RATIONAL DESIGN AND SYNTHESIS OF CHEMICAL PROBES FOR O-GLCNACASE AND OGT

by

Julia E. Heinonen
Bachelor of Arts, Simon Fraser University, 2005

THESIS SUBMITTED IN PARTIAL FULFILLMENT OF
THE REQUIREMENTS FOR THE DEGREE OF

MASTER OF SCIENCE

In the
Department of Chemistry

SIMON FRASER UNIVERSITY

Summer 2010

APPROVAL

Name: **Julia Heinonen**

Degree: **Master of Science**

Title of Thesis: **Rational Design and Synthesis of Chemical Probes for *O*-GlcNAcase and OGT**

Examining Committee:

Chair: **Dr. Paul Li**
Associate Professor, Department of Chemistry

Dr. David Vocadlo
Senior Supervisor
Associate Professor, Department of Chemistry

Dr. Robert Britton
Supervisor
Assistant Professor, Department of Chemistry

Dr. Gary Leach
Supervisor,
Associate Professor, Department of Chemistry

Dr. Robert Young
Internal Examiner
Professor, Department Chemistry

Date Defended/Approved: July 21, 2010

Declaration of
Partial Copyright Licence

ABSTRACT

The attachment of GlcNAc via a β-*O*-linkage to serine or threonine residues of various nucleocytoplasmic proteins is a common posttranslational modification in multicellular eukaryotes. A glycosyl transferase, UDP-*N*-acetyl-D-glucosamine: polypeptide-*N*-acetylglucosaminyl transferase (OGT) acts to install *O*-GlcNAc while a β-*N*-acetylglucosaminidase, *O*-GlcNAcase, removes this modification from proteins. A dynamic relationship between *O*-GlcNAc and phosphorylation has been proposed and is implicated in cellular signalling and disorders such as Alzheimer disease. In this thesis, the facile syntheses of two series of inhibitors of *O*-GlcNAcase are described. The potency of these compounds toward *O*-GlcNAcase is also detailed. Several of these compounds are highly potent and selective inhibitors of *O*-GlcNAcase. Additionally, 2-acetamido-2-deoxy-5-thio-D-glucopyranosose was synthesized as an analogue of GlcNAc. This compound was used for cell studies and to synthesize *para*-methoxyphenyl 2-acetamido-2-deoxy-5-thio-D-glucopyranoside as a potential substrate for *O*-GlcNAcase. Together, these compounds should serve as useful chemical probes to study the function of *O*-GlcNAc in cells and *in vivo*.

For my great grandmother Rice,
grandma Heinonen and parents,
with love.

ACKNOWLEDGEMENTS

I would first like to express my gratitude to my colleagues, who have been by my side, and helped me every step of the way through this journey. Their willingness to collaborate and solve problems as a team has been exceptional. I would especially like to thank Dr. Tong Li, Dr. Ramesh Kaul and Jenny Ji for their thoughtful input to my synthetic projects. Their experience and good humour made the tough spots a lot easier to overcome. During kinetic experiments, I received direction and thoughtful advice from Dr. Matthew Macauley, Garrett Whitworth and David Shen, and I thank them for their patience and helpful input in learning various kinetic techniques. I was fortunate to collaborate with several talented biochemists whom were able to take the synthetic tools that I made and bring them to life through their applications in cell and *in vivo* studies: thank you to Scott Yuzwa and Xioyang Shen for their hard work using Thiamet-G and to Dr. Tracey Gloster, Wesley Zandberg and David Shen for their work with 5SGlcNAc and *p*MP-5SGlcNAc. I would especially like to thank Dr. David Vocadlo for the incredible research opportunities he has provided me with, and both his support and criticism throughout my research, which has ultimately helped shape me into a more detailed, mature scientist.

Finally, I would like to thank my fantastic family and friends for their encouragement and love every step of the way. I especially thank my parents and Bryan for encouraging me through the most challenging moments. Your support and love mean the world to me.

TABLE OF CONTENTS

LIST OF FIGURES

LIST OF SCHEMES

LIST OF ABBREVIATIONS

General terms

calcd.	calculated
eq.	equivalents
expts.	experiments
δ+	partially positive
δ-	partially negative
h	hour(s)
HRMS	high resolution mass spectrometry
pH	acid dissociation constant
pK_a	negative log of the acid ionization constant (Ka)
r.t.	room temperature
U.V.	ultraviolet

Units of measure

Å	Ångstrom(s)
°C	degree Celsius
g	gram(s)
nm	nanometer(s)
nM	nanomole per litre
µM	micromole per litre
mg	milligram(s)
mL	millilitre(s)
mM	millimole(s) per litre
mmol	millimole(s)
mol	mole(s)
M	molar
m/z	mass to charge ratio
MHz	megahertz
ppm	parts per million
%	percentage

General chemistry terms

α	alpha
β	beta
cat.	catalytic
D	dextrorotatory
in vacuo	under vacuum
L	levorotatory
S_N1	unimolecular nucleophillic substitution reaction
S_N2	bimolecular nucleophillic substitution reaction
S_Ni	nucleophillic substitution with internal return
TLC	thin layer chromatography

Biological terms

APP	amyloid precursor protein
ADP	adenosine diphosphate
Asn	asparagine
Asp	aspartate
ATP	adenosine triphosphate
*Bt*GH84	*B. thetaoiotaomicron*
CAZy	*C*arbohydrate *A*ctive *E*n*zy*mes
DNA	deoxyribonucleic acid
GH	glycosyl hydrolase
GlcNAc	2-acetamido-2-deoxy-D-glucopyranose
GDP	guanidine diphosphate
GTP	guanidine triphosphate
HBSP	hexosamine biosynthetic pathway
His	Histidine
IC_{50}	50% maximal inhibitory concentration
in vitro	in glass
in vivo	in life
K_{cat}	catalytic rate constant (turnover number)
K_D	dissociation constant
K_i	inhibition constant
K_m	Michaelis constant
Leu	leucine
Lys	lysine

O-GlcNAc	2-acetamido-2-deoxy-D-glucopyranose
O-GlcNAcase	β-*N*-acetylglucosaminidase
OGT	UDP-*N*-acetyl-D-glucosamine:polypeptide-*N*-acetylglucosaminyl transferase
PHF	paired helical filaments
PC-12	phenochromocytoma cells
Pro	proline
PTM	post translational modification
RNA	ribonucleic acid
UDP	uridine diphosphate
V	rate
V_{max}	maximum rate

Chemical Terms

$CaCO_3$	calcium bicarbonate
$CDCl_3$	deuterated chloroform
CO_2	carbon dioxide
CF_3COOH	trifluoroacetic acid
DBU	1,8-Diazabicyclo[5.4.0]undec-7-ene
DCM	dichloromethane
DCC	dicyclohexylcarbodiiimide
DMF	dimethylformamide
EDC	*N*-(3-dimethylaminopropyl)-*N'*-ethylcarbodiimide
Et_3N	triethylamine
HCl	hydrochloric acid
H_2O	dihydrogen monoxide
K_2CO_3	potassium carbonate
$MgSO_4$	magnessium sulphate
NAG-thiazoline	1,2-deoxy-2'-methyl-α-D-glucopyranoso- [2,1-*d*]-Δ2'-thiazoline
$NaHCO_3$	sodium bicarbonate
NaOMe	sodium methoxide
NBut-GT	1,2-dideoxy-2'-propyl-α-D-gluco-pyranoso[2,1-*d*]-Δ2'-thiazoline
p	para
PUG-Nac	*O*-(2-acetamido-2-deoxy-D-glucopyranosylidene)amino-*N*-phenylcarbamate
5-SglcNAc	2-acetamido-2-deoxy-5-thio-α-D-glucopyranose
$SnCl_4$	tin (IV) chloride

THF	tetrahydrofuran
Thiamet-G	1,2-dideoxy-2'-aminoethyl-α-D-glucopyranoso[2,1-*d*]-Δ2'-thiazoline

Techniques and related terms

^{13}C-NMR	carbon nuclear magnetic resonance
^{1}H-NMR	proton nuclear magnetic resonance
d	doublet
dd	doublet of doublets
E.A.	elemental analysis
HRMS	High Resolution Mass Spectrometry
J	coupling constant
m	multiplet
NMR	Nuclear Magnetic Resonance
ppm	parts per million
s	singlet
t	triplet
TLC	thin layer chromatography
δ	chemical shift

Chapter 1: *O*-GlcNAc, *O*-GlcNAcase, *O*-GlcNAc transferase, and their roles in science and medicine.

1.1 *O*-GlcNAc, a simple sugar modification, can be reciprocal to phosphorylation.

2-acetamido-2-deoxy-D-glucopyranose (GlcNAc) is an aminosugar, differing from glucose by replacement of the 2-hydroxyl group with a 2-acetamido group (Figure 1.1). Glucose is the biosynthetic precursor to GlcNAc.[1] However, the roles that GlcNAc play in eukaryotic cells are varied and differ significantly from those played by glucose.[2-7]

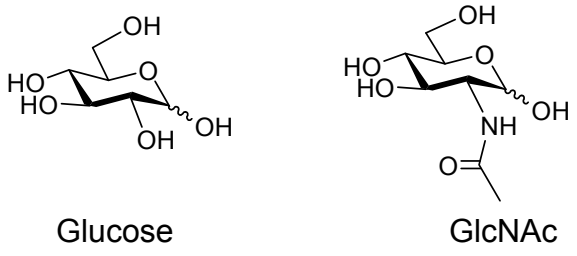

Figure 1.1 The structural differences between glucose and GlcNAc.

One role that GlcNAc plays is to modify intracellular proteins.[7-9] A protein that has GlcNAc attached to the hydroxyl group of a serine or threonine residue is referred to as an *O*-GlcNAc modified protein. The anomeric configuration of the GlcNAc residue *O*-glycosidically linked in this way is exclusively β, and to date, the addition of other sugars to *O*-GlcNAc to make longer chains has not been described. Because it is only after the protein has been synthesized within the

cell that *O*-GlcNAc is added, this modification is a post-translational modification (PTM).[9,10] *O*-GlcNAc was first discovered over twenty years ago by Torres and Hart.[9]

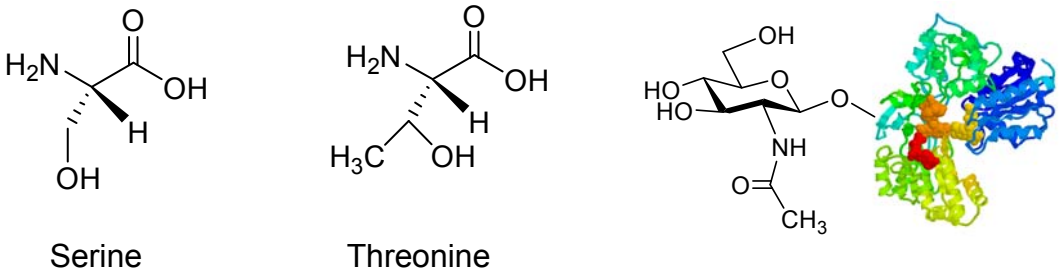

Figure 1.2 Amino acid acceptors for GlcNAc.
Above are shown the amino acids, threonine and serine. When found within certain proteins, serine or threonine residues can act as acceptors for the *O*-GlcNAc modification. Beside these two amino acids is illustrated an *O*-GlcNAc modified protein (note the β-glycosidic linkage).

It is important to appreciate that the *O*-GlcNAc modification is a reversible PTM. Indeed, the *O*-GlcNAc modification is dynamic, where the addition and removal of the sugar may occur several times during the lifetime of a protein.[11,12] This dynamism suggests that *O*-GlcNAc plays a role in signalling pathways similar to the well established signalling pathways mediated by phosphorylation.[10,13] The ability of *O*-GlcNAc to be added and subsequently cleaved off proteins in a cyclical manner arises from the action of two key enzymes; UDP-*N*-acetyl-D-glucosamine:polypeptide-*N*-acetylglucosaminyl transferase (OGT)[14,15] and β-*N*-acetylglucosaminidase (*O*-GlcNAcase).[16,17] OGT uses uridine 5′ diphospho-*N*-acetyl-D-glucosamine (UDP-GlcNAc, Fig. 1.3) as a glycosyl donor to transfer GlcNAc residues to the threonine and serine residues of target protein acceptors[14,18] (Fig. 1.4). UDP-GlcNAc is biosynthesized within eukaryotic cells from glucose through a series of steps that form what is referred to as the

hexosamine biosynthetic pathway (HBSP).[1] In contrast, *O*-GlcNAcase, is responsible for cleavage of *O*-GlcNAc off of modified proteins, thereby returning the proteins to their unmodified states (Figure 1.4).[16,17]

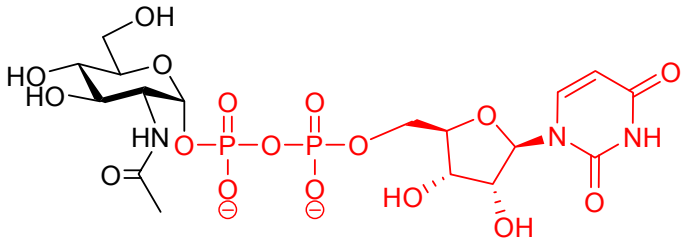

Figure 1.3 UDP-GlcNAc donor substrate of OGT.
UDP-GlcNAc is the donor substrate used by the glycosyl transferase OGT. This enzyme is responsible for transferring GlcNAc onto proteins. The nucleotide diphosphate, highlighted in red, is a good leaving group making the glycosyl transfer kinetically feasible and thermodynamically favourable.

Interestingly, it has been shown in a small number of cases that residues that can be *O*-GlcNAc modified can also sometimes be phophorylated through the action of a class of enzymes known as kinases.[19] Kinases are well known to transfer phosphate groups from donors such as adenosine triphosphate (ATP) or adenosine diphosphate (ADP) to a variety of biological substrates, including serine and threonine residues.[19] A group of enzymes known as phosphatases can function to remove phosphate moieties from such phosphorylated proteins.[20] This reciprocal dynamic relationship is illustrated in Figure 1.4:

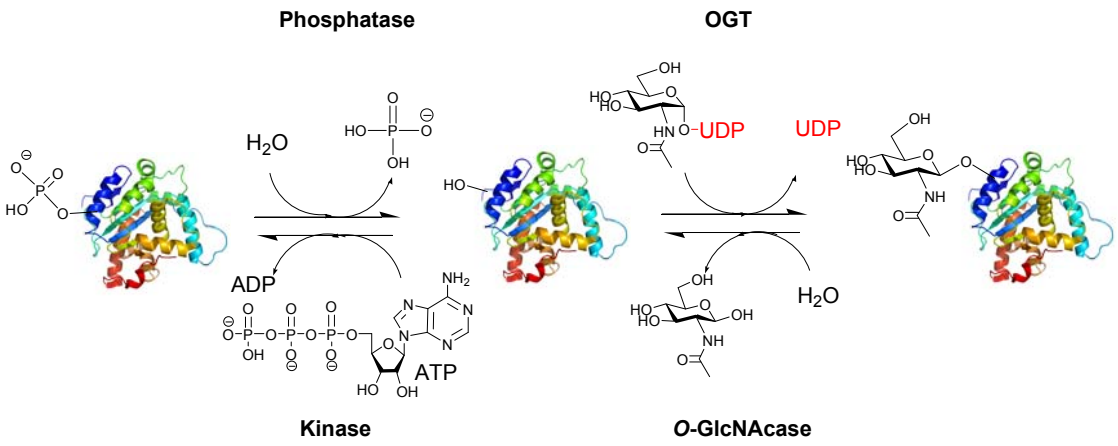

Figure 1.4 The dynamic relationship of *O*-GlcNAcylation and phosphorylation on proteins is mediated by several enzymes.
OGT is the enzyme responsible for transferring GlcNAc from UDP-GlcNAc onto various protein acceptors to β-*O*-GlcNAc. Conversely, *O*-GlcNAcase is responsible for the cleavage of the glycosidic bond of *O*-GlcNAc, consequently liberating the hydroxyl group of the protein and releasing GlcNAc. Free hydroxyl groups can in some cases be competitively modified either by OGT or by a kinase. Kinases phosphorylate these residues using ATP donors as a source of the phosphoryl group. A phosphatase can return the phosphorylated protein site to an unmodified state.

The fact that phosphorylation seems to sometimes occur at the same or adjacent sites[21] to where the *O*-GlcNAc modification can be found suggests that *O*-GlcNAc, in collaboration with phosphorylation, may play a role in regulating cellular processes as a dynamic team. Much research remains to be done in order to understand the roles played by *O*-GlcNAc in the working of cells. However, the *O*-GlcNAc modification appears critically important and has been found to be essential for embroyonic stem cell viability.[22]

The *O*-GlcNAc modification has also been implicated in several different disease states within humans. Research has suggested that the *O*-GlcNAc modification may play a role in the development of diabetes,[23,24] Alzheimer disease,[25-27] cardiovascular disease,[28-30] and cancer.[31,32] It also seems to play a

role in immune system function.[33,34] In light of these proposed roles played by *O*-GlcNAc in several disease states, it is clear that research performed to gain greater understanding of this dynamic modification, as well as its regulation, could have significant implications in both basic research and medical applications.

1.2 The addition and removal of sugar modifications: the fine work of glycosyl transferase and glycoside hydrolase enzymes.

Proper processing of the *O*-GlcNAc modification depends upon the action of OGT and *O*-GlcNAcase. OGT is an enzyme that is a part of the superfamily of enzymes known as the glycosyl transferases, enzymes that transfer sugars to a variety of biological substrates. In contrast, *O*-GlcNAcase is part of the large superfamily of glycoside hydrolases, which are responsible for the cleavage of glycosidic bonds found in various glycoconjugates. A general understanding of these two classes of enzymes will be useful for the discussion within this thesis. An overview of the catalytic mechanisms of these two classes of enzymes is therefore provided below.

1.2.1 Glycoside Hydrolases

Glycoside hydrolases (GH) are enzymes that are responsible for the cleavage of glycosidic bonds of sugars linked to other sugars, lipids, or proteins.[35,36] Glycosidic bonds are remarkably stable and it has been estimated that the half life for spontaneous hydrolysis of a single glycosidic bond is approximately 5 million years![37] Glycoside hydrolases can increase the rate of glycosidic bond cleavage by up to 10^{17} times,[37] making glycoside hydrolases one

of the most proficient superfamilies of enzymes.[37] Because of the wide range of glycan structures that exist in nature, there is also a wide range of glycoside hydrolases that process these structures. Due to the large number and diversity of the glycoside hydrolases found within the glycoside hydrolase superfamily, they have been subdivided into various families according to their amino acid sequence and structural similarities. This well established classification system, CAZy (*C*arbohydrate *A*ctive *E*n*zy*mes, http://www.cazy.org), is a highly useful and widely referenced classification system.[38] Glycoside hydrolases that are found in the same family often act on the same sugars and almost always use highly similar mechanisms. Generally speaking there are two possible ways that glycoside hydrolases act on substrates, and this partly defines their catalytic mechanism: the stereochemistry of the product can be either retained or inverted relative to that of the substrate.[35]

Inversion of stereochemistry at the anomeric center involves one chemical step in which a molecule of water acts as a nucleophile to displace the leaving group.[35] The nucleophilicity of the water molecule is enhanced by a general base catalytic residue and departure of the leaving group is aided by a general acid catalytic residue (Figure 1.5). Both these residues have been found most commonly to be enzymic carboxyl groups.[35]

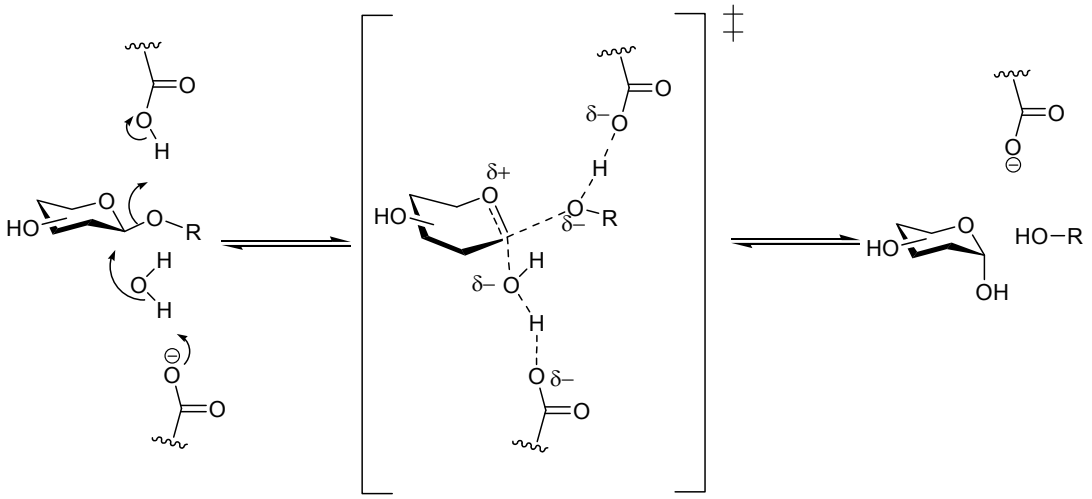

Figure 1.5 Inverting mechanism for a glycoside hydrolase.
An inverting catalytic mechanism is thought to proceed via a concerted one step process through a dissociative transition state. General acid catalysis from an enzymic carboxylic acid aids departure of the leaving group, while a second carboxylate residue acts as a general base and enhances the nucleophilicity of a water molecule.

With this general scenario in mind for an inverting mechanism, inversion of stereochemistry at the anomeric center may proceed along either an S_N1, or an S_N2 reaction coordinate. Classically speaking, with S_N1 reactions, the stereochemistry of the product can either be inverted or retained with respect to the stereochemistry of the starting material. This is the case because, during an S_N1 reaction a discrete cation is formed,[39] and the nucleophile can attack either face of this planar carbocation. These geometrically different processes lead to a mixture of retained and inverted stereochemistry in the resulting products.[39] An enzymatic S_N1 reaction, however, can result in exclusively inverted products since the face of the carbocation that would lead to a retained product may be blocked by the leaving group, which may diffuse out of the enzyme active site relatively slowly. Although there is no experimental evidence for an S_N1 reaction

occurring for any inverting glycoside hydrolases, the scenario certainly remains possible. In contrast, for an S_N2 mechanism, the incoming nucleophile attacks the anomeric center at the same time that the leaving group departs. The geometric requirements of the reaction ensure that such a process always leads to an inverted product.[39]

Two different, yet related, catalytic mechanisms are used by glycoside hydrolases that use a retaining mechanism. The first mechanism is a two step process where, in the first step of the reaction, a general acid catalyst facilitates departure of a leaving group while another residue acts as a nucleophile to displace the leaving group and stabilize an enzyme sequestered intermediate, which is most likely a covalent glycosyl enzyme intermediate. The second step of this mechanism is essentially the reverse of the first step; a general base catalyst facilitates the attack of a molecule of water at the anomeric center, intercepting the enzyme sequestered intermediate and forming a hemiacetal product having retained stereochemistry at the anomeric center relative to that of the substrate.[35] Both residues are generally enzymic carboxylates although exceptions are known.[35] Because it is generally believed that for retaining glycoside hydrolases the intermediate is a covalent glycosyl-enzyme intermediate, this type of mechanism is often referred to as a double displacement mechanism[35] (Figure 1.6). The second retaining mechanism involves the nucleophillic participation of the *N*-acetyl group found at position two of the pyranose ring of naturally occurring hexosamines such as GlcNAc.[35,40] In this scenario, a general acid catalytic residue aids departure of the leaving group. Attack of the nucleophilic *N*-

acetyl group is aided by a second residue in the active site that orients and polarizes this *N*-acetyl group, most likely by acting as a general base.[41] The net result is the formation of an enzyme sequestered oxazoline intermediate[40] (Figure 1.7). This intermediate is then broken down by the general base catalyzed attack of water at the anomeric center, as well as a general acid catalyzed opening of the oxazoline ring. The stereochemical constraints of the reaction ensure that the process occurs only with retention of configuration at the anomeric center.[35] This mechanism is known as a substrate-assisted catalytic mechanism or an anchimeric assistance mechanism. There are some rare mechanistic exceptions for retaining glycoside hydrolases but these will not be discussed here and the reader is advised to see a recent review for a discussion of these alternatives.[35]

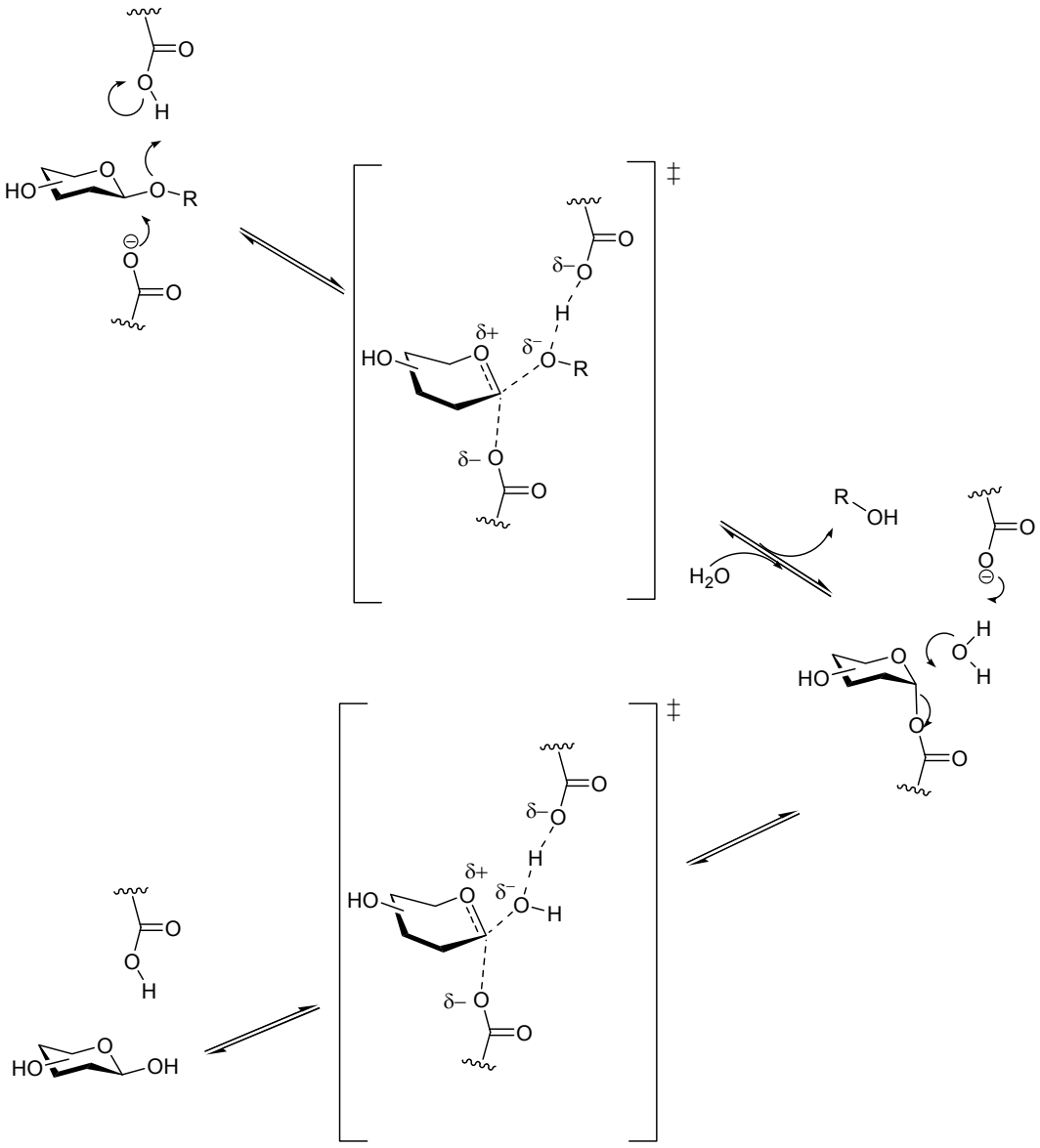

Figure 1.6 The retaining mechanism for glycoside hydrolases involving an enzymic nucleophile.

Two carboxyl groups play key catalytic roles in retaining glycoside hydrolases. One acts as a general acid to facilitate departure of the leaving group from the anomeric center. A second carboxyl group residue acts as a catalytic nucleophile to attack the anomeric center. A covalent enzyme intermediate is likely formed and is then broken down in a second step that is the near reverse of the first step.

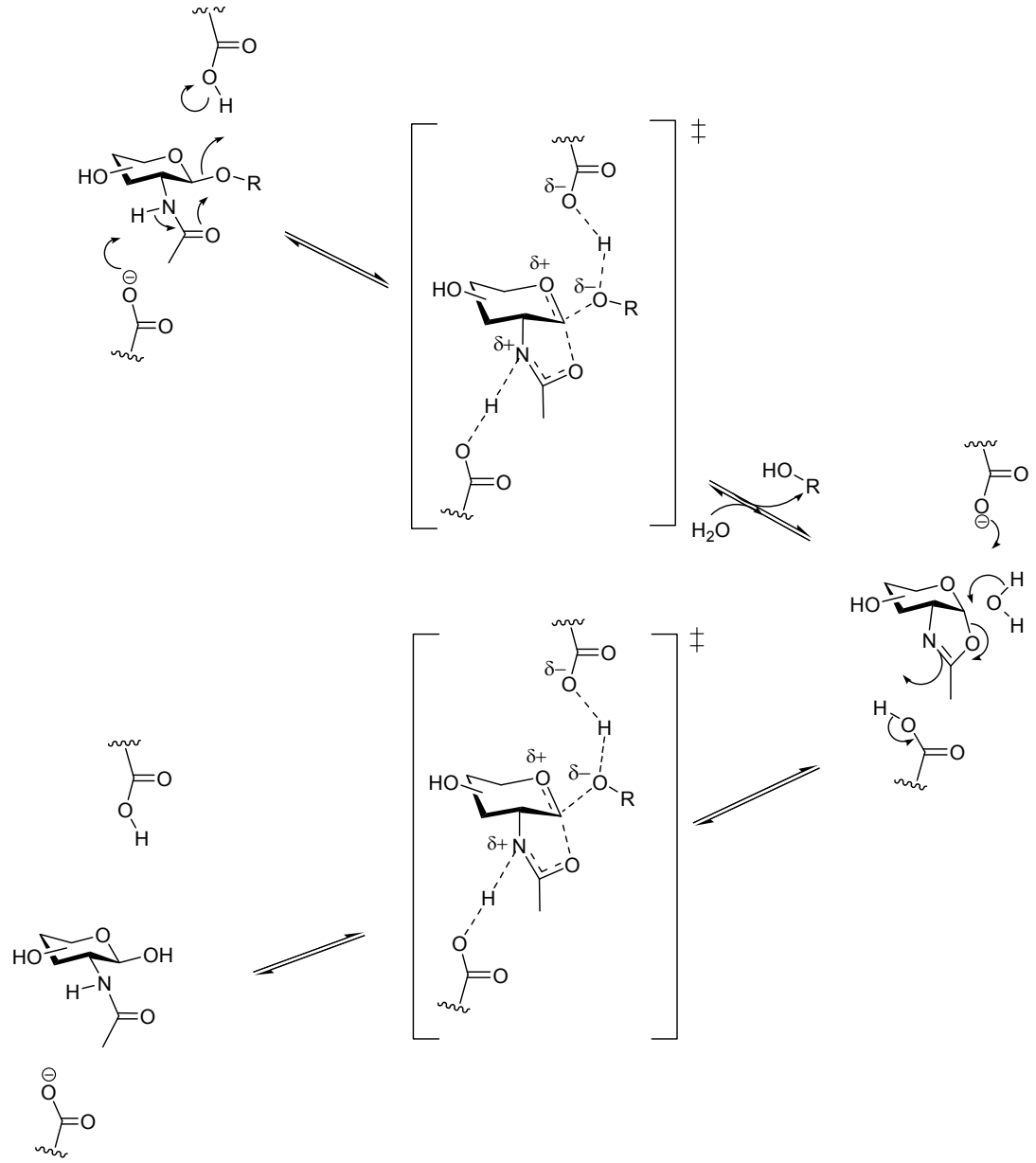

Figure 1.7 The retaining mechanism for glycoside hydrolases involving anchimeric assistance.

The anchimeric assistance mechanism involves two key catalytic carboxyl groups. One acts as a general acid to aid departure of the leaving group while a second group acts to polarize the *N*-acetyl group to act as a nucleophile. Attack of the *N*-acetyl group of the anomeric center displaces the leaving group and results in the formation of an oxazoline intermediate.The second step is the near reverse of the first step and produces the hemiacetal product having the same anomeric configuration as the substrate.

1.2.2 Inhibitors of Glycoside Hydrolases

Inhibitors of glycoside hydrolases can be subdivided into two broad classes; those that bind covalently to their target enzyme and those that bind non-covalently.[42] Covalent inhibitors associate with the target enzyme and then react to form a covalent bond between the inhibitor and the enzyme.[43,44] Typically, a nucleophilic residue within the active site of the enzyme reacts with an electrophillic moiety present on the inhibitor. The formation of this covalent adduct leads to loss of activity because the inhibitor physically blocks access of the substrate to the active site and also because the inhibitor often modifies an active site residue that is critical for catalytic action (Figure 1.8).[42] In contrast to such inactivators, a non-covalent inhibitor associates with the target enzyme through non-covalent interactions such as van der Waals, hydrogen bonding, and ionic interactions. Inhibition by these molecules is reversible (Figure 1.8).[42]

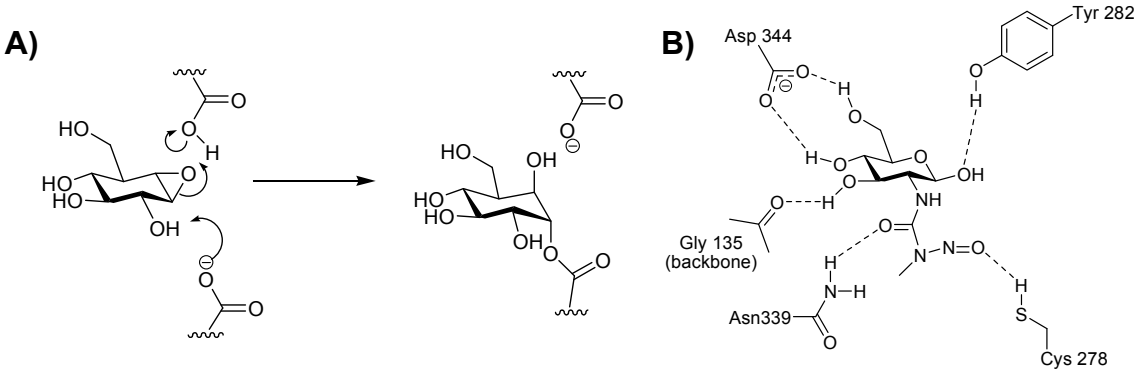

Figure 1.8 Covalent inhibition contrasted with non-covalent inhibition of glycoside hydrolase enzymes.
A) The mechanism of inactivation of a retaining β-glucosidase by conduritol β-epoxide. Note how the aspartate residue in the active site acts as a nucleophile to open the epoxide, forming a covalent bond to the inhibitor, leading to inactivation of the enzyme. B) In constrast, one can see the types of interactions between a non-covalent inhibitor streptazotocin with *Bt*GH84, a bacterial homologue of *O*-GlcNAcase.[45]

Covalent inhibitors are useful for several purposes, the most common of which is to identify active site residues. Labeled active site residues can be identified by X-ray crystallography or mass spectrometry.[42,43] The identified residues can then be altered by site-directed mutagenesis and kinetic analysis of the mutant enzymes can be used to confirm whether or not the identified residue has an essential catalytic function or simply serves a structural role.[42] In addition, highly specific covalent inactivators can be used to selectively inactivate a target enzyme in cells to observe the effect of eliminating the enzyme activity within cells.[46]

The inhibitors that will be discussed in this thesis are those that associate with *O*-GlcNAcase through non-covalent means. Non-covalent inhibitors are preferred as potential therapeutics and as research tools since there is less likelihood these molecules will adventitiously inactivate unrelated enzymes. Notably, many good non-covalent inhibitors are inspired to some extent by the proposed transition state structure stabilized by the enzyme being targeted. The transition state is a fleeting species wherein bonds are breaking and forming in a concerted manner. In the 1940's, Pauling proposed that inhibitors with the highest affinity for an enzyme are those possessing a structure resembling that of a "strained activated complex" (now termed a transition state).[47,48] The transition states for glycoside hydrolases are generally thought to possess oxocarbenium ion character. This arises from the transition state having only partial bonds formed with the attacking nucleophile and the leaving group as well as delocalization of the lone pair of electrons of the endocyclic oxygen. In these

dissociative transition states the anomeric carbon is believed to possess trigonal character (sp^2 hybridization) at both the endocyclic oxygen and anomeric carbon.[35,49] This double bond character in the pyranose ring means that there is some distortion from the ground state conformation of the substrate to a more planar and energetically unfavourable half chair or boat conformation.[35,49,50] Such transition state conformations, are something to consider when designing inhibitors of glycoside hydrolases. An additional point to consider when designing glycoside hydrolase inhibitors is the build up of partial positive charge on the endocyclic oxygen and anomeric pyranose at the transition state.

The first rational approach to inhibitor design is to replicate to some extent the charge distribution in the transition state, most often by using a piperidine derivative having a nitrogen atom at the position usually occupied by O-5 or C-1 of the pyranose ring. Such piperidine rings are protonated at physiological pH and are believed to mimic the transition state.[51] An example of such an inhibitor is Nojirimycin, which is the first natural product found to inhibit a glycoside hydrolase. This compound was isolated from a strain of *Streptomyces* in 1966 and was found to possess antibiotic properties.[52] Nojirimycin was also found to be capable of inhibiting both α- and β-glucosidases.[53] From this scaffold several derivatives were created, including deoxynojirimycin and deoxygalactonojirimycin, which were found to inhibit α- and β-mannosidases and galactosidases, respectively (Figure 1.9).[44]

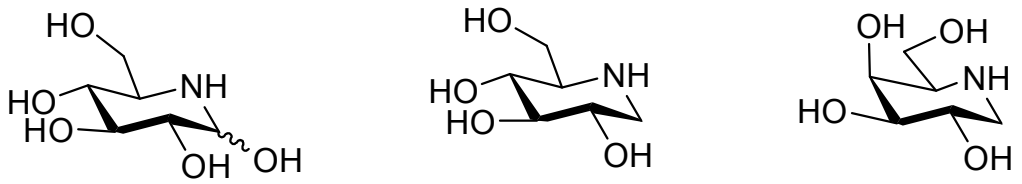

Figure 1.9 Structure of Nojirimycin and derivatives.
The structures of Nojirimycin, deoxynojirimycin and deoxygalactonojirimycin are shown from left to right respectively. Each is a well known inhibitor of different α- and β-glycosidases. The inhibitory potency of these compounds is due to the amino group within the ring at the position normally occupied by the endocyclic oxygen.

A second rational approach to creating a successful inhibitor for glycoside hydrolases is to engineer the molecule to adopt a shape resembling that of the transition state used by the enzyme of interest.[51,54] This approach can be an effective way to enhance binding to enzymes that have specific binding pockets where key catalytic groups are strategically positioned. If the inhibitor is oriented within the active site in a way that allows it to interact with key catalytic residues in a manner similar to how a transition state structure might bind, then it is likely the inhibitor will capture some transition state binding energy and bind fairly well. Examples of inhibitors that mimic the geometry of the transition state are glucolactones and gluconolactans and these are often good inhibitors, though they lack any charge.[54]

Of course, not all inhibitors of glycoside hydrolases are transition state mimics.[55] There are plenty of examples of inhibitors that bind successfully simply by having a structure that can position itself and interact favourably in the active site through serendipitous hydrogen bonds, van der Waals interactions, and electrostatic interactions. Indeed, there are examples of glycosidase inhibitors that do not have any features of carbohydrates. Some examples of such

inhibitors include proteins[56,57], cyclopeptides[58], and relatively simple amines[59]. Reflecting on this last point, it is important to maintain an open mind when designing inhibitors of glycoside hydrolases and avoid becoming hindered by trying to approach the problem from only one angle.

1.2.3 Glycosyl Transferases

All glycosyl transferases catalyze glycosidic bond formation using sugar donors that contain a substituted phosphate leaving group.[60] Activated donor sugars are most often nucleoside diphosphate sugars such as UDP-GlcNAc (Figure 1.3) or guanidine diphosphate (GDP) mannose. In other cases, however, nucleoside monophosphate sugars or lipid phosphate sugars are glycosyl donors. The structures that accept the transferred glycosyl unit are called acceptors and are most commonly other sugars, but can also be proteins, lipids, nucleic acids, or other small molecules.[60] Generally speaking, the glycosyl unit is transferred onto the nucleophillic oxygen of the hydroxyl substituent of the acceptor, but transfer can also occur to other atoms, such as nitrogen, sulphur and carbon.[60] With these basics in mind, a topic of interest regarding the glycosyl transferases is their mechanism of action. There are two possible stereochemical outcomes of the reactions catalyzed by this class of enzymes; the product can either be retained or inverted with respect to the stereochemistry of the donor sugar (Figure 1.10).[60] As with glycoside hydrolases, glycosyltransferases have been divided into many families based on amino acid sequence similarities. The classification system CAZy (*C*arbohydrate *A*ctive En*zy*mes, http://www.cazy.org) is a useful resource for those interested in glycosyl transferases.[38]

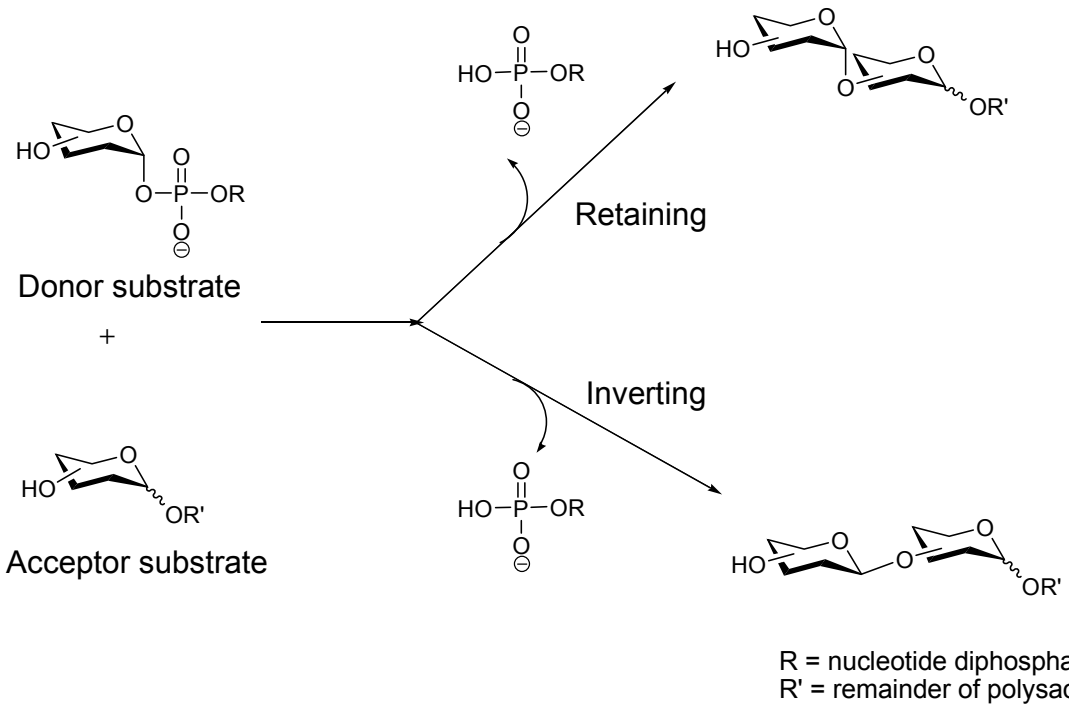

Figure 1.10 Stereochemical outcomes for glycosyl transferase reactions.
The two possible stereochemical outcomes for a glycosyl transferase catalyzed glycosyl transfer from a nucleotide diphosphate sugar onto a hydroxyl group of an acceptor sugar. The acceptor can also be a protein, lipid, or nucleic acid.

Each glycosyl transferase is stereospecific and catalyzes its reaction using only one of the stereochemical outcomes. The catalytic mechanism of inverting glycosyl transferases involves a single displacement of the phosphate leaving group through what is generally believed to be a dissociative S_N2 reaction mechanism.[60] An active site residue of the enzyme serves as a general base to aid the attack of the incoming nucleophile (the acceptor) and displacement of the activated phosphate leaving group (Figure 1.11). It has been found that inverting glycosyl transferases with bound acceptors often show conserved residues such as carboxylates or imidazoles that are within hydrogen bonding distance of the nucleophillic hydroxyl group undergoing reaction, consistent with their roles as general base catalysts.[61,62] In further support of this proposed mechanism, it has

been found that site directed mutagenesis of an active site carboxyl residue of an inverting glycosyl transferase from the GT2 family of enzymes, known as ExoM, resulted in complete loss of catalytic activity.[62] Also, a histidine residue has been unambiguously shown to be the general base in the sialyltransferase *Campylobacter jejuni* alpha-2,3/2,8-sialyltransferase (CstII) from the gycosyltransferase family 42.[61] Some glycosyl transferases use a divalent metal ion, such as Mn^{2+} or Mg^{2+}, to aid departure of the nucleotide diphosphate. Those that do not use a positively charged metal ion often have positively charged amino acid residues, within the active site to fulfil this role.[60]

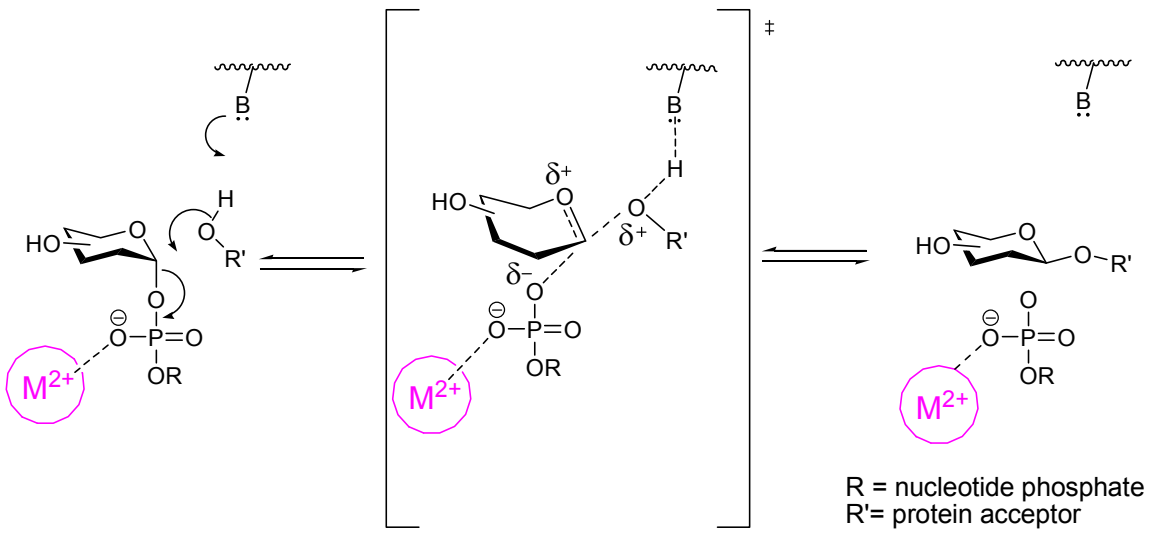

Figure 1.11 Inverting mechanism of glycosyl transferases.
Inverting glycosyl transferases are generally believed to use a direct-displacement S_N2 reaction mechanism that results in inverted configuration at the anomeric center. The glycosyl transferase shown here is a metal ion dependant enzyme.

For retaining glycosyl transferases, two catalytic mechanisms have been proposed. One of these is a double-displacement mechanism involving a covalently bound glycosyl enzyme intermediate in which the sugar residue is attached to an appropriately positioned nucleophile within the active site. The

reason why this mechanism is described as a ‘proposed’ mechanism is that mechanistic characterization of glycosyl transferases is quite challenging (Figure 1.12). There has not yet been any concrete evidence that a covalently linked intermediate does exist, although there have been numerous studies seeking to provide scientific support for this hypothesis. Perhaps the issue in supporting this potential mechanism is finding the appropriate techniques to trap the putative intermediate. Only further studies will provide a clear understanding.

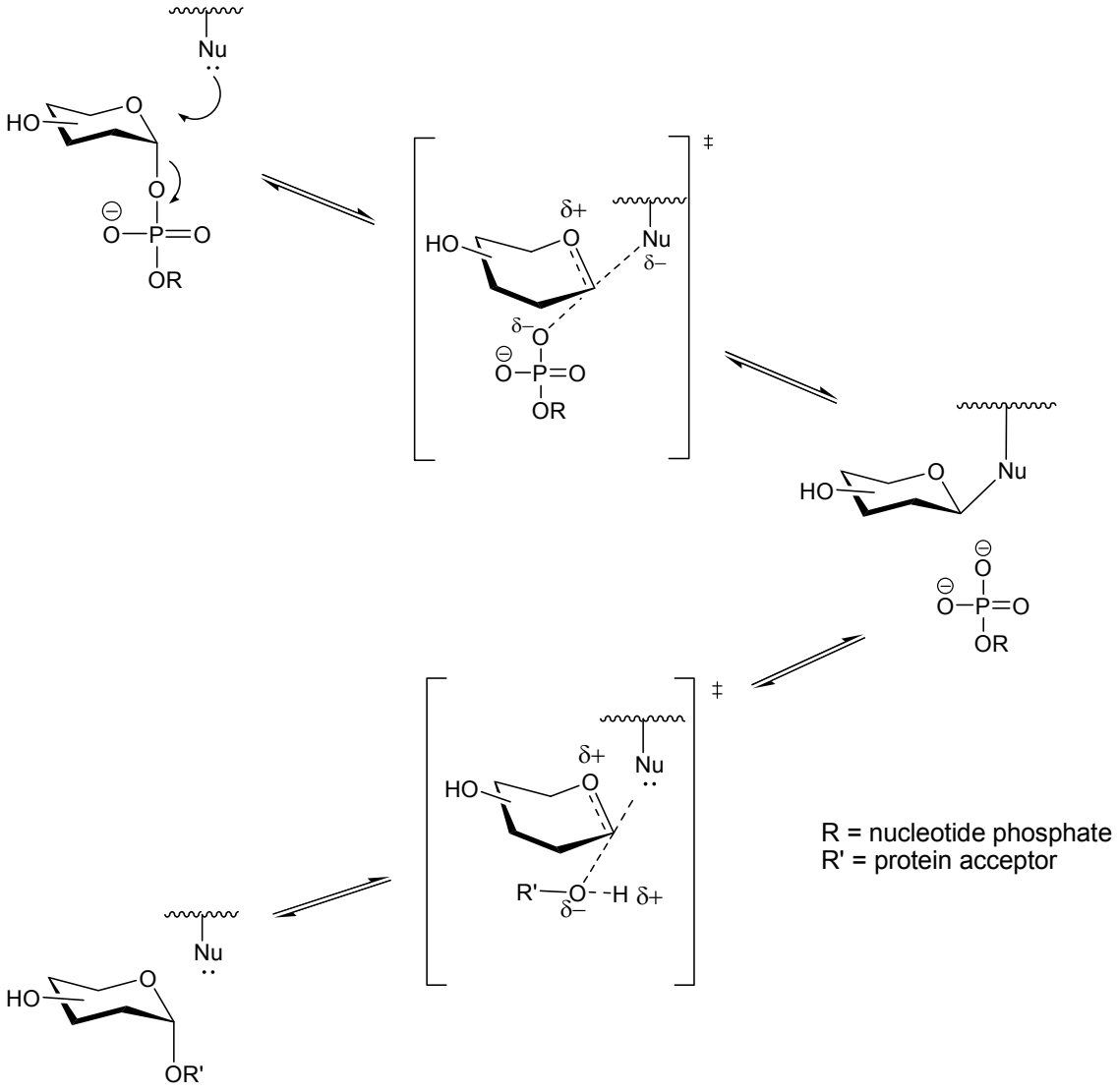

Figure 1.12 Proposed retaining mechanism for glycosyl transferses.
A hypothetical scheme illustrating what the proposed mechanism of a retaining glycosyl transferase may look like. The exact mechanistic details are yet to be uncovered for any retaining glycosyl transferase.

A second proposed catalytic mechanism that leads to exclusive retention of stereochemistry in retaining glycosyl transferases is a non-concerted process. This proposed mechanism is a special type of S_N1 reaction, known as S_Ni, and occurs when a discrete ion pair intermediate forms. This mechanism is termed S_Ni because the 'i' denotes the internal return of a nucleophile to the same face

from which the leaving group departed. This mechanism was first described to account for the products observed to arise from the decomposition alkyl chlorosulphites.[60,63] The unique features that account for the retention of stereochemistry in the case of alkyl chlorosulphites are that the leaving group undergoes decomposition, leading to the production of a nucleophile that is held as an ion pair on the same face as the leaving group. Decomposition of the leaving group species and attack of the newly formed nucleophile occurs at a rate that exceeds any other attack on the electrophile. Many authors now propose this type of S_N1 mechanism for glycosyl transferases that lead to retention of stereochemistry.[60] In the case of glycosyl transferases, the acceptor is positioned adjacent to the leaving group such that it can only attack the same face of the glycosyl cation intermediate from which the leaving group departed.

The take home message for the glycosyl transferases is that they function to attach sugars to different substrate acceptors within the cell, yet their precise mechanisms of action remain to be clarified. The main glycosyl transferase that will be discussed in this thesis is OGT, which is an inverting glycosyl transferase.

1.2.4 Inhibitors of Glycosyl Transferases

The development of potent and selective inhibitors of glycosyl transferases is still in its infancy.[64,65] This is partly due to many unknowns regarding the mechanistic details of how glycosyl transferases function. However, the importance of the development of inhibitors for this class of enzymes is well recognized.[64,66-68] In addition to their potential as valuable scientific tools that should aid in the study of glycobiology, selective inhibitors of

glycosyl transferases have potential applications as therapeutics for diseases that are linked to carbohydrate-protein interactions.[64] Despite this potential, and the considerable effort that has been put into developing inhibitors for members of this class of enzymes, most compounds have been found to be quite poor and only a minority have been found to be potent.[65] Of these potent glycosyl transferase inhibitors, only a handful can engage their targets in cells.[32,69-73]

Despite the challenges of generating inhibitors for glycosyl transferases, a few general observations have been collected over the last twenty years. Some carbohydrate-based inhibitors that have seen success in inhibiting glycosyl transferases are those that contain nitrogen in the place of the endocylclic oxygen of the carbohydrate ring or at the position of the anomeric center. This may be partly due to the fact that the ring nitrogen of these inhibitors is basic and is protonated under physiological conditions (pH 7.4).[44,51,54] The resulting cationic species can interact with anionic groups within the active site of glycosyl transferases. Some noteworthy examples of amino-based sugar inhibitors for glycosyl transferases include some of the structures illustrated in Figure 1.13.[74-76]

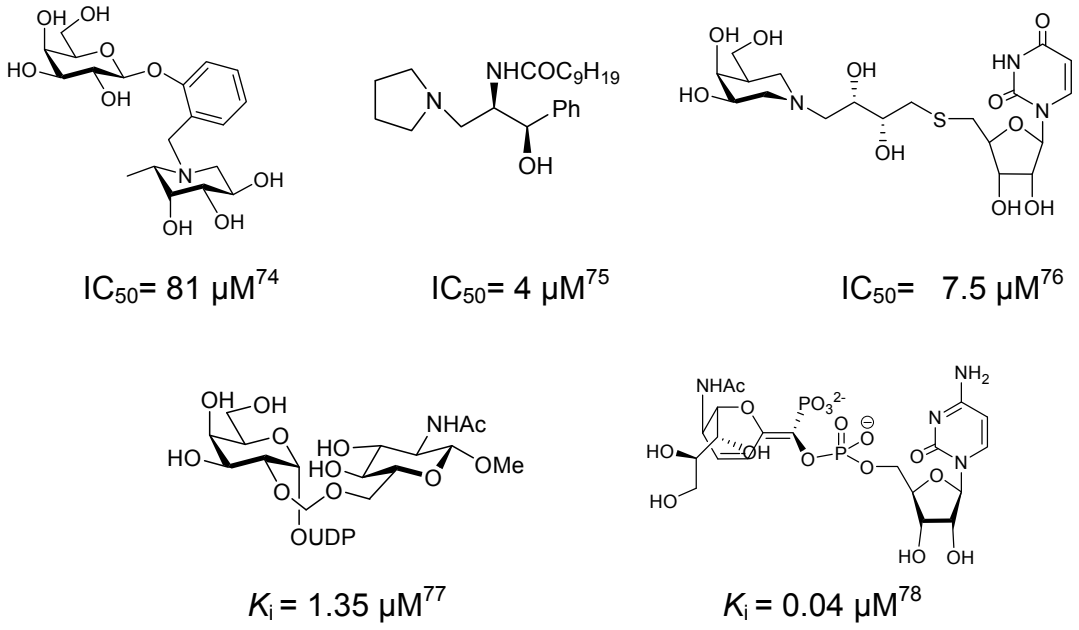

Figure 1.13 Examples of some moderately successful glycosyl transferase inhibitors. The above structures are examples of glycosyl transferase inhibitors that possess significant binding to different glycosyl transferases. From left to right, these inhibitors target mammalian α-1,3-fucosyltransferase,[74] ceramide glucosyltransferase,[75] α-1,3-galactosyltransferase,[76] β-1,4-galactosyltransferase,[77] and an α-2,6-Sialyltransferase,[78] respectively.

It is obvious that the binding affinities of the inhibitors illustrated in figure 1.13 are modest and though all inhibit their targets fairly well *in vitro*, none have been shown to act in cells. Each has a basic nitrogen atom, which likely aids in binding to their targets for reasons discussed earlier. Despite the observation that an appropriately positioned nitrogen atom seems to be helpful for succesful inhibition of glycosyl transferases there is clearly room for improvement. In terms of developing inhibitors that may act as therapeutics, they need to be able to permeate through cellular membranes in order to act *in vivo*; something that has only been accomplished for glycosyl transferase inhibitors in a very limited number of cases.[32,69,70,72,73]Challenges in developing inhibitors of glycosyl

transferases also arise from the intrinsic features of the glycosyl transferases themselves. For example, the transition state for glycosyl transferases is complex and often involves four distinct structures; the sugar donor, the sugar/protein acceptor, a metal cation, as well as the enzyme itself.[60,79] These groups all play a role in the transition state, making it difficult to emulate with a simple small-molecule inhibitor (Figure 1.14).

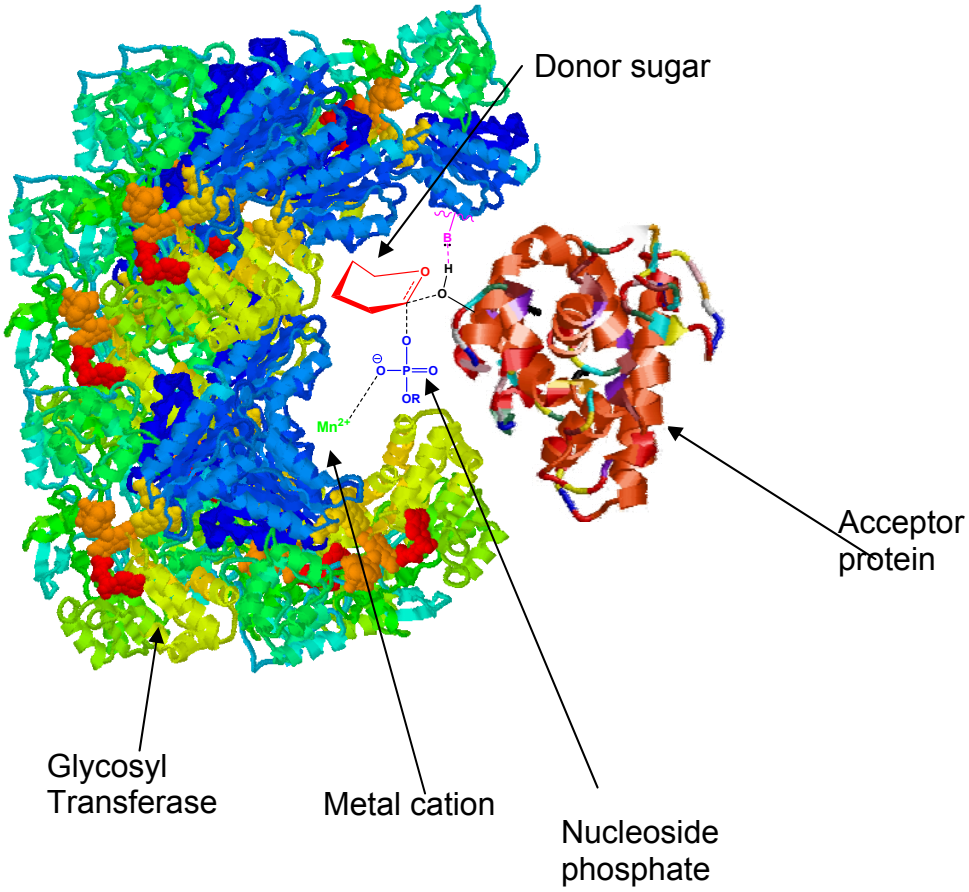

Figure 1.14 Common components involved in a glycosyl transferase transition state. The transition state of glycosyl transferases is complex. It often involves four distinct groups.

One reason it is useful to have an understanding of the transition state structures used by glycosyl transferases is that transition state structures are generally thought to interact very tightly with the enzyme. As was discussed in detail in section 1.2.2 about glycoside hydrolases, the preferential tight binding of the transition state is believed to confer much of the catalytic power of enzymes. As a result of this tight binding, proposed transition state structures are often used as inspiration for inhibitor design. However, it is evident that with glycosyl transferases, emulating the transition state structure is difficult. Further, binding of acceptor substrates and nucleosides to glycosyl transferases tends to be relatively weak; these species often bind to glycosyl transferases with K_D values in the mM range.[64] As a consequence, generating substrate or bisubstrate analogues that inhibit these enzymes can also be difficult. It is known, however, that glycosyl transferases, including OGT, bind UDP and UDP-GlcNAc quite tightly with K_D values often in the low micromolar range. Therefore, understanding the binding of glycosyl donor substrates and UDP is worthwhile. The pyrophosphate moiety of the sugar-nucleoside diphosphate donors has been well documented as being important in binding, especially since the anionic charges makes this portion of the sugar able to form favourable ionic interactions with cationic groups within the active site.[60,80] These areas of positive charge in the active site of glycosyl transferases may present themselves in the form of one or more positively charged amino acid residues,[60,81] as seen in Figure 1.15 for OGT. Alternatively the cationic group may be a divalent metal cation, often Mn^{2+}.[60,82]In light of this, maintaining the pyrophosphate bridge of the donor sugar

may prove beneficial for inhibitor binding. Alternatively, incorporating moieties that mimic the charge or characteristics of the diphosphate group may also be a productive approach to generating good inhibitors of glycosyl transferases.

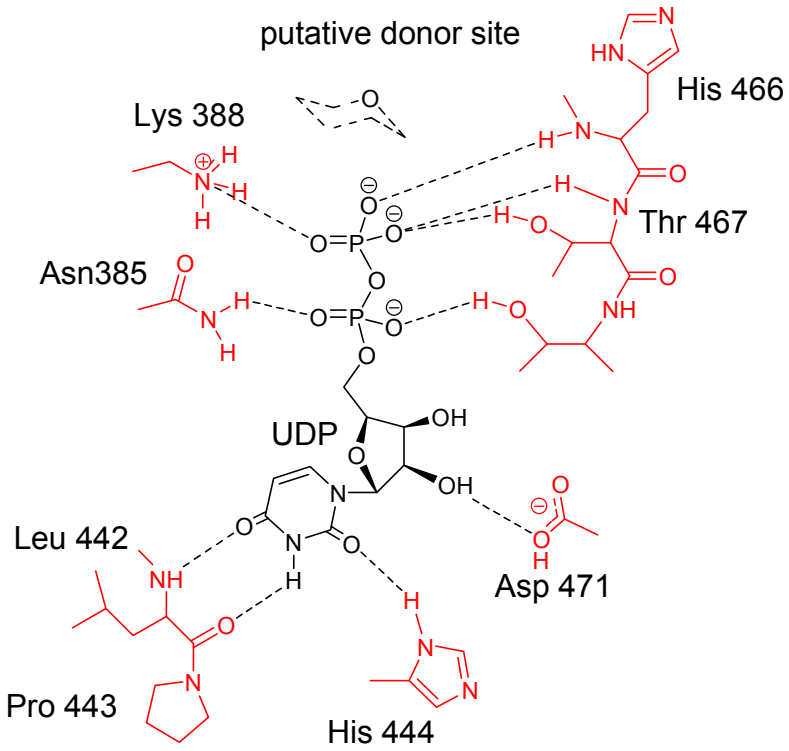

Figure 1.15 Binding interactions between UDP and OGT.
In red are shown the amino acid residues from a bacterial homologue of OGT and how they interact with the UDP portion of the nucleotide sugar donor. Various hydrogen bonding and ionic interactions form between this portion of the donor and the enzyme active site. This suggests the importance of incorporating this phosphate bridge, or a polar mimic of this group, when designing inhibitors of OGT and other glycosyl transferases.[81]

Clearly, there is a long way to go in terms of generating potent inhibitors of glycosyl transferases that can be used in tissues. It might be beneficial if much of the current research efforts regarding glycosyl transferases focused on gaining a better understanding of the mechanisms of these enzymes, since this knowledge could make design of good inhibitors more feasible.

1.3 *O*-GlcNAcase, the enzyme of central significance to the following studies

A more detailed discussion of *O*-GlcNAcase will be of importance to define the purposes of the research presented in this thesis. Although the focus of this thesis is on the synthetic processes used to make various small molecule targets, each final compound was synthesized to test the function of *O*-GlcNAcase or OGT. One of the reasons *O*-GlcNAcase is of interest to the glycoscience community is that it has been proposed to play key regulatory roles within mammals.[83-87] Some fundamental research over the past two decades supports this claim: the *O*-GlcNAc modification is present on a wide range of proteins and it is found on RNA polymerase, which may have implications on protein expression. Changes in *O*-GlcNAc levels have also been proposed to alter the behaviour of specific proteins by modulating protein-protein interactions,[85,86,88] DNA binding,[89] and enzyme activity.[87,90,91] Interestingly, in some cases the proteins that are *O*-GlcNAc modified have also been found to be phosphorylated, at the exact same or adjacent sites as *O*-GlcNAc can be found.[92-94] Because phosphorylation has long been known to play regulatory roles within cells, it has been postulated that *O*-GlcNAc also plays a role in these processes since it has the capacity to block phosphorylation at some sites.[94] This relationship between *O*-GlcNAc and phosphorylation is mediated in part by *O*-GlcNAcase since this enzyme is responsible for the removal of *O*-GlcNAc.

Consistent with its proposed involvement in various cellular processes, *O*-GlcNAc has been suggested to have roles in some disease states, although such proposals require further scientific studies to gain compelling support. For

example, it has been shown that increased *O*-GlcNAc levels correlate with insulin resistance and it has therefore been suggested that increased *O*-GlcNAc induces with the development of type 2 diabetes.[23,24] However, it remains unclear if increased *O*-GlcNAc levels cause diabetes.[95] It is important to maintain clear distinctions between research pointing to correlative observations and research that provide clear causative links. To date, *O*-GlcNAc levels have been correlated with several disease states but there is limited evidence supporting a causative link. In light of these observations, it is evident that investigating the dynamic levels of *O*-GlcNAc in cells is worthwhile. Specific tools to investigate the roles of *O*-GlcNAc within the cellular environment are likely to be useful in making these new discoveries.

One useful tool to aid the study of *O*-GlcNAc would be the development of highly selective and potent inhibitors of *O*-GlcNAcase. Using appropriate inhibitors, we can study the repercussions of increased *O*-GlcNAc levels in cells *in vivo*. This ability may help us to gain greater insight as to which processes or disease states are dependant on increased *O*-GlcNAc in the cell, and this in turn may point to potential areas where further research be directed. A major aim of this thesis is to develop an inhibitor that can permeate into cells, is potent, and is selective for *O*-GlcNAcase.

1.4 The *O*-GlcNAc modification and its possible role in the development and progression of Alzheimer disease.

Alzheimer disease is a neurological disorder characterized by two primary pathological features.[25] The first of these are the β-amyloid plaques, which are

abnormal aggregates of a peptide derived from proteolytic processing of the amyloid precursor protein (APP). β-amyloid plaques are found in the interneuronal tissue of diseased individuals.[25] The second diagnostic pathology found in Alzheimer disease are neurofibrillary tangles, which are abnormal aggregates of the microtubule associated protein tau, occurring within neurons.[6] Tau normally functions to stabilize microtubules within cells, however, cells that accumulate neurofibrillary tangles die.[6]

One of the key features of tau present in neurofibrillary tangles is that it is abnormally hyperphosphorylated.[96] As much as 4-fold greater levels of phosphorylation are seen on tau in the brains of Alzheimer patients compared to phosphorylation levels found on tau from brain tissue of individuals who had suffered no neurodegeneration.[97] This hyperphosphorylation of tau is generally thought to be the factor leading to its aggregation into paired helical filaments (PHF), which are the species that spontaneously assemble to form neurofibrillary tangles.[96,98] Interestingly, tau has been shown to be *O*-GlcNAc modified and a reciprocal relationship between *O*-GlcNAc and phosphorylation has been proposed for tau.[25,27] The dynamic balance between phosphorylation and *O*-GlcNAcylation points to some very interesting possibilities as to how one might be able to alter this balance using chemical tools. Since there is a connection between tau being present in a hyperphosphorylated state and its aggregation into pathological tangles,[96] then perhaps by decreasing tau phosphorylation we may be able to decrease the rate of formation of neurofibrillary tangles. One way in which this might be achieved is by inhibition of *O*-GlcNAcase. By blocking the

action of *O*-GlcNAcase, we could increase *O*-GlcNAc on tau and this might prevent tau hyperphosphorylation and the formation of neurofibrillary tangles (Figure 1.16).

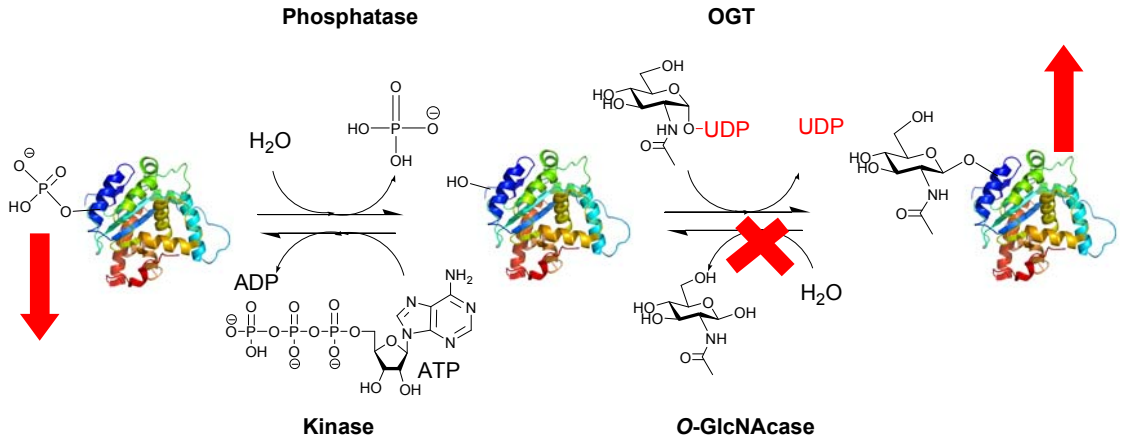

Figure 1.16 Increasing *O*-GlcNAc modification and decreasing phosphorylation on cellular proteins may be accomplished using an *O*-GlcNAcase inhibitor.
Blocking the action of *O*-GlcNAcase with a selective and potent inhibitor that is also cell permeable, would increase the levels of *O*-GlcNAc modification of proteins *in vivo*. Because several of the sites that are *O*-GlcNAc modified appear to be reciprocally phosphorylated, increasing the levels of *O*-GlcNAc modification could decrease levels of phosphorylation. This may be an effective method to block hyperphosphorylation of tau *in vivo*, thereby providing a potential therapeutic approach for preventing neurofibrillary tangles.

We aimed to test some hypotheses discussed above by first designing an inhibitor that is cell permeable, selective, potent, and able to enter into the brain *in vivo*. The role that I played in this endeavour was to synthesize several compounds that could be used to investigate these ideas. This was ultimately achieved by creating a panel of rationally designed inhibitors based on previous studies carried out by our group on the catalytic mechanism of *O*-GlcNAcase. The process of inhibitor design and the principles used will be discussed in detail in Chapter 2 of this thesis.

1.5 Aims and goals: Research relating to *O*-GlcNAcase and the *O*-GlcNAc modification.

In light of the information presented thus far, it is evident that there is reason for enthusiasm for research relating to the *O*-GlcNAc modification. On a personal note, when I began research in the Vocadlo laboratory I was extremely interested in contributing to this pool of growing knowledge, specifically in uncovering the potential role of *O*-GlcNAc in Alzheimer disease. It is evident, however, both from experience as a graduate student as well as from the vast body of research reported, that both directed research, with the aims of accomplishing specific goals, balanced with an open and mindful curiosity to what one might find along the way, is conducive to successful science. In keeping with this line of thinking some interesting and unexpected results were met. The details of each aim that will be discussed in each chapter are outlined here:

1) **Synthesis of inhibitors of *O*-GlcNAcase – Chapter 2.**
2) **Testing of inhibitors of *O*-GlcNAcase – Chapter 2.**
3) **Synthesis of 2-acetamido-2-deoxy-5-thio-D-glucopyranose (5SGlcNAc), a structural variant of GlcNAc: a possible inhibitor of OGT (in a UDP-donor form). - Chapter 3.**
4) **Synthesis of glycosides of 2-acetamido-2-deoxy-5-thio-β-D-glucopyranosides as substrates and probes for *O*-GlcNAcase. - Chapter 3**

It is evident from this summarized list of aims, that our overall interests for this thesis are to; a) create new, rationally designed, highly selective and potent inhibitors of *O*-GlcNAcase as potential tools for scientific research and to investigate the role of *O*-GlcNAc in diseases that have been proposed to be involved with the dysfunction of the *O*-GlcNAc modification and b) to investigate the scope of what kind of substrates might be processed by *O*-GlcNAcase.

Chapter 2: Synthesis and testing of inhibitors of *O*-GlcNAcase.

2.1 Rational inhibitor design: basic principles.

The synthesis of enzyme inhibitors that have *in vivo* efficacy is challenging. Several parameters must be considered when designing such inhibitors including; selectivity for the target enzyme, potency, solubility, pharmacokinetics, and the ability of the compound to cross cellular membranes to reach intracellular targets. Of these parameters, effective binding to the target is of foremost importance and is often optimized early on. When possible, careful analysis of the target's active site is beneficial in the design of potent inhibitors.[99-103] It is important that the size, shape, and polarizability of the inhibitor are appropriately matched to the amino acid residues present in the targeted active site.[104] Harnessing favourable polar, ionic, hydrogen bonding or hydrophobic interactions can greatly increase the strength of binding of an inhibitor.[51,105,106]

One way to obtain leads to enzyme inhibitors is to consider the properties of the natural substrate.[107,108] If a substrate can bind well to the active site of its target, then a compound having a similar structure may also bind well. Complicating such an approach to inhibitors, however, is that some enzymes need to alter their conformation to bind their substrate effectively or bind the substrate in a conformation that is uncommon in solution.[109-112] Furthermore it is known that intermediates and transition state structures found along the reaction

coordinate bind most tightly to the active site.[47,48,51,113] This last point highlights the importance of gaining an understanding of the catalytic mechanism of the target enzyme, including transition state and/or intermediates formed during the catalytic cycle. Since transition state and intermediate structures tend to bind well, trying to emulate these structures is often fruitful for designing potent inhibitors.[114-117]

A second parameter that is important is inhibitor selectivity.[40,107,117] When designing an inhibitor for a target enzyme that might be useful as a research tool it is important to have an understanding of functionally related enzymes. Off target effects arising from either inhibition of functionally related enzymes, or entirely different proteins, can lead to detrimental effects in cells or animal models.[118] An example of this comes from a consideration of the lysosomal β-hexosaminidases, which are functionally related to *O*-GlcNAcase in that they also cleave terminal β-linked *N*-acetylglucosamine residues off from glycoconjugates.[40] Inhibition of these two β-hexosaminidases has the potential to lead to serious problems since their dysfunction is known to lead to congenital disorders known as Tay Sachs and Sandhoff's diseases.[119] In these disorders a series of glycosylated lipids known as gangliosides accumulate within neurons, leading to a host of complications and eventual death.

These two considerations, amongst others including pharmacokinetics, solubility, and cellular permeability are important considerations when designing enzyme inhibitors, and collectively play a role in an approach to creating inhibitors known as "rational design".

2.2 Rational design of inhibitors for *O*-GlcNAcase.

When designing inhibitors for *O*-GlcNAcase, key amino acid residues present within the active site were considered. A series of analogues were designed having different substituents, but key structural features were retained in all compounds. These common features were directly inspired by a lead compound synthesized previously, which we were using as a starting point to generate inhibitors with improved potency for *O*-GlcNAcase and selectivity over the two functionally related lysosomal hexosaminidases, discussed previously in Section 2.1. This lead molecule, 1,2-dideoxy-2'-propyl-α-D-glucopyranoso[2,1-*d*]-Δ2'-thiazoline, was synthesized previously by Garrett Whitworth in our laboratory,[40] and is often abbreviated as 'NButGT' (Figure 2.1).

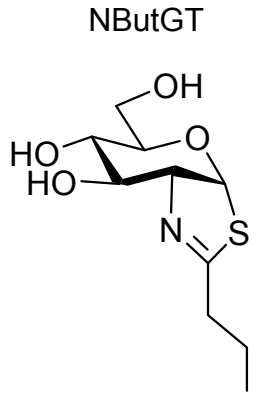

Figure 2.1 Structure of NButGT.

NButGT has a K_i value of 600 nM (K_i is defined as the inhibitor concentration required to inhibit half of all enzyme activity in solution) and a selectivity of 700-fold for *O*-GlcNAcase over the functionally related lysosomal β-hexosaminidases. This was an encouraging lead compound, but there was room for improvement.[117] Our approach to improving upon this compound was to

consider which parts of NButGT made it an effective inhibitor and which parts could be altered to improve its potency and selectivity. To gain an appreciation for which parts of NButGT were key to inhibition of *O*-GlcNAcase, a brief history of the development of NButGT and other *O*-GlcNAcase inhibitors will be described in the following section.

2.3 The history leading to the development of NButGT.

Historically, the two main compounds used as inhibitors of *O*-GlcNAcase were 2-deoxy-2({[methyl(nitroso)amino]carbonyl}amino)-β-D-glucopyranose (streptozotocin) and *O*-(2-acetamido-2-deoxy-D-glucopyranosylidene)amino-*N*-phenylcarbamate (PUGNAc) (Figure 2.2).[16,17,120-122] These two inhibitors were effective in blocking the action of *O*-GlcNAcase, however were not ideal for use in cells or *in vivo* due to off-target effects.

PUGNAc

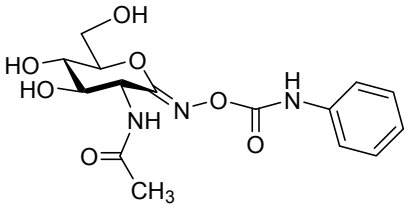

Streptozotocin

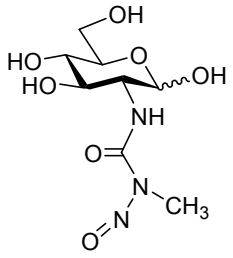

Figure 2.2 Structures of PUGNAc and streptozotocin.

Streptozotocin is able to inhibit *O*-GlcNAcase, but is not a potent inhibitor of this enzyme (K_i = 2 mM).[121] Additionally, it is observed to have cytotoxic effects in cells[123] through alkylation of DNA and the production of radical species.[123,124] These cytotoxic effects lead to cell death, and therefore make streptozotocin

inappropriate for cellular experiments to study the effects of *O*-GlcNAcase inhibition.[125] PUGNAc is a potent inhibitor of human *O*-GlcNAcase (K_i = 52 nM),[16] but is also a potent inhibitor of the human lysosomal β-hexosaminidases (K_i = 52 nM).[40] Because PUGNAc inhibits all of these enzymes, it is not ideal for cellular or *in vivo* experiments to study the effects of selectively inhibiting *O*-GlcNAcase. Therefore, development of potent and selective inhibitor of *O*-GlcNAcase was needed, as it would be a valuable research tool to study the dynamics of the *O*-GlcNAc modification in cells or animal models.

Understanding the mechanism of *O*-GlcNAcase was expected to be useful for the development of a selective inhibitor. Macauley, Whitworth, and co-workers sought to study its mechanism by conducting several in depth enzyme kinetic studies and then using this information to generate a small library of inhibitors that were cell permeable, potent, and selective for *O*-GlcNAcase.[40] As a first step, three alternative catalytic mechanisms were considered for *O*-GlcNAcase. These included a single step inverting mechanism, a double displacement retaining mechanism, and a double displacement retaining mechanism involving substrate-assisted catalysis (see Figures 1.5, 1.6, 1.7 for an overview of these mechanisms). A key difference between these mechanisms is the involvement of the 2-acetamido group of the substrate; only in the substrate- assisted catalytic mechanism does it play an active role. In order to address the possible involvement of this group, several substrate analogues were synthesized, each bearing differing levels of fluorine substitution on the N-acetyl group. The added fluorine atoms on the N-acetyl group decrease the basicity of the amide oxygen.

Decreasing the nucleophilicity in this way was predicted to decrease the rate of catalysis if *O*-GlcNAcase does use a substrate-assisted mechanism (Figure 2.3).[40]

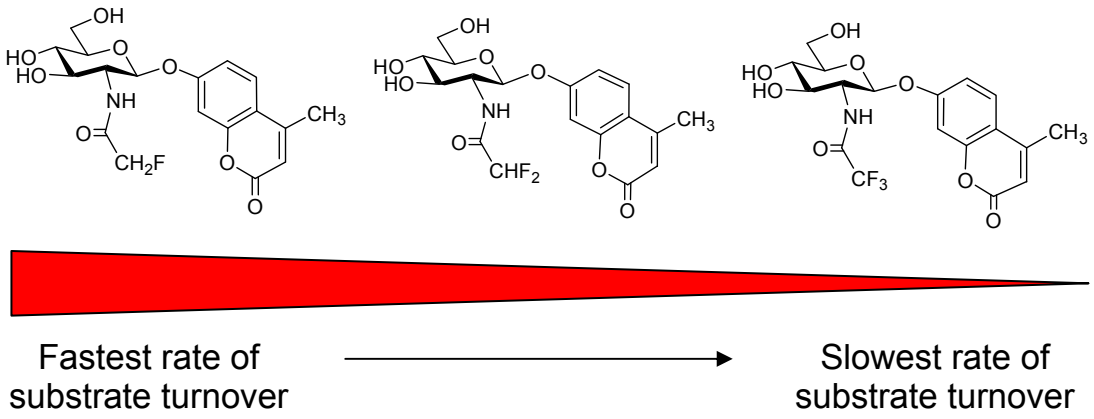

Figure 2.3 Three fluoro-analogues of GlcNAc and their predicted rates of processing by *O*-GlcNAcase.
The rates of catalysis were measured as a function of fluorescence generated by the *O*-GlcNAcase-catalyzed liberation of the 4-methylumbulliferyl leaving group of the substrates.

Though the human lysosomal β-hexosaminidases are in a different CAZy family, and are unrelated to *O*-GlcNAcase they were already known to use substrate-assisted catalysis.[40] These compounds were therefore tested with one of these human hexosaminidase enzymes to validate the approach. As predicted, when the number of fluorines was increased, a decrease in second order rate constant was observed with this enzyme. A similar pattern was also seen with *O*-GlcNAcase. Through this experiment, as well as further kinetic studies, that will not be discussed in detail here, it was concluded that *O*-GlcNAcase, in common

with lysosomal β-hexosaminidase, uses a substrate assisted catalytic mechanism.[40]

A further experiment to test this conclusion was performed. 1,2-deoxy-2'-methyl-α-D-glucopyranoso-[2,1-*d*]-Δ2'-thiazoline (NAG-thiazoline) (Figure 2.4) was previously designed to mimic the putative bicyclic oxazoline intermediate (Figure 2.4) formed in the course of the substrate-assisted catalytic mechanism for a plant hexosaminidase. This compound was tested with human *O*-GlcNAcase with the expectation being that it would inhibit the enzyme.

NAG-thiazoline

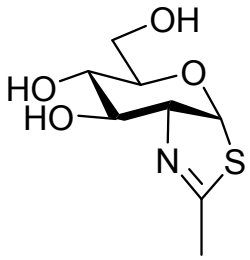

oxazoline intermediate

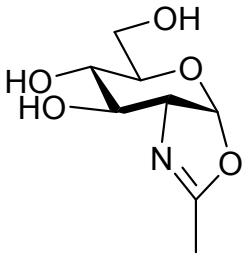

Figure 2.4 Structure of NAG-thiazoline (left) contrasted with the structure of the oxazoline intermediate (right).

It was discovered that this compound was a potent inhibitor of *O*-GlcNAcase (K_i = 180 nM),[40] binding 21,000 fold more tightly than the parent saccharide. It was hypothesized that this tight binding may be attributed to it mimicking a transition state structure resembling the oxazoline intermediate.[40] These studies collectively led to the clear conclusion that *O*-GlcNAcase hydrolyzes *O*-GlcNAc from proteins using a substrate-assisted catalytic mechanism.

Several observations from these studies, as well as ones involving streptozotocin, led to the development of the first class of selective inhibitors of *O*-GlcNAcase by Whitworth, Macauley, and coworkers.[40] One observation was that the structure of a human lysosomal β-hexosaminidase reveals a snug pocket that tightly accommodates the methyl substituent of the acetamido group of GlcNAc.[126] Additionally, streptozotocin, which has a sterically bulky *N*-acyl group, shows some weak 10-fold preference for *O*-GlcNAcase over β-hexosaminidase.[40,127] It was hypothesized in the Vocadlo group that this bulky group impaired the bonding of streptozotocin to the lysosomal β-hexosaminidase. These observations aided the development of seven inhibitors where the 2'-position of the thiazoline ring was elaborated with alkyl chains of differing lengths, starting with a methyl group and progressing to a hexyl chain (Figure 2.5). It was predicted that the differing chain lengths of these compounds would confer selectivity for *O*-GlcNAcase over the lysosomal β-hexosaminidases. As predicted, the findings from the studies involving these compounds revealed that increasing the chain length of each compound resulted in a decrease in potency for β-hexosaminidase. An addition of even one methylene unit to the alkyl chain attached to the thiazoline ring resulted in a 460-fold increase in the K_i value of the inhibitor for β-hexosaminidase. Furthermore, it was found that an increase in chain length in the inhibitors was much better tolerated by *O*-GlcNAcase (Figure 2.5) and these inhibitors were consequently highly selective for *O*-GlcNAcase over β-hexosaminidase, suggesting that *O*-GlcNAcase has significant space in the region surrounding the 2-acetamido group of substrates.[40]

Whitworth, Macauley, and associates made significant achievements in discovering the mechanism for *O*-GlcNAcase. These mechanistic studies enabled the generation of inhibitors of *O*-GlcNAcase; some with significant potency and excellent selectivity compared to the previously available inhibitors, PUGNAc and streptozotocin.

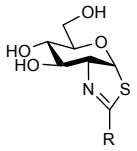

R group	*O*-GlcNAcase K_i (μM)	β-hexosaminidase K_i /*O*-GlcNAcase K_i
—CH_3	0.07	0.070
—CH_2CH_3	0.12	32
—$(CH_2)_2CH_3$	0.23	340
—$(CH_2)_3CH_3$	1.5	4,600
—$(CH_2)_4CH_3$	57	11,000
—$CH(CH_3)_2$	1.6	720
—$CH_2CH(CH_3)_2$	5.7	4,000

Figure 2.5 Data showing the inhibition of *O*-GlcNAcase by thiazoline analogues synthesized by Whitworth *et al.* and their selectivity for *O*-GlcNAcase over β-hexosaminidase (pH 6.5).[40]
It is clear that longer 'R' group chain lengths are better tolerated by *O*-GlcNAcase than the β-hexosaminidases.[40]

2.4 Design of new thiazoline analogue inhibitors of *O*-GlcNAcase.

It is clear, based on the studies performed by Macauley and Whitworth, that the thiazoline moiety which confers mimicry of the transition state (resembling the putative oxazoline intermediate) is key to the potency of the inhibitors.[40] It was also clear that the selectivity of NButGT for *O*-GlcNAcase over the functionally related lysosomal β-hexosaminidase enzymes was due to the presence of an alkyl chain attached to the thiazoline ring. Therefore, it was

reasoned that retaining such bulky groups on the 2'-position of the thiazoline ring would be important for retaining selectivity.

We aimed to synthesize analogues that possessed different substituents attached to the 2'-position of the thiazoline ring moiety and investigate the ability of these analogues to inhibit *O*-GlcNAcase. On the basis of detailed mechanistic studies by Cetinbas and co-workers in the Vocadlo laboratory that revealed key residues in the active site interacting with the substrate, it was predicted that having an electron-donating group, such as an amine directly attached to the thiazoline ring of the new analogues would increase binding affinity. The basis for this hypothesis was that Asp[174] of human *O*-GlcNAcase was found to be important in catalysis; it is proposed to interact with the amide group of the substrate, and act as a general base having a pKa of ~5.[41,128] This low pKa indicated that this carboxyl residue would be negatively charged at physiological pH. The pKa of the thiazoline ring of NButGT itself was also quite low, pKa = 5.5, therefore this inhibitor would not be protonated at physiological pH and no favourable interaction between the endocyclic nitrogen of the inhibitor and enzyme carboxylate would take place.[117] The proposals regarding the position and function of this residue were later supported by the structure acquired by collaborators Rebecca Dennis and Prof. Gideon Davies at the University of York, (see Figure 2.6 of a bacterial homologue of *O*-GlcNAcase from *B. thetaoiotaomicron* (*Bt*GH84)).[129] By generating a 2'-aminothiazoline ring, the pK_a of the endocyclic nitrogen was predicted to increase, in keeping with the aminooxazoline ring of allosamizoline,[130] making it likely this compound would be

protonated under physiological conditions. It was expected that protonation of this group would introduce a hydrogen bonding or ionic interaction with Asp242 not possible with NButGT, thereby increasing its affinity for *O*-GlcNAcase. Such an interaction would be reminiscent of the interaction of the basic protonated aminooxazoline ring of allosamizoline observed in complex with a plant chitinase (Figure 2.6).[130] Selectivity for *O*-GlcNAcase over the lysosomal β-hexosaminidases could be retained by maintaining an alkyl chain at the 2'-position of the thiazoline ring (Figure 2.6). A variety of different substituents could also be attached to the thiazoline ring. This would provide more information as to what might make an effective inhibitor of *O*-GlcNAcase by defining the space of *O*-GlcNAcase's active site and capturing possible adventitious interactions.

NButGT with key residues *Bt*GH84 *O*-GlcNAcase[117]

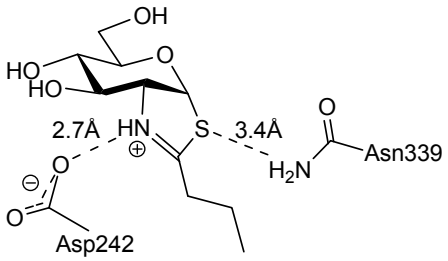

allosamizoline with plant chitinase[130]

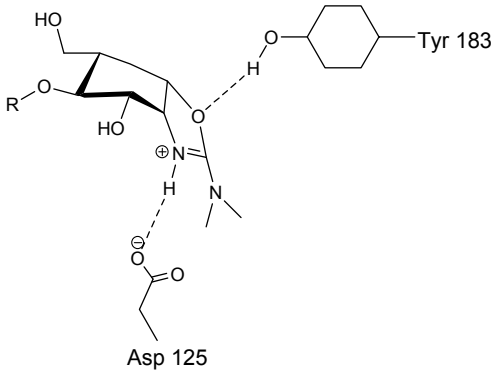

Figure 2.6 Interactions between NButGT (left) with key residues of *Bt*GH84 *O*-GlcNAcase contrasted with allosamizoline with plant chitinase (right).

Results and Discussion

2.5 Synthesis of Second Generation Inhibitors of *O*-GlcNAcase: An Overview of Synthetic Methods.

The synthesis of the new inhibitors for *O*-GlcNAcase synthesized here can be divided into two main groups: an aminothiazoline series (those inhibitors that possess a 2'-amino group on the thiazoline ring) and an alkylthiazoline series (those that possess 2'-alkyl, substituted alkyl, or aryl substituents on the thiazoline ring). The synthesis of thiazolines on carbohydrate scaffolds is well established and several literature procedures were helpful in the synthesis of these analogues.[40,131-133] There were two general synthetic routes used to make these analogues of NButGT, which are summarized in Schemes 2.1 and 2.2. These compounds were accessed using well established chemistry[40,131,134]in either three or four step routes. One route involved the acylation of commercially available amine **1**. The second route involved reaction of a well known isothiocyanate intermediate[135] with various amines.[131,136] The subsequent steps, including the conversion of amides to thioamides[134] and cyclization of thioamides and thioureas to thiazolines, have been reported for related carbohydrate scaffolds. The deprotection conditions used are general methods used reliably for carbohydrates.[40,134] For more detailed procedures, refer to the methods found in Section 2.9.

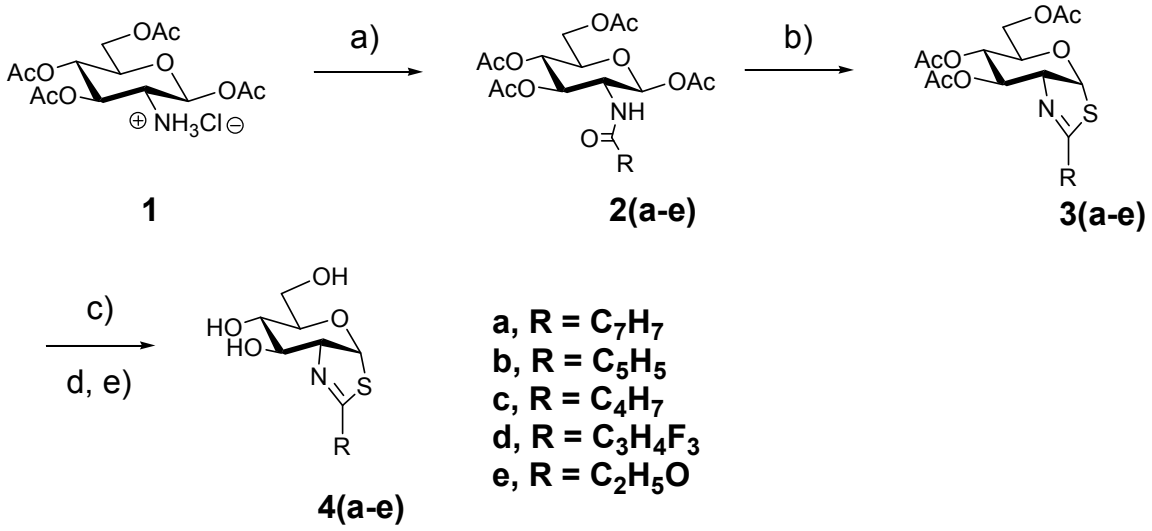

Scheme 2.1 Overview of the synthesis of (4a-e).

a) 1 (1 eq.) desired carboxylic acid (1.2 eq.) and EDC or DCC (2.5 eq.) or acid chloride (1.2 eq.). Plus Et_3N (2 eq.) in DCM or DMF, r.t.; b) 2a-e (1 eq.), Lawesson's reagent (0.6 eq.), toluene, 80-85°C; c) 3a-e, K_2CO_3 (cat.) d) MeOH, r.t. e) AcOH, MeOH.

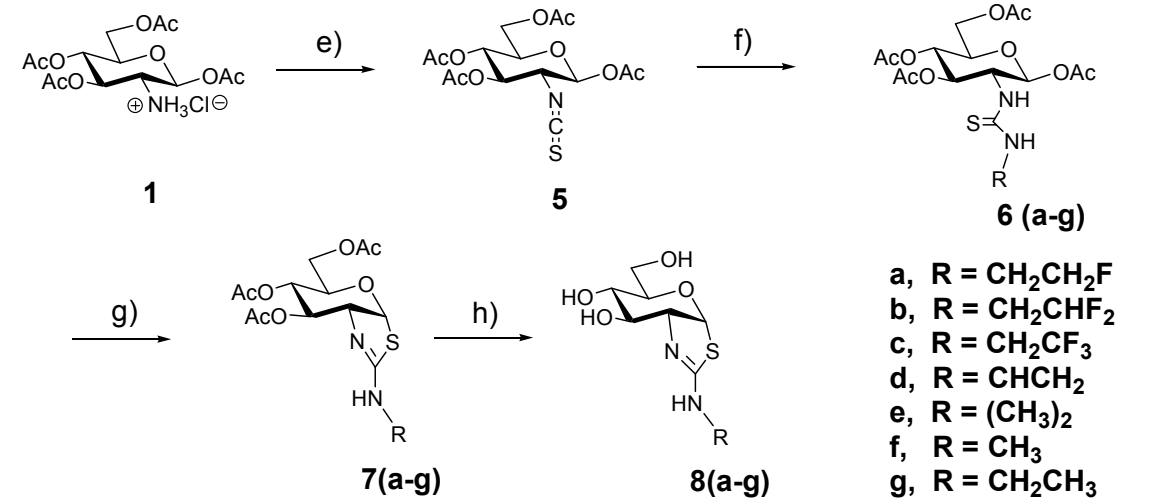

Scheme 2.2 Overview of methods for the synthesis of 8a-g.

e) 1 (1 eq.), thiophosgene (2 eq.), $CaCO_3$ (3 eq.), DCM, H_2O, r.t.; f) 5 (1 eq.), amine or HCl·amine of the desired 'R' substituent (1.2 eq.), Et_3N (1.2 eq.), acetonitrile, r.t.; g) 6a-g (1 eq.), Lewis acid (either $SnCl_4$ (4 eq.) or trifluoroacetic acid (7.5 eq.)), DCM, r.t.; h) 7a-g, K_2CO_3 (cat.), r.t..

2.6 Discussion of synthetic methods.

Coupling reactions between 1,3,4,6-tetra-*O*-acetyl-2-amino-2-deoxy-β-D-glucopyranose hydrochloride and various carboxylates were carried out using EDC or DCC to introduce the desired groups and generate various alkyl thiazolines having different 2'-substituents. These coupling reactions were relatively straightforward. The main issue encountered at this step was isolating the desired compounds during the work-up procedure, as most of these compounds were partially soluble in water. Back extracting each aqueous layer with DCM was required to ensure the synthesized compounds were effectively recovered from aqueous layers. Separation of the desired products from excess reagents and minor side products was generally simple, but sometimes separation by flash silica column chromatography was challenging due to poor separations. In such cases more than one chromatography step was needed for complete product recovery.

Generation of thioamide intermediates and subsequent cyclization[40,134] to form thiazolines **3a-e** required, for best yields, that the reactions be kept dry and maintained under an atmosphere of N_2. Heating the reaction to 80-85°C was imperative to drive the reaction forward and also aided the dissolution of the Lawesson's reagent in the toluene.[134] It was most common for the thiazoline products to have a higher R_f value than the starting material on TLC (ethyl acetate:hexanes 1:1), but sometimes the differences in polarity were only slight, making purification by silica column chromatography difficult. It was found to be important, to obtain reasonable yields (50% or higher), that the product was

isolated immediately following concentration of the reaction mixture under high vacuum. Yields for formation of thiazolines **3a-e** were rarely high and were typically around 50%. This relatively low yield may be due to the number of side products that often formed as judged by TLC analysis.

For the synthesis of 2'-aminothiazoline inhibitors formed from the known isothiocyanate **5** (Scheme 2.2),[137] care was required in handling the highly reactive isothiocyanate. It was important that the coupling reaction to form thioureas **6a-g**, was kept dry to avoid the possibility of water reacting with the isothiocyanate. The work up procedure used to obtain thioureas **6a-g** generally required back extraction of all aqueous layers to obtain good yields.

For cyclization of thioureas **6a-g** to form thiazolines **7a-g**, an acid catalyst was dissolved with the compounds in a solution of DCM under an atmosphere of N_2. When using $SnCl_4$,[131] it was imperative that the reaction was dry, since moisture was found to lead to degradation of thiazoline products, most likely due to the formation of HCl. Thiazoline compounds can be sensitive to Brønstead acids, especially in aqueous conditions due to the acid lability of the thiazoline ring. Once the cyclization reaction was complete as judged by TLC analysis (15 h), reactions were treated with a solution of saturated $NaHCO_3$ until the evolution of CO_2 ceased and the pH of the solution was between 7 and 8. Quenching of $SnCl_4$ was a crucial step, since when too little saturated $NaHCO_3$ was added to the crude mixture, degradation of the thiazoline products **7a-g** occurred after the work-up procedure. It was later found that using TFA (7.5 eq.) instead of $SnCl_4$ was advantageous for cyclizing thiourea compounds **6a-g** to thiazolines **7a-g**.

Using this work up procedure, the product contained less impurities and there was the added advantage of not having to deal with tin waste. The use of TFA was only used in two cyclization procedures, but its future use for creating 2'-aminothiazoline analogues is highly recommended.

The deprotection of analogues **4a-e** and **8a-g** in methanol was completed by addition of a catalytic amount of either K_2CO_3[107] or NaOMe.[40,134] Both methods worked well, however, one advantage of using K_2CO_3 (cat.) was that the reaction could simply be filtered and concentrated directly, whereas with NaOMe it was important that the reaction was neutralized with a dilute solution of acetic acid in methanol.[134] Because these final compounds were sometimes heat sensitive, it was advantageous to concentrate the reactions under high vacuum without heating.

2.7 K_i values for synthesized inhibitors.

K_i values for *O*-GlcNAcase were measured by Dixon plot analysis (see the appendix for details). Either 4-methylumbelliferyl 2-acetamido-2-deoxy-β-D-glucopyranoside or 4-nitrophenyl 2-acetamido-2-deoxy-β-D-glucopyranoside was used as a substrate for *O*-GlcNAcase. Assays were carried out at 37°C at pH 7.4 using fluorescence or absorbance, respectively (see methods section(s) 2.12 and 2.13 for further details).

There were two families of inhibitors synthesized containing different groups attached to the thiazoline ring. It is clear that the potency of these two families against *O*-GlcNAcase vary greatly (Figure 2.7).

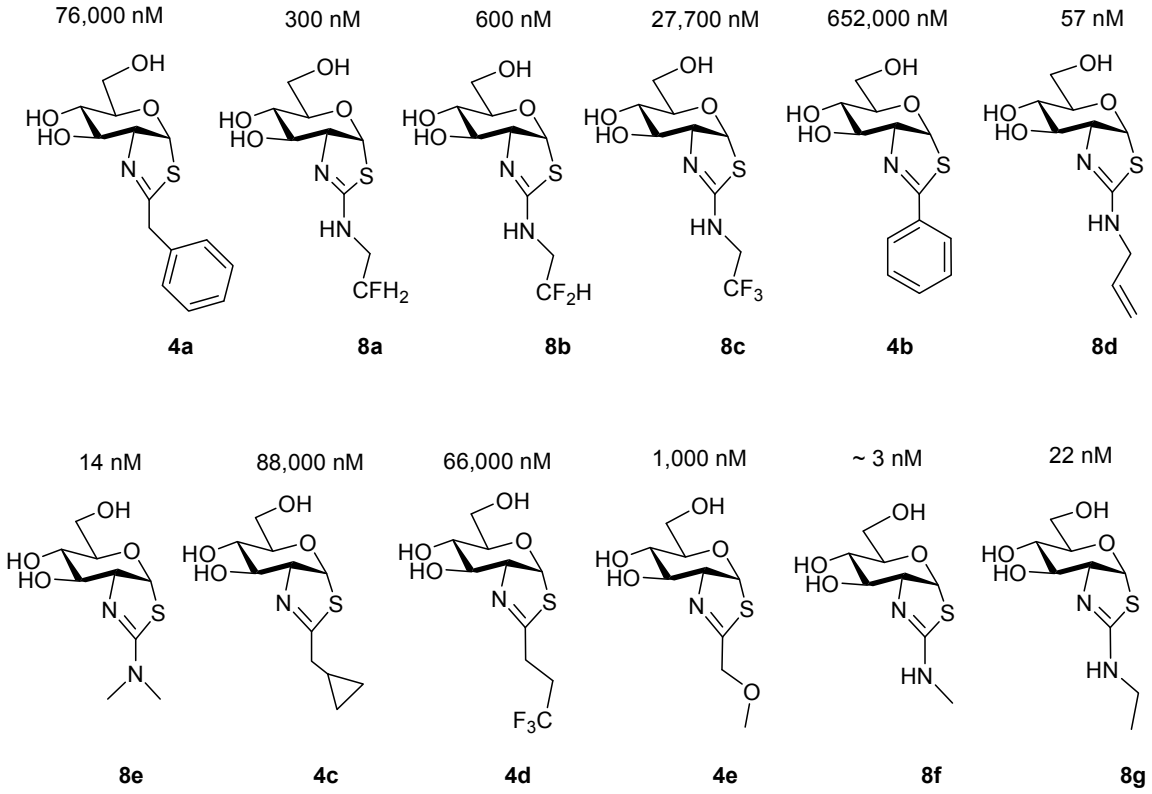

Figure 2.7 Twelve inhibitors synthesized and their respective K_i values for inhibition of *O*-GlcNAcase.

Our prediction that increasing the basicity of the thiazoline ring would improve binding affinity to *O*-GlcNAcase proved correct. Again, this is likely due to the exocyclic nitrogen donating electron density into the thiazoline ring, increasing the pK_a of the endocyclic nitrogen and so making it protonated under physiological conditions. This protonated exocyclic nitrogen introduces a new ionic interaction with the catalytic aspartate residue discussed earlier. To further investigate this hypothesis, some fluorinated aminothiazoline analogues were synthesized (compounds 8a 8b and 8c). It is evident that increasing the number of fluorine atoms on the aminoethyl chain correlates with an increased K_i value.

The electron withdrawing fluorine atoms limit the ability of the exocyclic nitrogen to donate electrons to the endocyclic nitrogen, thereby decreasing the pKa of the endocyclic nitrogen and making it less likely to be present in a protonated form under physiological conditions. Furthermore, it is apparent that larger 2'-substituents are less tolerated than smaller groups, and groups above a certain size bind very poorly 4a-e.

Although the K_i values for inhibitors of *O*-GlcNAcase are generally lower for those compounds containing less bulky exocyclic groups, it is important to incorporate some steric bulk attached to the thiazoline ring in order to maintain selectivity for *O*-GlcNAcase over the lysosomal β-hexosaminidases.[40] Therefore, as will be discussed in greater detail, 1,2-dideoxy-2'-aminoethyl-α-D-gluco-pyranoso[2,1-*d*]-Δ2'-thiazoline (Thiamet-G, compound **8g**) was the inhibitor that gained most attention from our laboratory, despite there being two other inhibitors (compounds **8e** and **8f**) that had lower K_i values than Thiamet-G against *O*-GlcNAcase. The lower K_i values observed for **8e** and **8f** are most probably due to their having less bulky 2'-amino substituents. However, we expected these two inhibitors to be less selective for *O*-GlcNAcase over the β-hexosaminidases because of the lesser 2'-steric bulk. Indeed, Thiamet-G was the compound that still demonstrated potent inhibition of *O*-GlcNAcase while maintaining excellent selectivity (37,000-fold) for *O*-GlcNAcase over lysosomal β-hexosaminidases based on measurements made by Garrett Whitworth.[107]

2.8 Thiamet-G shows promise as a selective *in vivo* inhibitor and is a possible lead for Alzheimer disease treatment.

We were pleased to discover the inhibitory potency of Thiamet-G toward *O*-GlcNAcase. Thiamet-G showed superior binding affinity and selectivity (K_i of 22 nM and 37,000 fold selectivity for human *O*-GlcNAcase over human lysosomal β-hexosaminidase) compared to the lead structure NButGT (K_i = 600 nM, selectivity for *O*-GlcNAcase over β-hexosaminidase enzymes is 700-fold).[40] Thiamet-G was also shown by Scott Yuzwa to cross cellular membranes as well as being bioavailable.[107]

In addition to this inhibitor being a potentially useful tool to study the effects of increased *O*-GlcNAcylation levels within cells, it also has potential as a lead to devise new therapeutics for Alzheimer disease.[107] As mentioned in Chapter 1, Alzheimer disease has been correlated with increased levels of phosphorylation of the protein tau, a microtubule associated protein present in the central nervous system. Tau has been found to be hyperphosphorylated in Alzheimer disease. This high level of phosphorylation of tau is correlated with the formation of neurofibrillary tangles in the brain, which is one of the two main disease pathologies present in Alzheimer disease. In several cases it is known that the same, or nearby sites on proteins that are *O*-GlcNAc modified can also be phosphorylated.[7,21] This is also likely true for tau, given the recent results found through studies performed by Scott Yuzwa in our laboratory as well as others.[25,27,107] As a result, it seemed plausible that increasing *O*-GlcNAcylation on tau may successfully decrease levels of phosphorylation, thereby potentially contributing to slowing Alzheimer pathology at a molecular level. Upon

discovering Thiamet-G, investigation of these possibilities was quickly undertaken by talented biochemist colleagues, Yuzwa, Macauley, and Shan, in our laboratory. Although I will not discuss the biochemical details of the investigations, I will briefly summarize some of their results.

It was of interest to investigate in detail how Thiamet-G inhibits *O*-GlcNAcase at the molecular level. Because the structure of human *O*-GlcNAcase is not available, a structure of *Bt*GH84, a bacterial homologue of *O*-GlcNAcase discussed previously, was used to investigate this issue. A crystal structure of Thiamet-G bound to *Bt*GH84 was obtained by Prof. Gideon Davies and Rebecca Dennis from the University of York.[107] The main difference between binding of Thiamet-G to *O*-GlcNAcase, compared to NButGT, was the formation of the predicted interaction between the protonated endocyclic nitrogen of the thiazoline ring and the catalytic aspartate residue (Asp242 in *Bt*GH84). The distances between the Asp242 and the endocyclic and exocyclic nitrogens of Thiamet-G are 2.7 and 2.8 Å, respectively. Figure 2.8 illustrates the interactions of *Bt*GH84 with Thiamet-G:

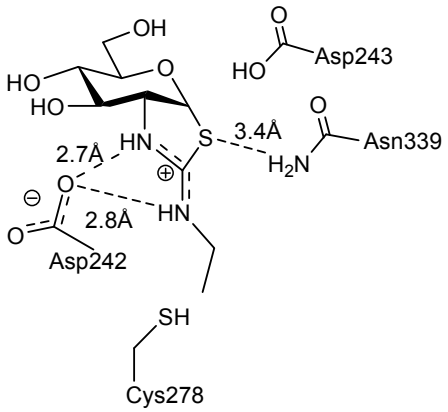

Figure 2.8 Interactions between Thiamet-G with key residues of *Bt*GH84 *O*-GlcNAcase.[107]

Members of the Vocadlo laboratory carried out experiments to investigate whether Thiamet-G could successfully increase *O*-GlcNAc levels in cells. PC-12 cells were used, as they are a well characterized neuronal cell model. It was found that Thiamet-G inhibits *O*-GlcNAcase and increases *O*-GlcNAc levels in PC-12 cells in both a dose and time dependent manner. It was also found that Thiamet-G reduces tau phosphorylation at various residues in the same cell line.[107] These findings have implications both in basic research as well as research relating to Alzheimer disease. The next big questions were whether administering Thiamet-G *in vivo* would have comparable results to those found in cells and whether Thiamet-G was capable of crossing the blood brain barrier within animals. In order to address these questions, Thiamet-G was administered intravenously at four different doses to Sprague Dawley rats (rats that are bred specifically for scientific research purposes). It was found that Thiamet-G is capable of crossing the blood brain barrier to increase brain *O*-GlcNAc levels in a dose dependent manner.[107] It was also found that *in vivo* administration of

Thiamet-G reduces tau phosphorylation in all areas in the brains of treated rats.[107] In the future Thiamet-G could be a valuable lead for generating potential therapeutics for Alzheimer disease as well as being a valuable stepping-stone to new discoveries. Currently, long term studies are underway in our laboratory to investigate the effect of Thiamet-G on tau pathology in animal models that show tau hyperphosphorylation and aggregation to form neurofibrillary tangles.

2.9 Methods

Several analogues (compounds **4a-e, 8a-g**) were prepared using common synthetic methods. Section 2.9.1 describes the general methods used to synthesize the 2'-alkylthiazoline series (Scheme 2.1) and 2'-aminothiazoline series of inhibitors (Scheme 2.2). The yields and methods used to prepare each analogue are summarized in Figure 2.9.

2.9.1 Preparation of amides (2a-e) from compound (1).

Two methods were used to prepare amides **2a-e**. The first method involved the use of *N,N*'-dicyclohexylcarbodiimide (DCC) or *N*-(3-dimethylaminopropyl)-*N'*-ethylcarbodiimide (EDC) (2.5 eq.) to couple the desired carboxylic acid (1.2 eq.) along with amine **1** (1eq.). These reagents were suspended together in dimethylformamide (DMF) and upon addition of triethylamine (2 eq.) a homogeneous solution was obtained and the reaction was then stirred overnight. Upon completion of the reaction, as judged by TLC analysis, the crude reaction mixture was extracted with ethyl acetate. The organic fraction was then washed with saturated sodium bicarbonate, and brine.

Each aqueous layer was back extracted with ethyl acetate. The combined organic layers were dried using $MgSO_4$, filtered, and concentrated under vacuum. The crude residue was subjected to flash silica column chromatography using a solvent system of ethyl acetate and hexanes, in the appropriate ratio (typically 1:1), to afford the desired amides.

The second method to prepare amides **2a-e** involved reaction of **1** (1 eq.) with the desired acid chloride (1.2 eq.) dissolved in DCM. *N,N*–diisopropylethylamine (2.2 eq.) was added to the mixture to act as a base. The reaction mixture was stirred (1.5 h), and upon completion of the reaction as judged by TLC analysis, it was diluted with DCM. The mixture was washed with saturated sodium bicarbonate, which was subsequently back extracted with DCM. The pooled organic layers were dried with $MgSO_4$, filtered, and concentrated under vacuum. The crude residue was subjected to flash silica column chromatography using a solvent system of an appropriate ratio of ethyl acetate and hexanes (typically 1:1), to obtain the desired amides.

2.9.2 Preparation of per-*O*-acetylated thiazoline analogues (3a-e) from (2a-e).

The general method used has been previously reported for related compounds, however some minor changes were made.[134] Each amide **2a-e** (1eq.) was suspended in toluene and Lawesson's reagent (0.6 eq.) was added. The reaction mixture was heated (80-85 ºC) and stirred until the reaction was complete as judged by TLC analysis (2-3 h). The crude reaction mixture was concentrated *in vacuo*. The product was immediately purified by flash silica

column chromatography using an appropriate solvent system composed of ethyl acetate and hexanes (typically 1:1).[40,134]

2.9.3 Preparation of deprotected thiazolines 4a-e.

The deprotected thiazolines were generated using procedures previously described in the literature for related compounds with minor modifications.[40,107,134]A catalytic amount of anhydrous NaOMe or K_2CO_3 was added to a solution of the protected thiazoline **3a-e**. The resulting mixture (pH 9-10) was stirred until the reaction was judged complete by TLC analysis (typically 1 h). In cases where NaOMe was used, a solution of glacial acetic acid in methanol (pH 4) was added dropwise to the reaction mixture until the solution became neutral or slightly basic (pH 7-8). For reactions using K_2CO_3, the K_2CO_3 was removed by filtration upon completion of the reaction. The solvent was removed under high vacuum at room temperature for both reaction methods. The desired products were isolated as syrups by flash silica column chromatography using a solvent system of DCM and methanol in ratios ranging from 5:1 to 10:1, as appropriate.

2.10 Aminothiazoline series: synthetic methods.

2.10.1 Preparation of isothiocyanate 5 from amine 1.

Isothiocyanate **5** was prepared as previously described with minor modifications.[137] Amine **1** (8.44 g, 22.04 mmol, 1 eq.) and calcium carbonate (6.62 g, 66.1 mmol, 3 eq.) were combined, followed by addition of DCM (14 mL) and H_2O (14 mL). Thiophosgene (3.80 g, 33.05 mmol, 1.5 eq.) was added drop

wise, followed by additional DCM (11 mL) and H_2O (11 mL). The mixture was stirred at room temperature (<1 h). The reaction mixture appeared bright yellow and separated into two immiscible layers once stirring ceased. The aqueous layer was back extracted with DCM. The combined organic layers were dried using $MgSO_4$, filtered, and concentrated to afford the crude product as a brownish yellow solid (6.87 g, 80%). ^{1}H-NMR data were consistent with the literature data for this previously known compound[137] and the material was used without further purification.

2.10.2 Preparation of thioureas 6a-g.

The preparation of thioureas **6a-g** from isothiocyanate **5** was carried out in acetonitrile as the solvent and various desired hydrochloride salts of amines or free amines (1.2 eq.). When using **5** (1 eq.) and the hydrochloride salt of the desired amine as starting materials, triethylamine was also added to the reaction mixture (1.2 eq.). Reactions were stirred at room temperature until judged complete by TLC analysis (typically under 1 hr). The organic layer was washed with aqueous saturated sodium bicarbonate and the aqueous layer was subsequently back extracted with DCM. The combined organic layers were dried with $MgSO_4$, filtered, and concentrated under vacuum. The desired products were then purified from the crude residue by flash silica column chromatography using a solvent system composed of an appropriate ratio of ethyl acetate and hexanes (typically 1:1).

2.10.3 Preparation of the per-acetylated 2'-aminothiazoline derivatives 7a-g.

Thiourea derivatives **6a-g** were cyclized to the corresponding thiazolines using the following general procedure: the thiourea derivative **6a-g** was dissolved in DCM at room temperature. Acid was added to the solution, either $SnCl_4$ (4 eq.) or trifluoroacetic acid (7.5 eq.). The generation of related aminothiazoline compounds using Lewis acid catalysis was described previously.[131] The reaction was stirred under an atmosphere of nitrogen until judged complete by TLC analysis (15 h). The reactions promoted using trifluoroacetic acid were washed twice with saturated aqueous sodium bicarbonate and the aqueous layers were back extracted three times with DCM. The combined organic fractions were dried with $MgSO_4$, filtered, and concentrated under vacuum. Reactions using $SnCl_4$ as a Lewis acid promoter were quenched with saturated sodium bicarbonate solution until the evolution of CO_2 from the reaction mixture ceased and the pH of the solution became neutral or slightly basic (pH 7-8). The resulting aqueous layer was extracted three times with DCM. The combined organic layers were dried with $MgSO_4$, filtered, and concentrated under vacuum. With both cyclization approaches the reactions were purified using flash silica column chromatography using a solvent system of an appropriate ratio of ethyl acetate and hexanes (typically 1:1).

2.10.4 Preparation of deprotected 2'-aminothiazoline analogues 8a-g.

Catalytic amounts of anhydrous K_2CO_3 were added to a solution of the appropriate 2'-aminothiazoline **7a-g**. The basic solution was stirred under an atmosphere of N_2 until the reaction was judged complete by TLC analysis

(typically 1 h). The reactions were filtered and the solvent was then removed under vacuum. The desired materials were isolated as syrups by flash silica column chromatography using a solvent system of DCM and methanol in ratios ranging from 5:1 to 10:1, as appropriate. The yields attained for each step of the analogue syntheses are summarized in Figure 2.9.

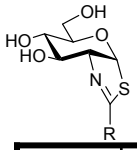

'R' group attached via:	Cyclized using:	Deprotection:
Amine **1** reacted with 2-methoxyacetyl chloride (73%)	Lawesson's Reagent (16%)	catalytic NaOMe (52%)
Amine **1** reacted with 2-cyclopropylacetyl chloride (89%)	Lawesson's Reagent (89%)	catalytic NaOMe (quantitative)
Amine **1**, benzoic acid reacted with EDC, DMAP (80%)	Lawesson's reagent (58%)	catalytic NaOMe (51%)
Amine **1**, 4,4,4-trifluorobutanoic acid reacted with EDC, DMAP (80%)	Lawesson's reagent (39%)	catalytic NaOMe (51%)
Amine **1** reacted with 2-phenylacetic acid, EDC, DMAP (80%)	Lawesson's reagent (60%)	catalytic K_2CO_3 (46%)
Amine **1** reacted with isothiocyanatoethane, Et_3N (98%)	Tin (IV) Chloride (90%)	catalytic K_2CO_3 (quantitative)
Isothiocynate **5** reacted methylanamine hydrochloride, Et_3N (62%)	Tin (IV) Chloride (76%)	catalytic K_2CO_3 (64%)
Isothiocynate **5** reacted with 2-fluoroethylamine, Et_3N (62%)	Tin (IV) Chloride (44%)	catalytic K_2CO_3 (90%)
Isothiocynate **5** reacted with 2,2-difluoroethylamine, Et_3N (56%)	Tin (IV) Chloride (75%)	catalytic K_2CO_3 (74%)
Isothiocynate **5** reacted, 2,2,2-trifluoroethylamine, Et_3N (70%)	Tin (IV) Chloride (65%)	catalytic K_2CO_3 (47%)
Isothiocynate **5** reacted With dimethylamine-hydrochloride, Et_3N (91%)	Trifluoroacetic acid (42%)	catalytic K_2CO_3 (75%)
Amine **1** reacted with 3-isothiocyanatoprop-1-ene, Et_3N (81%)	Trifluoroacetic acid (90%)	catalytic K_2CO_3 (18%)

Figure 2.9 Summary of synthetic methods and yields for twelve inhibitors of *O*-GlcNAcase.
Methods and yields are shown for each step used to prepare the different inhibitors. The general scaffold common to each analogue is illustrated at the top left of the table and the varying 'R' group functionalities are illustrated in the first column.

2.11 Synthesized second generation inhibitors for *O*-GlcNAcase: NMR and elemental data.

The following data includes the structures and NMR data for the complete series of second generation inhibitors for *O*-GlcNAcase, as well as their synthetic intermediates, synthesized using the general procedures described in section 2.6.

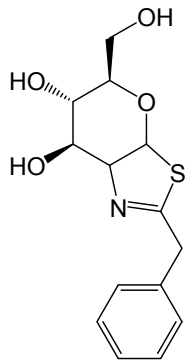

4a

(2a) 1,3,4,6-Tetra-*O*-acetyl-2-[(2-phenylacetyl)amino]-2-deoxy-β-D-gluco pyranose

^{1}H-NMR (500 MHz, $CDCl_3$) δ (ppm) 7.33 (m, 2H), 7.27 (m, 1H), 7.21 (apparent triplet, J = 7.1 Hz, 2H), 5.65 (apparent triplet, *J* = 8.9 Hz, 2H), 5.10 (m, 2H), 4.23 (m, 2H), 4.10 (dd, *J* = 12.5, 2.1 Hz, 1H), 3.78 (m, 1H), 3.47 (s, 2H), 2.07 (s, 3H), 2.00 (s, 3H), 1.99 (s, 3H), 1.90 (s, 3H); ^{13}C-NMR (125 MHz, $CDCl_3$) δ (ppm) 171.30, 171.12, 170.89, 169.56, 169.48, 134.60, 129.28, 129.26, 127.72, 92.57, 73.13, 72.32, 67.97, 61.85, 53.21, 44.19, 20.96, 20.95, 20.79, 20.71.

(3a) 3,4,6-Tri-*O*-acetyl-1,2-dideoxy-2'-phenylmethyl-α-D-glucopyranoso[2,1-d]-Δ 2'-thiazoline

^{1}H-NMR (500 MHz, $CDCl_3$) δ (ppm) 7.23 (m, 5H), 6.16 (d, *J* = 7.1 Hz, 1H), 5.60 (m, 1H), 4.92 (d, *J* = 9.4 Hz, 1H), 4.52 (m, 1H), 4.08 (m, 1H), 3.96 (m, 2H), 3.76

(dd, *J* = 14.6, 1.2 Hz, 1H), 3.37 (m, 1H), 2.12 (s, 3H), 2.09 (s, 3H), 2.01 (s, 3H); ^{13}C-NMR (125 MHz, $CDCl_3$) δ (ppm) 171.56, 170.40, 169.40, 169.20, 135.22, 128.94, 128.61, 127.30, 88.30, 76.17, 70.40, 69.03, 68.39, 63.05, 41.10, 20.87, 20.78, 20.61.

(4a) 1,2- dideoxy-2'-phenylmethyl-α-D-glucopyranoso[2,1-d]-Δ2'-thiazoline
^{1}H-NMR (500 MHz, MeOH, d_4) δ (ppm) 7.27 (m, 5H), 6.34 (d, *J* = 7.0 Hz, 1H), 4.36 (apparent triplet, *J* = 5.6 Hz, 1H), 4.15 (apparent triplet, *J* = 4.9 Hz, 1H), 3.85 (m, 1H), 3.7 (dd, *J* = 12.1, 1.3 Hz, 1H), 3.62 (m, 2H), 3.35 (m, 2H); ^{13}C-NMR (125 MHz, MeOH, d_4) δ (ppm) 174.36, 137.08, 130.21, 129.78, 128.34, 90.51, 80.09, 76.33, 74.38, 71.14, 63.31, 42.16; HRMS (*m*/*z*): $[M+H]^+$ calcd for $C_{14}H_{17}NO_4S$: 296.0957; found 296.0964.

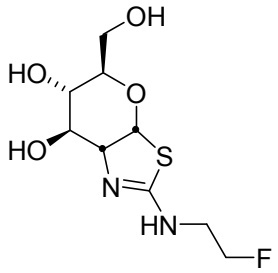

8a

(6a) 1,3,4,6-Tetra-*O*-acetyl-2-deoxy-2-[[[(2-fluoroethyl)amino] thioxomethyl]amino]-β-D-glucopyranose

^{1}H-NMR (500 MHz, $CDCl_3$) δ (ppm) 6.64 (apparent triplet, *J* = 5.4 Hz, 1H), 6.48 (d, *J* = 9.3 Hz, 1H), 5.71 (d, *J* = 8.6 Hz, 1H), 5.23 (apparent triplet, *J* = 9.7 Hz, 1H), 5.09 (apparent triplet, *J* = 9.7 Hz, 1H), 4.59 (m, 1H), 4.50 (m, 1H), 4.23 (dd, *J* = 12.5, 4.6 Hz, 1H), 4.10 (m, 1H), 3.84 (m, 2H), 2.08 (s, 3H), 2.04 (s, 3H), 2.02 (s, 3H), 2.00 (s, 3H), 1.20 (t, *J* = 7.3, 2H); ^{13}C-NMR (125 MHz, $CDCl_3$) δ (ppm)

183.87, 171.52, 170.62, 169.34, 92.68, 83.01, 82.41 (d, *J* = 166.3 Hz, 1C), 72.87, 72.48, 67.76, 61.51, 60.30, 57.37, 20.90, 20.75, 20.60, 20.57.

(7a) 3,4,6-Tri-*O*-acetyl-1,2-dideoxy-2'-[(2-fluoroethyl)amino]-α-D-gluco pyranoso[2,1-d]-Δ 2'-thiazoline

^{1}H-NMR (500 MHz, $CDCl_3$) δ (ppm) 6.21 (d, *J* = 6.5 Hz, 1H), 5.37 (apparent triplet, *J* = 3.1 Hz, 1H), 4.92 (dd, *J* = 9.5, 2.2 Hz, 1H), 4.64 (m, 1H), 4.54 (m, 1H), 4.45 (m, 1H), 4.32 (dd, *J* = 6.3, 4.1 Hz, 1H), 4.11 (m, 2H), 3.78 (m, 1H), 3.57 (m, 2H), 2.07 (s, 3H), 2.04 (s, 3H), 2.03 (s, 3H); ^{13}C-NMR (125 MHz, $CDCl_3$) δ (ppm) 170.54, 169.51, 169.39, 89.34, 82.44 (d, *J* = 165.6 Hz, 1C), 81.11, 71.62, 71.33, 68.78, 68.40, 63.07, 44.62, 20.84, 20.68, 20.62.

(8a) 1,2-dideoxy-2'-[(2-fluoroethyl)amino]-α-D-glucopyranoso[2,1-d]-Δ2'-thia zoline

^{1}H-NMR (500 MHz, MeOH, d_4) δ (ppm) 6.31 (d, *J* = 6.4 Hz, 1H), 4.56 (m, 1H), 4.46 (m, 1H), 4.06 (apparent triplet, *J* = 6.1 Hz, 1H), 3.92 (apparent triplet, *J* = 5.6 Hz, 1H), 3.78 (dd, *J* = 11.8, 2.1 Hz, 1H), 3.56 (m, 5H); ^{13}C-NMR (125 MHz, MeOH, d_4) δ (ppm) 163.19, 91.06, 91.04, 83.83 (d, *J* = 166.8Hz, 1C), 82.50, 76.34, 75.61, 71.12, 63.26; HRMS (*m*/*z*): $[M+H]^+$ calcd for $C_9H_{15}FN_2O_4S$: 267.0716 (M+H); found 267.0619.

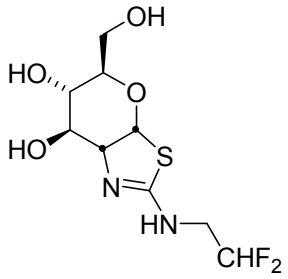

8b

(6b) 1,3,4,6-Tetra-*O*-acetyl-2-deoxy-2-[[[(2,2-difluoroethyl)amino] thioxomethyl]amino]-β-D-glucopyranose

^{1}H-NMR (500 MHz, $CDCl_3$) δ (ppm) 6.69 (m, 2H), 5.94 (t, *J* = 56.1 Hz, 1H), 5.72 (d, *J* = 8.6 Hz, 1H), 5.23 (apparent triplet, *J* =10.1 Hz,1H), 5.09 (apparent triplet, *J* = 9.6 Hz, 1H), 4.21 (m, 1H), 4.06 (m, 2H), 3.95 (m, 1H), 3.84 (m, 2H), 2.06 (s, 3H), 2.03 (s, 3H), 2.00 (s, 3H), 1.99 (s, 3H); ^{13}C-NMR (125 MHz, $CDCl_3$) δ (ppm) 184.55, 171.47, 170.81, 169.48, 113.36 (t, *J* = 241.5 Hz, 1C), 92.51, 72.82, 72.44, 67.84, 61.60, 60.38, 57.38, 20.68, 20.53, 20.52, 20.38.

(7b) 3,4,6-Tri-*O*-acetyl-1,2-dideoxy-2'-(2,2-difluoroethyl)amino-α-D-gluco pyranoso[2,1-d]-Δ 2'-thiazoline

^{1}H-NMR (500 MHz, $CDCl_3$) δ (ppm) 6.22 (d, *J* = 6.5 Hz, 1H), 6.00 (m, 1H), 5.36 (m, 1H), 5.27 (s, 1H), 4.92 (m, 1H), 4.32 (m, 1H), 4.10 (m, 2H), 3.73 (m, 2H), 3.51 (m, 1H), 2.09 (s, 3H), 2.05 (s, 3H), 2.04 (s, 3H); ^{13}C-NMR (125 MHz, $CDCl_3$) δ (ppm) 170.97, 169.88, 169.82, 159.97, 113.64 (t, J = 241.2 Hz, 1C), 90.36, 72.46, 71.62, 69.20, 68.67, 63.52, 21.18, 20.96, 20.94, 14.38.

(8b) 1,2-dideoxy-2'-(2,2-difluoroethyl)amino-α-D-glucopyranoso[2,1-d]-Δ2'-thiazoline

^{1}H-NMR (500 MHz, MeOH, d_4) δ (ppm) 6.34 (d, *J* = 6.4 Hz, 1H), 6.01 (m, 1H), 4.08 (m, 1H), 3.93 (apparent triplet, *J* = 5.4 Hz, 1H), 3.80 (dd, *J* = 11.9, 2.3 Hz, 1H), 3.56 (m, 5H); ^{13}C-NMR (125 MHz, MeOH, d_4) δ (ppm) 205.31, 161.92, 114.22 (t, *J* = 245.1 Hz, 1C), 90.09, 75.17, 74.23, 69.85, 62.07; Elemental analysis calculated: C - 38.02, H - 4.96, N - 9.85; Found: C - 37.71, H - 5.00, N - 9.48.

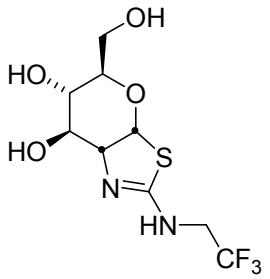

8c

(6c) 1,3,4,6-Tetra-*O*-acetyl-2-deoxy-2-[[[(2,2,2-trifluoroethyl)amino] thioxomethyl]amino]-β-D-glucopyranose

^{1}H-NMR (500 MHz, $CDCl_3$) δ (ppm) 6.74 (m, 2H), 5.73 (d, *J* = 8.5 Hz, 1H), 5.26 (apparent triplet, *J* = 9.8 Hz, 1H), 5.05 (apparent triplet, *J* = 9.6 Hz, 1H), 4.35 (m, 1H), 4.22 (m, 2H), 4.07 (m, 2H), 3.87 (m, 1H), 2.04 (s, 3H), 2.03 (s, 3H), 1.99 (s, 3H), 1.98 (s, 3H); ^{13}C-NMR (125 MHz, $CDCl_3$) δ (ppm) 184.84, 171.76, 171.63, 170.88, 169.62, 122.47 (q, *J* = 279.3 Hz, 1C) 92.44, 72.77, 72.42, 68.04, 61.66, 60.44, 57.52, 20.59, 20.52, 20.46, 20.36.

(7c) 3,4,6-Tri-*O*-acetyl-1,2-dideoxy-2'-[(2,2,2-difluoroethyl)amino]-α-D-gluco pyranoso[2,1-d]-Δ2'-thiazoline

^{1}H-NMR (500 MHz, $CDCl_3$) δ (ppm) 6.20 (d, *J* = 6.6 Hz, 1H), 5.72 (s, 1H), 5.33 (dd, *J* = 3.7, 2.3 Hz, 1H), 4.87 (d, *J* = 10.4 Hz, 1H), 4.30 (dd, *J* = 6.5, 3.8 Hz, 1H), 4.04 (m, 3H), 3.80 (m, 1H), 3.74 (m, 1H), 2.05 (s, 3H), 2.02 (s, 3H), 2.00 (s, 3H); ^{13}C-NMR (125 MHz, $CDCl_3$) δ (ppm) 170.58, 169.70, 169.40, 159.58, 124.01 (q, *J* = 279.2 Hz, 1C) 89.61, 71.51, 71.20, 68.82, 68.19, 63.10, 60.29, 20.75, 20.54, 20.50.

(8c)1,2-dideoxy-2'-[(2,2,2-difluoroethyl)amino]-α-D-glucopyranoso[2,1-d]-Δ2'-thiazoline

^{1}H-NMR (500 MHz, MeOH, d_4) δ (ppm) 6.35 (d, *J* = 6.4 Hz, 1H), 4.02 (m, 1H), 3.92 (m, 3H), 3.79 (dd, *J* = 11.9, 2.2 Hz, 1H), 3.68 (dd, *J* = 11.9, 6.1 Hz, 1H), 3.61 (m, 1H), 3.48 (dd, *J* = 9.1, 5.6 Hz, 1H); ^{13}C-NMR (125 MHz, MeOH, d_4) δ (ppm) 162.74, 126.16 (q, *J* = 277.9 Hz, 1C), 91.34, 76.59, 75.53, 71.07, 63.21, 45.13; HRMS (*m*/*z*): $[M+H]^+$ calcd for $C_9H_{13}O_4N_2SF_3$ 303.0626 (M+1); found 303.0616.

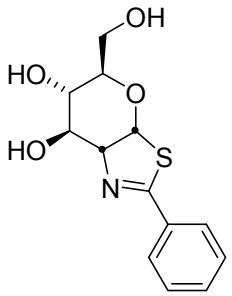

4b

(2b) 1,3,4,6-Tetra-*O*-acetyl-2-benzamido-2-deoxy-β-D-glucopyranose[138]

^{1}H-NMR (500 MHz, $CDCl_3$) δ (ppm) 7.69 (m, 2H), 7.40 (t, *J* = 7.4 Hz, 1H), 7.39 (t, *J* = 7.9 Hz, 2H), 6.52 (m, 1H), 5.80 (d, *J* = 8.8 Hz, 1H), 5.35 (apparent triplet, *J* = 10.7 Hz, 2H), 5.23 (t, *J* = 9.7 Hz, 1H), 4.60 (apparent triplet, *J* = 10.5 Hz, 1H), 4.30 (dd, *J* = 12.5, 4.8 Hz, 1H), 4.17 (dd, *J* = 12.5, 2.2 Hz, 1H), 2.11 (s, 3H), 2.07 (s, 3H), 2.07 (s, 3H), 2.00 (s, 3H); ^{13}C-NMR (125 MHz, $CDCl_3$) δ (ppm) 171.61, 170.67, 169.59, 169.26, 167.31, 133.55, 131.96, 128.70, 126.87, 92.75, 73.06, 72.72, 67.79, 61.73, 53.15, 20.84, 20.72, 20.61, 20.57.

(3b) 3,4,6-Tri-*O*-acetyl-1,2-dideoxy-2'-phenyl-α-D-glucopyranoso[2,1-d]-Δ2'-thiazoline

^{1}H-NMR (500 MHz, $CDCl_3$) δ (ppm) 7.87, (d, *J* = 7.1 Hz, 2H), 7.52 (t, *J* = 7.4 Hz, 1H), 7.46 (t, *J* = 7.8 Hz, 2H), 6.38 (d, *J* = 7.1 Hz, 1H), 5.74 (dd, *J* = 3.3, 1.6 Hz,

1H), 5.00 (d, *J* = 9.4 Hz, 1H), 4.75 (m, 1H), 4.13 (m, 2H), 3.62 (m, 1H), 2.19 (s, 3H), 2.08 (s, 3H), 2.07 (s, 3H); ^{13}C-NMR (125 MHz, $CDCl_3$) δ (ppm) 169.50, 109.59, 109.09, 102.86, 77.63, 77.56, 76.77, 67.04, 66.75, 54.08, 52.57, 48.87, 26.79, 26.72, 26.11, 25.00, 22.91.

(4b) 1,2-dideoxy-2'-phenyl-α-D-glucopyranoso[2,1-d]-Δ2'-thiazoline

^{1}H-NMR (500 MHz, MeOH, d_4) δ (ppm) 7.85 (d, *J* = 7.2 Hz, 2H), 7.51 (m, 1H), 7.45 (m, 2H), 6.49 (d, *J* = 6.9 Hz, 1H), 4.58 (dd, *J* = 6.7, 5.2 Hz, 1H), 4.26 (apparent triplet, *J* = 4.5 Hz, 1H), 3.76 (dd, *J* = 12.1, 2.5 Hz, 1H), 3.63 (m, 2H), 3.42 (m, 1H); ^{13}C-NMR (125 MHz, MeOH, d_4) δ (ppm) 169.25, 133.32, 131.57, 128.52, 128.18, 88.87, 80.21, 75.38, 73.35, 70.27, 62.27; Elemental analysis calculated: C -55.10, H - 5.37 N - 4.98; Found: C - 54.79, H - 5.65, N - 4.95.

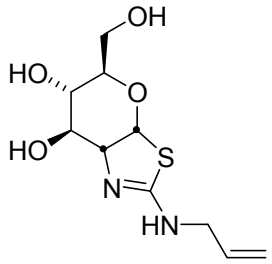

8d

(6d) 1,3,4,6-Tetra-*O*-acetyl-2-deoxy-2-[[[(2-prop-1-ene)amino]thioxomethyl] amino]-β-D-glucopyranose[139]

^{1}H-NMR (500 MHz, $CDCl_3$) δ (ppm) 6.48 (s, 2H), 5.77 (s, 1H), 5.71 (d, *J* = 8.6 Hz, 1H), 5.24 (m, 2H), 5.11 (m, 3H), 4.22 (dd, *J* = 12.5, 4.6 Hz, 1H), 4.05 (m, 2H), 3.80 (m, 1H), 2.05 (s, 3H), 2.03 (s, 3H), 2.00 (s, 3H), 1.98 (s, 3H), 1.19 (m, 1H); ^{13}C-NMR (125 MHz, $CDCl_3$) δ (ppm) 211.43, 171.85, 171.00, 169.60, 93.16, 73.21, 73.07, 68.00, 61.90, 57.94, 21.30, 21.10, 21.00, 20.85.

(7d) 3,4,6-Tri-*O*-acetyl-1,2-dideoxy-2'-[(2-prop-1-ene)amino]-α-D-gluco pyranoso[2,1-d]-Δ2'-thiazoline

^{1}H-NMR (500 MHz, $CDCl_3$) δ (ppm) 6.34 (s, 1H), 6.16 (d, *J* = 6.6 Hz, 1H), 5.81 (m, 1H), 5.31 (apparent triplet, *J* = 3.3 Hz, 1H), 5.16 (d, *J* = 17.2 Hz, 1H), 5.06 (d, *J* = 11.3 Hz, 1H), 4.83 (dd, *J* = 9.4, 2.4 Hz, 1H), 4.27 (dd, *J* = 6.0, 4.8 Hz, 1H), 4.02 (m, 2H), 3.81 (m, 3H), 2.01 (s, 3H), 1.98 (s, 3H), 1.97 (s, 3H); ^{13}C-NMR (125 MHz, $CDCl_3$) δ (ppm) 170.36, 169.38, 169.38, 159.98, 133.93, 116.06, 89.30, 72.25, 71.53, 68.88, 68.12, 62.97, 46.51, 20.71, 20.58, 20.49.

(8d)1,2-dideoxy-2'-[(2-prop-1-ene)amino]-α-D-glucopyranoso[2,1-d]-Δ2'-thiazoline

^{1}H-NMR (500 MHz, $CDCl_3$) δ (ppm) 6.31 (d, *J* = 6.4 Hz, 1H), 5.90 (m, 1H), 5.22 (m, 1H), 5.11 (m, 1H), 4.06 (apparent triplet, *J* = 4.1 Hz, 1H), 3.92 (apparent triplet, *J* = 5.6 Hz, 1H), 3.86 (m, 2H), 3.78 (dd, *J* = 11.7, 2.1 Hz, 1H), 3.63 (m, 2H), 3.47 (dd, *J* = 8.9, 5.3 Hz, 1H); ^{13}C NMR (125 MHz, MeOH, d_4) δ (ppm) 163.37, 135.89, 116.23, 90.95, 76.46, 75.57, 71.28, 63.35, 47.22; HRMS (*m*/*z*): $[M+H]^+$ calcd for $C_{10}H_{16}N_2O_4S$: 261.0909 (M+H); found 261.0909.

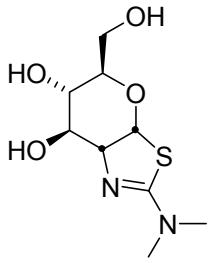

8e

(6e)1,3,4,6-Tetra-*O*-acetyl-2-deoxy-2[[(dimethylamino)thioxomethyl]amino]-β-D-glucopyranose[140]

^{1}H NMR (500 MHz, $CDCl_3$) δ (ppm) 5.77 (d, *J* = 8.4 Hz, 1H), 5.72 (d, *J* = 9.2 Hz, 1H), 5.31 (dd, *J* = 18.5, 9.4 Hz, 1H), 5.20 (m, 2H), 4.22 (dd, *J* = 12.5, 4.7 Hz, 1H), 4.10 (m, 1H), 3.81 (m, 1H), 3.17 (s, 6H), 2.08 (s, 3H), 2.06 (s, 3H), 2.02 (s, 3H), 2.00 (s, 3H); ^{13}C-NMR (125 MHz, $CDCl_3$) δ (ppm) 182.29, 171.83, 170.68, 169.94, 169.06, 93.28, 73.24, 72.99, 67.52, 61.71, 58.46, 40.63, 21.06, 20.78, 20.69, 20.53.

(7e) 3,4,6-Tri-*O*-acetyl-1,2-dideoxy-2'-dimethylamino-α-D-glucopyranoso[2,1-d]-Δ2'-thiazoline[140]

^{1}H NMR (500 MHz, $CDCl_3$) δ (ppm) 6.35 (d, *J* = 6.7 Hz, 1H), 5.32 (apparent triplet, *J* = 5.3 Hz, 1H), 4.92 (dd, *J* = 9.5, 5.1 Hz, 1H), 4.42 (apparent triplet, *J* = 6.1 Hz, 1H), 4.08 (m, 2H), 3.92 (m, 1H), 3.10 (s, 6H), 2.02 (s, 3H), 2.00 (s, 3H), 1.99 (s, 3H); ^{13}C NMR (125 MHz, $CDCl_3$) δ (ppm) 170.48, 169.89, 169.38, 87.73, 70.77, 69.76, 67.25, 65.65, 62.14, 49.83, 41.22, 20.41, 20.36, 20.35.

(8e)1,2-dideoxy-2'-dimethylamino-α-D-glucopyranoso[2,1-d]-Δ2'-thia zoline[140]

^{1}H NMR (500 MHz, MeOH, d_4) δ (ppm) 6.38 (d, *J* = 6.5 Hz, 1H), 4.07 (apparent triplet, *J* = 6.3 Hz, 1H), 3.87 (apparent triplet, *J* = 6.1 Hz, 1H), 3.81 (dd, *J* = 11.5, 1.6 Hz, 1H), 3.65 (m, 2H), 3.48 (dd, *J* = 6.0 Hz, 1H), 3.04 (s, 6H); ^{13}C NMR (125 MHz, MeOH, d_4) δ (ppm) 166.48, 91.82, 76.54, 75.78, 74.68, 70.76, 62.95, 40.40; HRMS (*m*/*z*): $[M+H]^+$ calcd for $C_9H_{16}N_2O_4S$: 249.0909 (M+H); found 249.0912.

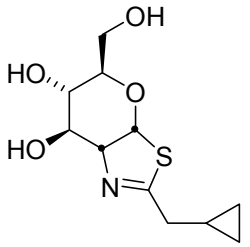

4c

(2c) 1,3,4,6-Tetra-*O*-acetyl-2-cyclopropaneacetamido-2-deoxy-β-D-gluco pyranose

^{1}H NMR (500 MHz, $CDCl_3$) δ (ppm) 6.22 (d, *J* = 9.6 Hz, 1H), 5.70 (d, *J* = 8.8 Hz, 1H), 5.21 (apparent triplet, *J* = 9.5 Hz, 1H), 5.10 (apparent triplet, *J* = 9.9 Hz, 1H), 4.09 (dd, *J* = 20.1, 10.5 Hz, 1H), 4.23 (dd, *J* = 12.5, 4.8 Hz, 1H), 4.09 (dd, *J* = 12.4, 2.1 Hz, 1H), 3.83 (m, 1H), 2.07 (s, 3H), 2.05 (s, 3H), 2.03 (d, *J* = 7.2 Hz, 2H), 2.01 (s, 3H), 2.00 (s, 3H), 0.85 (m, 1H), 0.51 (m, 2H), 0.10 (m, 2H); ^{13}C-NMR (125 MHz, $CDCl_3$) δ (ppm) 172.51, 171.00, 170.57, 169.36, 169.20, 92.46, 72.75, 72.40, 67.86, 61.67, 52.44, 41.42, 20.75, 20.61, 20.55, 20.46, 7.11, 4.42, 4.38.

(3c) 3,4,6-Tri-*O*-acetyl-1,2-dideoxy-2'-cyclopropylmethyl-α-D-glucopyranoso [2,1-d]-Δ2'-thiazoline

^{1}H NMR (500 MHz, $CDCl_3$) δ (ppm) 6.19 (d, *J* = 7.1 Hz, 1H), 5.55 (dd, *J* = 3.3, 1.6 Hz, 1H), 4.70 (d, *J* = 9.5 Hz, 1H), 4.46 (m, 1H), 4.07 (m, 2H), 3.54 (m, 1H), 2.43 (m, 2H), 2.10 (s, 3H), 2.05 (s, 3H), 2.04 (s, 3H), 0.99 (m, 1H), 0.55 (m, 2H), 0.22 (m, 2H); ^{13}C-NMR (125 MHz, $CDCl_3$) δ (ppm) 172.64, 170.47, 169.45, 169.19, 87.83, 76.02, 70.53, 69.24, 68.26, 63.31, 39.42, 20.89, 20.79, 20.65, 9.17, 5.01, 4.61.

(4c) 1,2-dideoxy-2'-cyclopropylmethyl-α-D-glucopyranoso[2,1-d]-Δ2'-thiazoline

^{1}H NMR (500 MHz, MeOH, d_4) δ (ppm) 5.90 (d, *J* = 7.0 Hz, 1H), 4.10 (apparent triplet, *J* = 5.5 Hz, 1H), 3.92 (apparent triplet, *J* = 4.1 Hz, 1H), 3.52 (dd, *J* = 12.0, 2.5 Hz, 1H), 3.38 (m, 2H), 3.14 (m, 1H), 2.23 (d, *J* = 7.2 Hz, 2H), 0.77 (m, 1H), 0.35 (d, *J* = 7.9 Hz, 2H), 0.03 (m, 2H); ^{13}C NMR (125 MHz, MeOH, d_4) δ (ppm) 175.52, 89.74, 79.81, 76.18, 74.18, 71.22, 63.39, 40.52, 10.08, 5.51, 5.40; Elemental analysis calculated: C - 50.95, H - 6.61, N - 5.40; Found: C - 50.65, H - 6.59, N - 5.39.

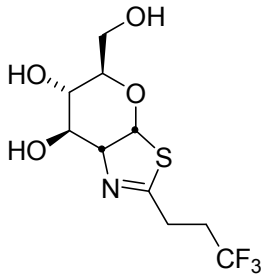

4d

(2d) 1,3,4,6-Tetra-*O*-acetyl-2-deoxy-2-(4,4,4-trifluorobutanamido)-β-D-gluco pyranose

^{1}H NMR (500 MHz, $CDCl_3$) δ (ppm) 5.90 (d, *J* = 9.4 Hz, 1H), 5.72 (d, *J* = 8.8 Hz, 1H), 5.18 (m, 2H), 4.29 (m, 1H), 4.12 (dd, *J* = 12.5, 2.1 Hz, 1H), 3.82 (m, 1H), 2.47 (m, 2H), 2.36 (m, 2H), 2.09 (s, 3H), 2.08 (s, 3H), 2.04 (s, 3H), 2.03 (s, 3H), 1.72 (s, 1H); ^{13}C-NMR (125 MHz, $CDCl_3$) δ (ppm) 171.36, 170.66, 169.91, 169.51, 169.28, 92.44, 72.84, 72.47, 67.75, 61.61, 53.10, 29.36 (q, J = 30.1 Hz, 1C) 20.78, 20.71, 20.57, 20.56.

(3d) 3,4,6-Tri-*O*-acetyl-1,2-dideoxy-2'-(3,3,3-trifluoropropyl)-α-D-gluco pyranoso[2,1-d]-Δ2'-thiazoline

^{1}H NMR (500 MHz, $CDCl_3$) δ (ppm) 6.30 (d, *J* = 7.2, 1H), 5.58 (m, 1H), 4.96 (dd, *J* = 9.3, 1.3 Hz, 1H), 4.51 (m, 1H), 4.14 (m, 2H), 3.53 (m, 1H), 2.83 (m, 2H), 2.58 (m, 2H), 2.16 (s, 3H), 2.11 (s, 3H), 2.10 (s, 3H); ^{13}C-NMR (125 MHz, $CDCl_3$) δ (ppm) 170.57, 169.47, 169.31, 168.87, 88.65, 76.18, 70.31, 69.10, 68.46, 63.26, 31.14, 30.90 (q, *J* = 30.1 Hz, 1C), 27.19, 20.95, 20.78, 20.72.

(4d)1,2-dideoxy-2'-(3,3,3-trifluoropropyl)-α-D-glucopyranoso[2,1-d]-Δ2'-thiazoline

^{1}H NMR (500 MHz, MeOH, d_4) δ (ppm) 6.40 (d, *J* = 7.0 Hz, 1H), 4.35 (m, 1H), 4.15 (apparent triplet, *J* = 3.9 Hz, 1H), 3.74 (dd, *J* = 12.1, 2.4 Hz, 1H), 3.59 (m, 2H), 3.32 (m, 1H), 2.80 (m, 2H), 2.60 (m, 2H); ^{13}C NMR (125 MHz, MeOH, d_4) δ (ppm) 207.59, 171.17, 90.71, 80.43, 76.31, 74.07, 71.27, 63.47, 32.12 (q, J = 30.9 Hz, 1C), 28.43; Elemental analysis calculated: C -39.87, H - 4.68, N - 4.65; Found: C - 39.90, H - 4.65, N - 4.58.

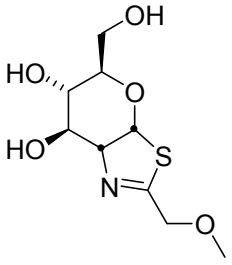

4e

(2e) 1,3,4,6-Tetra-*O*-acetyl-2-deoxy-2-methoxyacetamido-β-D-gluco pyranose[141]

^{1}H NMR (500 MHz, $CDCl_3$) δ (ppm) 6.58 (d, *J* = 9.6 Hz, 1H), 5.75 (d, *J* = 8.7 Hz, 1H), 10.33 (apparent triplet, *J* = 10.3 Hz, 1H), 5.12 (apparent triplet, *J* = 9.8 Hz,

1H), 4.27 (m, 1H), 4.14 (dd, *J* = 12.4, 2.1 Hz, 1H), 3.82 (m, 3H), 3.36 (s, 3H), 2.10 (s, 3H), 2.08 (s, 3H), 2.03 (s, 3H), 2.02 (s, 3H), 1.68 (s, 1H); ^{13}C-NMR (125 MHz, $CDCl_3$) δ (ppm) 170.64, 170.60, 169.98, 169.29, 92.28, 72.82, 72.17, 71.63, 67.76, 61.57, 59.29, 52.34, 20.87, 20.71, 20.58, 20.57.

(3e) 3,4,6-Tri-*O*-acetyl-1,2-dideoxy-2'-methoxymethyl-α-D-glucopyranoso [2,1-d]-Δ2'-thiazoline

^{1}H NMR (500 MHz, $CDCl_3$) δ (ppm) 6.18 (d, *J* = 7.3 Hz, 1H), 5.53 (dd, *J* = 3.3, 1.8 Hz, 1H), 4.89 (d, *J* = 9.4 Hz, 1H), 4.48 (m, 1H), 4.32 (dd, *J* = 14.3, 2.3 Hz, 1H), 4.22 (dd, *J* = 14.3, 2.4 Hz, 1H), 4.06 (m, 2H), 3.49 (m, 1H), 3.40 (s, 3H), 2.08 (s, 3H), 2.02 (s, 6H); ^{13}C-NMR (125 MHz, $CDCl_3$) δ (ppm) 171.59, 170.29, 169.23, 169.01, 86.59, 76.06, 71.51, 70.25, 68.97, 68.28, 63.05, 59.01, 20.72, 20.61, 20.50.

(4e) 1,2-dideoxy-2'-methoxymethyl-α-D-glucopyranoso[2,1-d]-Δ2'-thiazoline

^{1}H NMR (500 MHz, MeOH, d_4) δ (ppm) 6.37 (d, *J* = 6.9 Hz, 1H), 5.41 (m, 1H), 4.99 (m, 1H), 4.44 (m, 1H), 4.38 (apparent triplet, *J* = 5.6 Hz, 1H), 4.26 (m, 2H), 4.11 (s, 1H), 3.78 (m, 1H), 3.41 (s, 3H); ^{13}C-NMR (125 MHz, $CDCl_3$) δ (ppm) 173.22, 88.66, 77.90, 74.56, 73.41, 71.93, 68.90, 61.57, 59.36; HRMS (*m*/*z*): $[M+H]^+$ calcd for $C_9H_{15}NO_5S$: 250.0749 (M+H); Found: 250.0777.

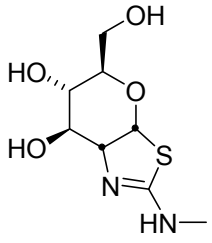

8f

(6f) 1,3,4,6-Tetra-*O*-acetyl-2-deoxy-2-[[(aminomethyl)thioxomethyl]amino]-β-D-glucopyranose

^{1}H NMR (500 MHz, $CDCl_3$) δ (ppm) 6.21 (s, 1H), 5.92 (s, 1H), 5.74 (d, *J* = 8.1 Hz, 1H), 5.20 (m, 2H), 4.28 (dd, *J* = 12.5, 4.6 Hz, 1H), 4.13 (m, 2H), 3.84 (m, 1H), 2.98 (s, 3H), 2.15 (s, 3H), 2.11 (s, 3H), 2.08 (s, 3H), 2.06 (s, 3H); ^{13}C-NMR (125 MHz, $CDCl_3$) δ (ppm) 171.78, 171.03, 169.81, 169.65, 93.01, 73.35, 72.90, 68.14, 62.00, 57.68, 53.76, 21.22, 21.03, 20.94, 20.80.

(7f) 3,4,6-Tri-*O*-acetyl-1,2-dideoxy-2'-aminomethyl-α-D-glucopyranoso[2,1-d]-Δ2'-thiazoline

^{1}H NMR (500 MHz, $CDCl_3$) δ (ppm) 6.21 (d, *J* = 6.5 Hz, 1H), 5.39 (dd, *J* = 4.1, 2.9 Hz, 1H), 4.90 (m, 1H), 4.34 (dd, *J* = 6.2, 4.3 Hz, 1H), 4.12 (m, 2H), 3.84 (m, 1H), 2.90 (s, 3H), 2.08 (s, 3H), 2.06 (s, 3H), 2.05 (s, 3H); ^{13}C-NMR (125 MHz, $CDCl_3$) δ (ppm) 170.89, 169.90, 169.72, 161.21, 90.03, 73.01, 72.24, 69.40, 68.67, 63.40, 31.19, 21.23, 21.10, 21.00.

(8f) 1,2-dideoxy-2'-aminomethyl-α-D-glucopyranoso[2,1-d]-Δ2'-thiazoline

^{1}H NMR (500 MHz, MeOH, d_4) δ (ppm) 6.14 (d, *J* = 6.4 Hz, 1H), 4.04 (t, *J* = 5.1 Hz, 1H), 3.90 (t, *J* = 5.1 Hz, 1H), 3.67 (m, 1H), 3.51 (m, 2H), 3.42 (m, 1H), 2.67 (s, 3H); ^{13}C NMR (125 MHz, MeOH, d_4) δ (ppm) 163.73, 88.52, 74.19, 73.61, 73.24, 69.28, 61.39, 29.83; HRMS (*m*/*z*): $[M+H]^+$ calcd for $C_8H_{14}N2O_4S$: 235.0674 (M+H); Found: 234.0753.

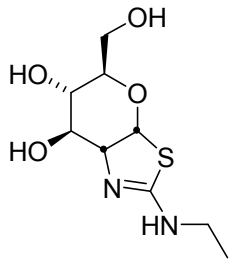

8g

(6g) 1,3,4,6-Tetra-*O*-acetyl-2-deoxy-2[[(aminoethyl)thioxomethyl]amino]-β-D-glucopyranose

^{1}H NMR (500 MHz, $CDCl_3$) δ (ppm) 6.12 (d, *J* = 15.0 Hz, 1H), 6.00 (s, 1H), 5.73 (d, *J* = 7.7 Hz, 1H), 5.19 (m, 1H), 4.81 (s, 1H), 4.28 (m, 1H), 4.12 (m, 1H), 3.85 (m, 1H), 3.40 (s, 1H), 2.14 (s, 3H), 2.10 (s, 3H), 2.08 (s, 3H), 2.05 (s, 3H), 1.81 (d, *J* = 40.2 Hz, 1H), 1.19 (m, 3H); ^{13}C-NMR (125 MHz, $CDCl_3$) δ (ppm) 171.88, 170.97, 169.60, 163.03, 93.12, 73.31, 72.99, 68.08, 61.95, 60.67, 57.84, 21.25, 21.07, 20.96, 20.81, 14.39.

(7g) 3,4,6-Tri-*O*-acetyl-1,2-dideoxy-2'-aminoethyl-α-D-glucopyranoso[2,1-d]-Δ2'-thiazoline

^{1}H NMR (500 MHz, $CDCl_3$) δ (ppm) 6.24 (d, *J* = 6.5 Hz, 1H), 5.43 (dd, *J* = 4.0, 2.7 Hz,1H), 4.96 (m, 1H), 4.37 (m, 1H), 4.14 (d, *J* = 4.3 Hz, 2H), 3.85 (m, 1H), 3.34 (m, 2H), 2.12 (s, 3H), 2.09 (s, 3H), 2.08 (s, 3H), 1.22 (t, *J* = 7.1 Hz, 3H); ^{13}C-NMR (125 MHz, $CDCl_3$) δ (ppm) 171.88, 170.97, 169.60, 93.12, 73.31, 72.99, 68.08, 61.95, 57.84, 21.25, 21.07, 20.96, 20.81, 14.28.

(8g) 1,2-dideoxy-2'-aminoethyl-α-D-glucopyranoso[2,1-d]-Δ2'-thiazoline

^{1}H NMR (500 MHz, MeOH, d_4) δ (ppm) 6.44 (d, *J* = 6.4 Hz, 1H), 4.09 (apparent triplet, *J* = 6.4 Hz, 1H), 3.89 (apparent triplet, *J* = 6.2 Hz, 1H), 3.82 (dd, *J* = 11.7,

1.8 Hz, 1H), 3.66 (m, 2H), 3.49 (dd, *J* = 9.0, 6.1 Hz, 1H), 3.35 (m, 2H), 1.22 (t, *J* = 7.3 Hz, 3H); ^{13}C NMR (125 MHz, MeOH, d_4) δ (ppm) 161.92, 89.72, 75.11, 74.57, 69.99, 62.07, 38.40, 38.35, 13.73; Elemental analysis calculated: C - 43.53, H - 6.49, N -11.28; Found: C - 43.82, H -6.62, N - 11.02.

2.12 Kinetic analysis of potent inhibitors using 4-methylumbelliferyl 2-acetamido-2-deoxy-β-D-glucopyranoside as a substrate.

Assays were carried out at 37 °C using 4-methylumbelliferyl 2-acetamido-2-deoxy-β-D-glucopyranoside as a substrate in a continuous assay where the linear rate of liberation of 4-methylumbelliferone was monitored by measuring its fluorescence emission (450 nm) using a CARY Eclipse fluorometer equipped with a temperature controller. Reactions (final volume of 150 µL) were initiated by the addition, *via* syringe, of enzyme (10 µL, $1.3X10^{-4}$ µg/µL final concentration) and monitored for 3 minutes. Recombinant human *O*-GlcNAcase is stable in the assay buffer (137 mM NaCl, 2.7 mM KCl, 10 mM Na_2HPO_4, 2 mM K_2HPO_4, with ~0.1% BSA) over the time of the assay. The inhibitors of interest were tested at 6 or more concentrations above and below the estimated K_i value. The K_i values were determined by Dixon plot analysis.

2.13 Kinetic analysis of moderate to poor inhibitors using 4-nitrophenyl 2-acetamido-2-deoxy-β-D-glucopyranoside (*p*NP-GlcNAc) as a substrate

Assays were carried out in triplicate at 37 °C in a Precision incubator, using 4-nitrophenyl 2-acetamido-2-deoxy-β-D-glucopyranoside (*p*NP-GlcNAc) as

a substrate in a stopped assay procedure. Absorbance values produced by the liberated 4-nitrophenolate were recorded at 400 nm using a Spectra max 340 spectrophotometer. Reactions (final volume of 50 µL) were initiated by the addition, *via* syringe, of enzyme (5 µL, to generate a final concentration of enzyme between $1.8X10^{-5}$µg/µL and 9.0 $X10^{-4}$ µg/µL) and were allowed to react for 30 minutes. Enzymatic reactions were stopped by the addition of 200 µL basic glycine quenching buffer (0.1M glycine, 1mM Zn_2Cl, 1mM $MgCl_2$, pH adjusted to 10.4 using 10 N NaOH). Absorbance values were determined from aliquots (100 µL) taken from the quenched reactions and subtracting the value obtained for a reaction containing no enzyme. Recombinant human *O*-GlcNAcase is stable in the assay buffer (137 mM NaCl, 2.7 mM KCl, 10 mM Na_2HPO_4, 2 mM K_2HPO_4, with ~0.1% BSA) over the time of the assay. The inhibitors of interest were tested at 6 or more concentrations above and below the estimated K_i value. The K_i values were determined by Dixon plot analysis.

Chapter 3: Synthesis of 2-acetamido-2-deoxy-5-thio-α-D-glucopyranose (5SGlcNAc) and derivatives.

3.1 Synthesis of 2-acetamido-2-deoxy-5-thio-α-D-glucopyranose (5SGlcNAc).

3.1.1 Rationale behind the synthesis of 5SGlcNAc.

As discussed in chapter 2, a bacterial homologue of *O*-GlcNAcase, *Bt*GH84, has been characterized fairly comprehensively.[40,41,128,129,142,143] Several studies have also clarified aspects of the catalytic mechanism and the natural function of *O*-GlcNAcase in cells. There remains, however, much to discover about how *O*-GlcNAcase is regulated in cells as well as its specific roles in certain diseases. Further studies to better understand its substrate specificity and detailed catalytic mechanism are also warranted. In this regard, investigating how tolerant *O*-GlcNAcase is to variation in substrate structure may provide further insight into its catalytic mechanism. It is also worth noting that sometimes molecules resembling the natural substrate, intermediate, or transition state can act as inhibitors of enzymes. For these reasons, studying substrate analogues for *O*-GlcNAcase was judged worthwhile and synthetic derivatives of 2-acetamido-2-deoxy-5-thio-D-glucopyranose (5SGlcNAc) were prepared. 5SGlcNAc differs from the natural substrate of *O*-GlcNAcase in that the endocyclic ring oxygen is replaced by sulphur (Figure 3.1).

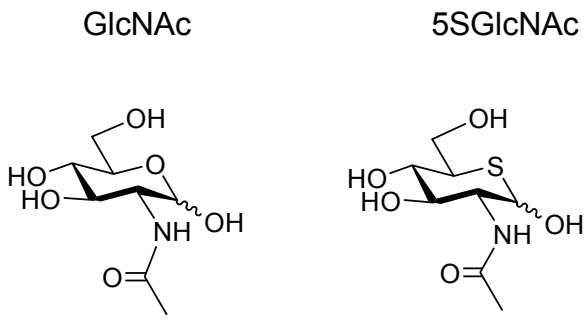

Figure 3.1 Structures of GlcNAc and 5SGlcNAc.

3.2 Results and Discussion: synthetic challenges and triumphs

3.2.1 Synthesis of 5SGlcNAc (18)

Despite the availability of published methods,[144,145] the synthesis of the target (5SGlcNAc, **18**)[144,145] was not trivial and the published methodology we followed was modified in order to obtain improved results. The procedures used are outlined in Scheme 3.1.

For the synthesis of 2-acetamido-2-deoxy-3,4:5,6-di-*O*-isopropylidine-aldehydo-D-glucose diethyl acetal (**10**), it was found that a much longer reaction time was required (24 h) than was quoted in the literature (2 h) in order to obtain comparable yields.[145] Additionally, at this step, rather than using a basic resin, potassium carbonate was added directly to the crude reaction mixture to neutralize the solution once the reaction was judged complete by TLC. It was found that to effect the benzoylation of 2-acetamido-2-deoxy-3,4-*O*-isopropylidine-aldehydo-D-glucose dimethyl acetal (**11**) to generate 2-acetamido-6-*O*-benzoyl-2-deoxy-3,4-*O*-isopropylidene-aldehydo-D-glucose dimethyl acetal (**12**), it was imperative that the reaction was carried out under dry conditions. Any moisture resulted in poor yields and the formation of undesired by-products.

Mesylation of intermediate **12** resulted in a good yield of 2-acetamido-6-*O*-benzoyl-2-deoxy-3,4-*O*-isopropylidine-5-*O*-mesyl-aldehydo-D-glucose dimethyl acetal (**13**). For both reactions, the already purified starting material was placed under high vacuum for at least 3 hours prior to setting up the reaction under an atmosphere of N_2.

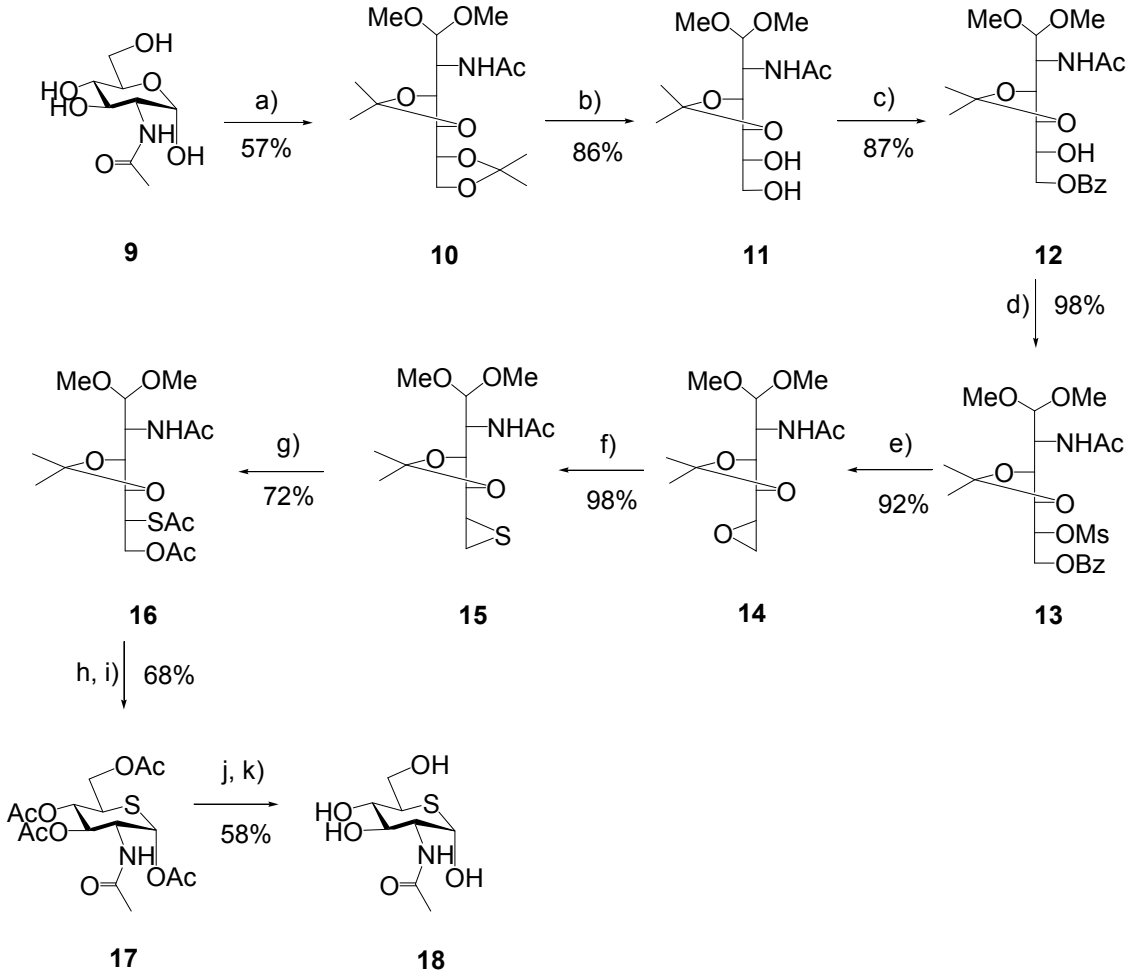

Scheme 3.1 Synthesis of Ac-5SGlcNAc (17) and 5SGlcNAc (18).
a) 2,2 Dimethoxypropane, p-tosic acid, dioxane, 80 °C, 24 h; b) 80% AcOH in H_2O, 40 °C, 2 h; c) Benzoyl chloride, pyridine, -20 °C, 6 h; d) Methane sulphonyl chloride, pyridine, 0 °C, 2 h; e) NaOMe, DCM -20→0 °C, 2 h; f) Thiourea, MeOH, 60 °C, 2 h; g) KOAc, AcOH, acetic anhydride, 160 °C, 20 h; h) 10:1 NaOAc, 10 M HCl, 40 °C, 24 h; i) Acetic anhydride, pyridine, 0 °C, 12 h; j) MeOH, NaOMe, r.t, 1h; k) AcOH, MeOH (pH 4).[144,145]

Synthesis of the epoxide, 2-acetamido-5,6-anhydro-2-deoxy-3,4-*O*-isopropylidene-aldehydo-L-idose dimethyl acetal (**14**), was relatively straightforward, however, care was required when neutralizing the basic reaction mixture with the acidic resin. If the reaction pH became even slightly acidic, degradation of product occurred rapidly upon concentrating the crude mixture *in vacuo*. Therefore, if needed, potassium carbonate was used to neutralize the pH if too much acidic resin had been added to the crude reaction mixture at this step. To successfully synthesize the thioepoxide, it was crucial that all glassware and reagents were dry. Drying the starting material **14**, as well as the thiourea, for several hours under high vacuum was required to obtain good yields.

The opening of the thioepoxide to generate intermediate **16** proved to be an extremely challenging step, and 72% was the best yield obtained. The key to increasing the yield of this reaction was a high reaction temperature (160 °C) and long (15-20 h) reaction time. Optimization of the global deprotection / reprotection step to yield per-*O*-acetylated 5SGlcNAc **17** was difficult. When following literature procedures,[144] poor yields were obtained (10-20%). It was found that a long reaction time (24 h) was required. The literature procedure[144] reports a 6 hour reaction time for this step, but to obtain comparable yields (75%) required at least 15 hour reaction time. Additionally, the desired material degraded when concentrating this reaction *in vacuo* with the application of heat; using high vacuum rotary evaporation without heating was needed to obtain the desired material in good yield. Acetylation of the crude product was achieved in a similar manner as described in the literature.[144] Again, concentrating the crude product

was successfully accomplished using high vacuum rotary evaporation with no heating. The final deprotection step was affected using the literature procedure.[144] It seems, however, that this product is also heat sensitive and isolation requires gradual concentration of only pure fractions obtained from column chromatography, to yield crystalline white needles.

3.2.2 5SGlcNAc: a possible metabolic inhibitor of the glycosyl transferase, OGT.

After purifying 5SGlcNAc, it was decided that it would be interesting to investigate whether this material would produce any measurable effects in cells. One scenario envisioned was that 5SGlcNAc might be incorporated in the place of *O*-GlcNAc on cellular proteins and accumulate, since it might be turned over slowly by *O*-GlcNAcase. Another scenario considered possible, though less likely, was that *O*-GlcNAc levels on proteins might drop; OGT might install 5SGlcNAc more slowly than GlcNAc and *O*-GlcNAcase might remove 5SGlcNAc more quickly than it is in-stalled. Interestingly, when Dr. Tracey Gloster (from our laboratory) treated cells with 5SGlcNAc, significant decreases in *O*-GlcNAc levels were observed. This led to the hypothesis that 5SGlcNAc is converted to uridine diphosphate 2-acetamido-2-deoxy-5-thio-α-D-glucopyranoside (UDP-5SGlcNAc, compound **19**, Figure 3.2) and this molecule might act as an inhibitor of OGT.

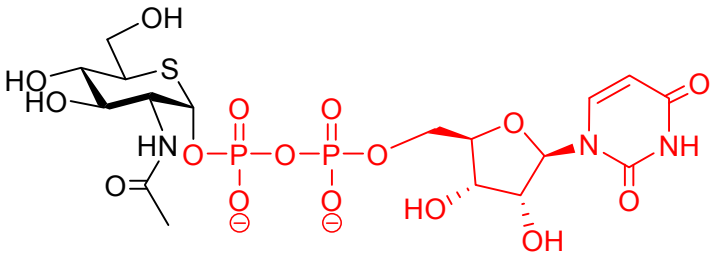

(19)

Figure 3.2 UDP-5SGlcNAc.

This observation and hypothesis was of great interest to our laboratory as there were no known cell permeable inhibitors of OGT, and the discovery of such a compound would be both novel and useful for research into understanding the role of *O*-GlcNAc in cells. Because *O*-GlcNAc modification levels have been implicated in several disease states, discovering a way of decreasing the levels of *O*-GlcNAc in cells could provide a means of investigating the molecular basis for involvement of *O*-GlcNAc in these diseases as well as its normal biological roles. This could be done by treating cells, and perhaps even animals, with this compound. To verify whether the results observed in cells were due to UDP-5SGlcNAc blocking OGT, Wesley Zandberg and Dr. Tracey Gloster chemoenzymatically synthesized this compound using the 5SGlcNAc that had been prepared. With this compound in hand, kinetic studies were undertaken by Dr. Tracey Gloster and David Shen in our laboratory to evaluate this compound as an inhibitor of OGT. To our excitement, it was found that UDP-5SGlcNAc did inhibit OGT with a K_i value of 8 μM. UDP-5SGlcNAc was also evaluated as a substrate for OGT and it was found that it was a poor substrate compared to UDP-GlcNAc.

3.3 Synthesis of para-methoxyphenyl 2-acetamido-2-deoxy-5-thio-β-D-glucopyranoside (*p*MP-5SGlcNAc): making a new substrate for *O*-GlcNAcase.

3.3.1 Synthesis of 2-acetamido-3,4,6-tri-*O*-acetyl-2-deoxy-5-thio-α-D-glucopyranosyl chloride: a putative glycosyl donor for glycosylation reactions.

Even though UDP-5SGlcNAc (**19**) was a poor substrate for OGT, and therefore transfers to proteins only very slowly, we were interested in studying whether glycosides of 5SGlcNAc could be substrates for *O*-GlcNAcase. Creating a β-glycoside of 5SGlcNAc presented several obstacles. The first approach to preparing such a substrate was to generate the glycosyl donor 2-acetamido-3,4,6-tri-*O*-acetyl-2-deoxy-α-D-glucopyranosyl chloride (Compound **20**, Scheme 3.2). Reflecting on previous work done in our laboratory where the synthesis of 2-acetamido-2-deoxy-β-D-glucopyranosides from 2-acetamido-3,4,6-tri-*O*-acetyl-2-deoxy-α-D-glucopyranosyl chloride was successfully achieved,[146] we expected that the analogous 2-acetamido-3,4,6-tri-*O*-acetyl-2-deoxy-5-thio-α-D-glucopyranosyl chloride (**20**) could be used to stereoselectively prepare 5-thio-β-D-*N*-acetylglucopyranosides. The basis for stereoselectivity was that the 2-acetamido group should provide anchimeric assistance to block the bottom face of a glycosyl cation intermediate such that nucleophilic attack occurs predominantly on the β-face of the pyranose ring. A β-configured glycoside is essential for testing as a substrate of *O*-GlcNAcase since this enzyme only catalyzes hydrolysis of β-glycosides. An α-configured product would thus be useless for testing as a substrate of *O*-GlcNAcase.

For the reasoning stated above, the synthesis of 2-acetamido-3,4,6-tri-*O*-acetyl-2-deoxy-5-thio-α-D-glucopyranosyl chloride (**20**) was undertaken using

conditions previously used for the synthesis of the oxygen analogue[146] (see methods section for reaction conditions and Scheme 3.2). After successful synthesis of the glycosyl donor **20**, several glycosylation attempts (including ones that worked with the oxygen analogue)[146] were made, unfortunately with no success. This caused us to re-evaluate our approach.

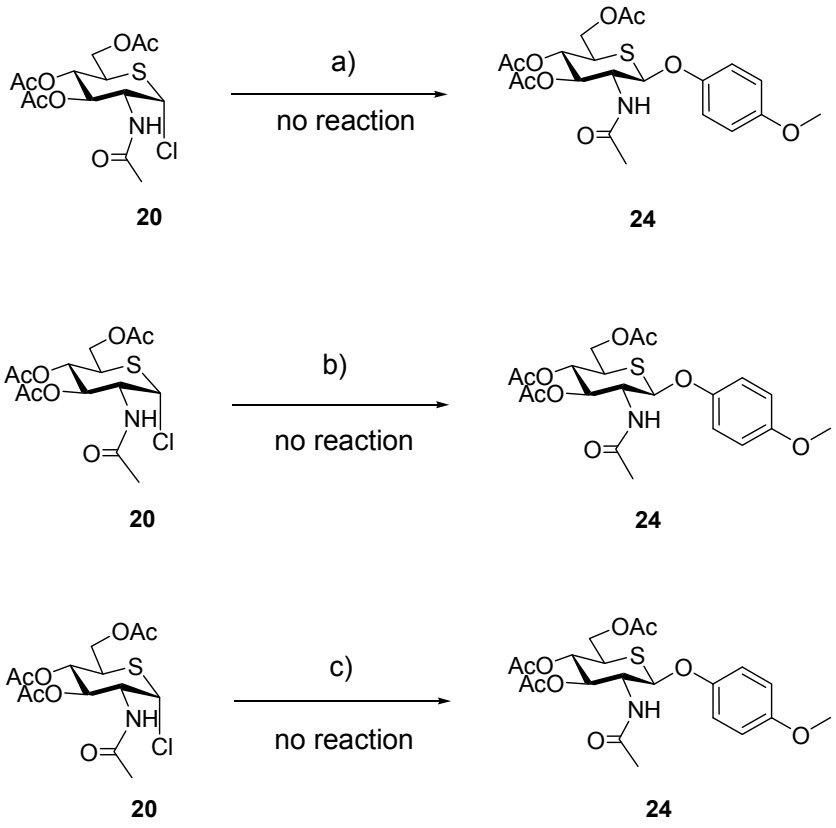

Scheme 3.2 Attempts at glycosylating 2-acetamido-3,4,6-tri-*O*-acetyl-2-deoxy-5-thio-α-D-glucopyranosyl chloride.
Several glycosylation attempts were made using with **20** as a glycosyl donor. No desired product was isolated from any of these attempts. a) *para*-Methoxyphenol, benzyltriethylammonium chloride, DCM, 1M NaOH, 24 h; b) Sodium *para*-methoxyphenolate, THF, r.t., 24 h; c) *para*-Methoxyphenol, NaOH, acetone, r.t., 24 h.

3.3.2 Synthesis of 2-acetamido-3,4,6-tri-*O*-acetyl-2-deoxy-5-thio-α-D-gluco pyranosyl trichloroacetimidate (22).

After some unsuccessful attempts to obtain our desired product using the chloride donor **20**, an alternative route was explored. Upon examination of the

literature, it was found that trichloroacetimidate 5-thiosugar donors had been successfully used when glycosylating various acceptors.[147-152] Therefore, the α-trichloroacetimidate sugar donor, 2-acetamido-3,4,6-tri-*O*-acetyl-2-deoxy-5-thio-α-D-glucopyranosyl trichloroacetimidate (**22**) was prepared with the anticipation that it would prove more useful than the chloride donor **20**. The general procedure for the synthesis of **22** is outlined in Scheme 3.3.

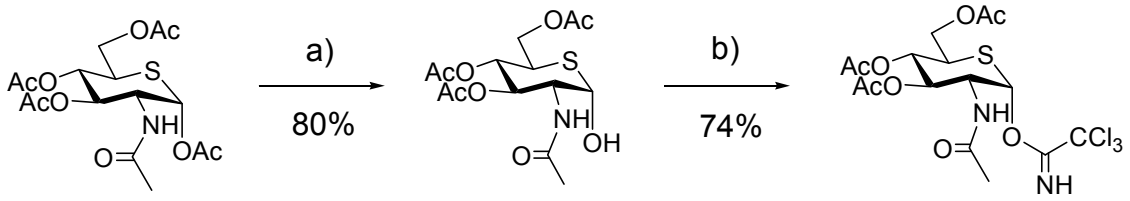

17 **21** **22**

Scheme 3.3 Synthesis of 2-acetamido-3,4,6-tri-*O*-acetyl-2-deoxy-5-thio-α-D-glucopyranosyl trichloroacetimidate glycosyl donor (22).
An alternative glycosyl donor was synthesized by introducing a trichloroacetimidate leaving group at the anomeric center.[148-152] a) Hydrazine acetate, DMF, r.t., 4 h; b) Trichloroacetonitrile, DBU (cat.), DCM, 0°C, 0.5 h.

3.4 Synthesis of a potential substrate for *O*-GlcNAcase.

3.4.1 Glycosylation of 2-acetamido-3,4,6-tri-*O*-acetyl-2-deoxy-5-thio-α-D-glucopyranosyl trichloroacetimidate (22) with para-methoxyphenol under low temperature conditions.

After isolating the trichloroacetimidate donor **22**, the next step was glycosylation. It was decided that this would be attempted at low temperature (-78 °C), as several references had successfully made use of various trichloroacetimidate donors under low temperature conditions.[150,152-154] The first glycosylation conditions that were explored are summarized in Scheme 3.4, and the detailed procedure is outlined at the end of this chapter (see methods section 3.6).

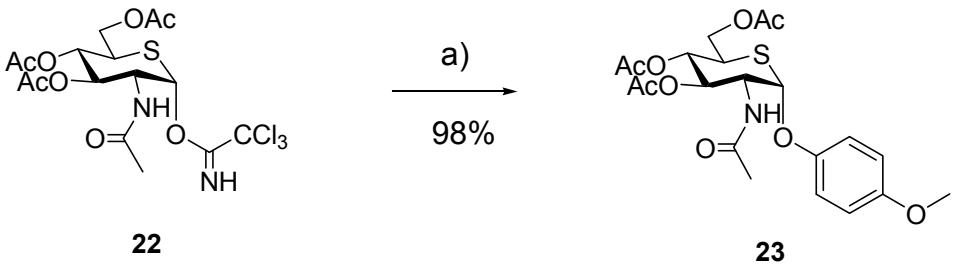

22 **23**

Scheme 3.4 An α-glycoside product is generated under low temperature reaction conditions.
a) *para*-Methoxyphenol, $BF_3{\cdot}OEt_2$ (cat.), DCM, - 78 °C, 1 h.

3.4.2 Back to the drawing board: an α-glycosylated product will not be useful, *O*-GlcNAcase only processes β-glycosides.

While it was encouraging to finally obtain a 5-thio glycoside product, it unfortunately and surprisingly did not possess the desired stereochemistry. Glycoside hydrolases are very specific as to which anomer of a sugar substrate they will process.[35] As mentioned previously, only β-glycosides are processed by *O*-GlcNAcase.[17] This makes the α-anomer useless for our purposes. However, all was not lost. This α-glycoside product was a step in the right direction. The obstacle was now how to obtain the β-configured version of this glycoside. Being somewhat puzzled by the stereochemical selectivity of this previous reaction, we consulted the literature for some potential explations of the observed results. We were relieved to discover that we were not the only ones to have faced this issue of stereoselectivity when using 5-thio sugar glycosyl donors. There were references that revealed that when using various 5-thio sugar donors, α-glycoside products greatly predominated.[147,149-151,155-157] This is an interesting phenomenon, and while there are currently no concrete explanations for this, it

seems that the endocyclic ring sulphur gives rise to a stronger anomeric effect than that observed for sugars containing an endocyclic ring oxygen.

In one interesting report, exclusive production of the β-anomer was obtained although this necessitated the use of a 2-phthamido group, which was not readily feasible given the synthetic route we used.[147] Fortunately, there were reaction conditions found in a few references that demonstrated how glycosylation conditions may be manipulated when using 5-thio sugar trichloroacetimidate donors, to achieve reasonable, though not exclusive selectivity for the β-glycoside.[151,153,157] The main difference contributing to the formation of the β-glycoside was the temperature under which the glycosylation reactions took place. It was found in the literature that by using a Lewis acid promoter, catalytic $BF_3 \cdot OEt_2$, and a higher temperature (-20 °C → r.t.), the β-anomer was generated to a much greater extent than what we had found when carrying out the reaction at -78 °C.[151,153,157] Following this promising lead from the literature, glycosylation using **22** was attempted again but using higher temperature conditions (see Scheme 3.5).

3.4.3 The synthesis of para-methoxyphenyl 2-acetamido-3,4,6-tri-*O*-acetyl-2-deoxy-5-thio-β-D-glucopyranoside.

The reaction conditions used to prepare para-methoxyphenyl 2-acetamido-3,4,6,-tri-*O*-acetyl-2-deoxy-5-thio-β-D-glucopyranoside (**24**) are summarized in Scheme 3.5 and a detailed synthetic procedure follows in the methods section 3.6.

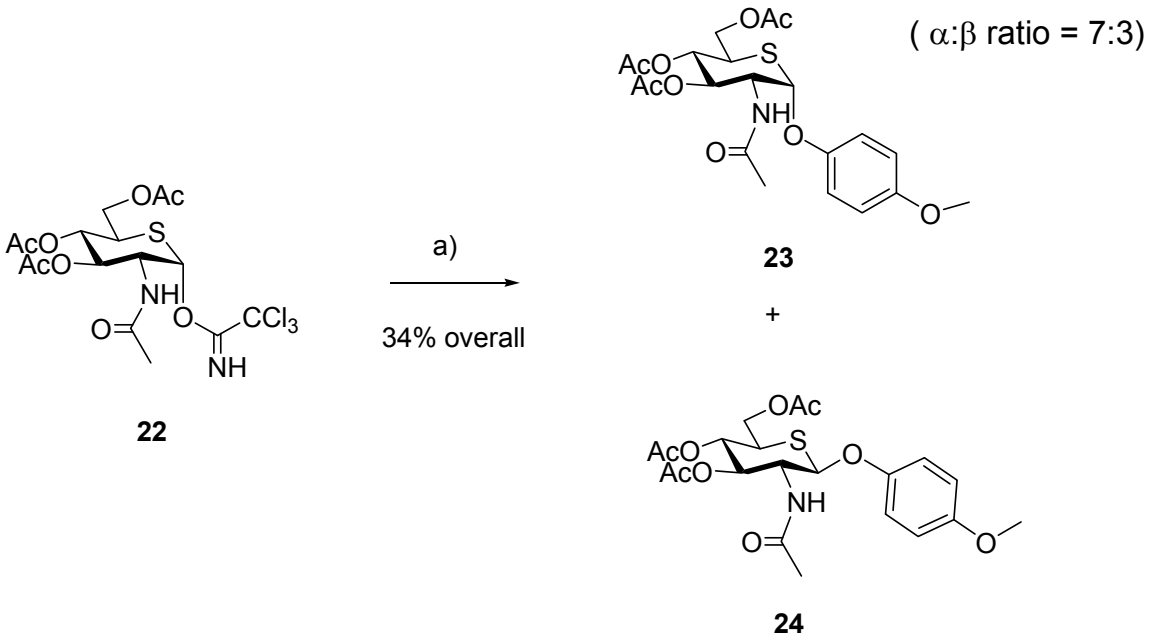

22

Scheme 3.5 An increase in reaction temperature increased the ratio of β- to α-glucosides. The glycosylation of **22** was achieved with a greater selectivity for the β-anomer than previously observed.[151,153,157] Ratios were determined using ^{1}H NMR spectroscopy of the isolated product mixture. a) *para*-Methoxyphenol, $BF_3{\cdot}OEt_2$ (cat.), DCM, -20 °C → r.t., 1 h.

Once each anomer was isolated, the next step was to remove the acetyl groups. Because each protected anomer was isolated in such a small quantity, it was decided that the deprotection would be performed first on the α-anomer (the less important compound) to identify appropriate reaction conditions. Upon successful deprotection of the α-anomer, deprotection of the β-anomer was carried out. The reaction conditions are summarized below in Scheme 3.6, followed by detailed procedures in the methods section.

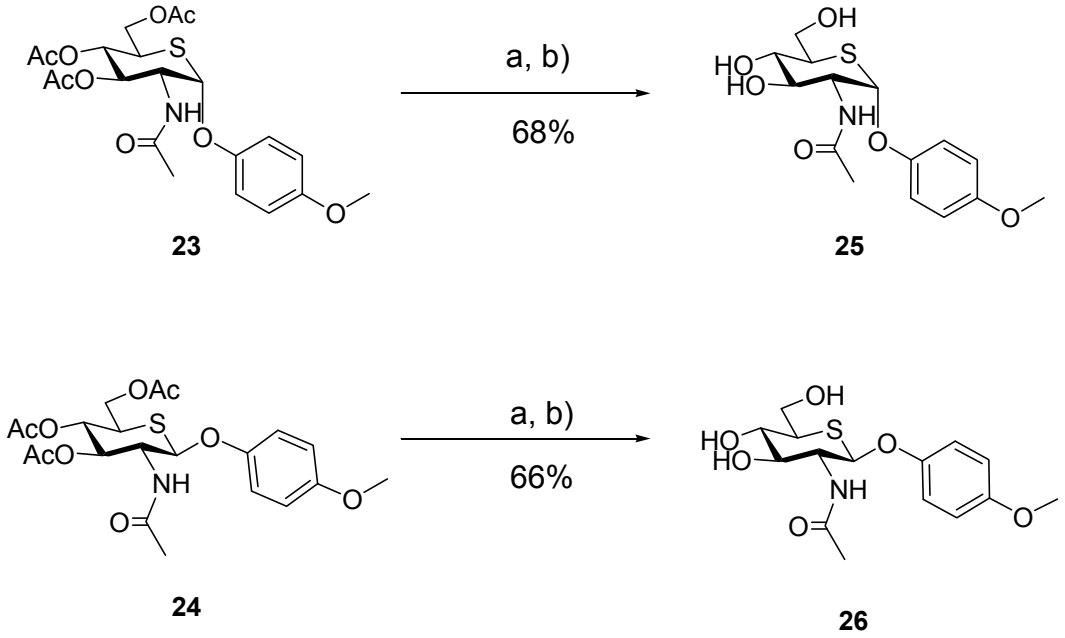

Scheme 3.6 Deprotection of *p*MP-5SGlcNAc 23 and 24 glycosylated products. Each deprotected anomer was obtained using standard deprotection procedures. a) NaOMe (cat.), MeOH, r.t., 0.5 h; b) AcOH, MeOH (pH 4).

3.4.4 *p*MP- 5SGlcNAc (26): isolated!

We were pleased to successfully isolate *p*MP-5SGlcNAc (**26**) with the appropriate stereochemistry at the anomeric center. It is interesting that the temperature was such an important factor for obtaining a reasonable yield of the β-glycoside. This temperature dependence on stereoselectivity has been documented in a few synthetic procedures involving 5-thiosugar donors, as mentioned earlier.[151,153,157] It is likely that this selectivity arises from kinetic differences that are apparent when using different reaction temperatures, as a thermodynamic explanation would require that there be reversibility of the glycosylation reaction, which is highly unlikely. A more detailed explanation will require further experimentation including closely monitored kinetic experiments.

Regardless, the isolation of this compound required some careful consideration and willingness to plunge forward toward alternative approaches when other strategies failed.

3.5 *p*MP-5SGlcNAc (26): a substrate for *O*-GlcNAcase.

Once *p*MP-5SGlcNAc (**26**) was prepared, our laboratory was curious to investigate if this compound could be a substrate for *O*-GlcNAcase. This question is fundamentally interesting since it could expand our understanding of the catalytic mechanism of *O*-GlcNAcase, as well as enlighten us as to how tolerant this enzyme is toward variants of its natural substrate. Dr. Tracy Gloster carried out kinetic studies and found that *O*-GlcNAcase was indeed capable of processing *p*MP-5SGlcNAc (**26**), with an enzymatic efficiency (k_{cat}/K_m) of 0.054 μM s^{-1} mg^{-1} mM^{-1}, which is only 5-fold less efficient than the processing of *p*MP-GlcNAc (k_{cat}/K_m = 0.27 μM s^{-1} mg^{-1} mM^{-1}), which more closely resembles the natural substrate. This shows that *O*-GlcNAcase tolerates substitution of the endocyclic ring oxygen with sulphur surprisingly well. This observation is interesting in light of the finding that UDP-5SGlcNAc acts as a poor substrate for OGT and suggests that the cationic character of the transition states differ between these two enzymes. These findings are likely just the early days of studies relating to understanding the processing and use of 5SGlcNAc (**18**) by OGT and *O*-GlcNAcase. Nevertheless, these discoveries are significant and a good step forward.

3.6 Methods

3.6.1 Detailed methods for the synthesis 5SGlcNAc

The synthesis of 5SGlcNAc (**18**) was carried out following the literature procedure established by Tanahashi *et al.*,[144] as well as that of Hasegawa *et. al.*[145] However, the conditions at certain steps were modified in order to obtain improved results. In all cases where the spectral characterization was available for literature compounds, the data was in good agreement. Owing to the absence of full characterization in the literature, data is provided here for each compound for completeness and for future reference.

2-Acetamido-2-deoxy-3,4:5,6-di-O-isopropylidine-aldehydo-D-glucose dimethyl acetal (**10**).[145] 15.0 g (67.8 mmol) of **9** was suspended in 1,4- dioxane (150 mL) at 80 °C. 2,2-dimethoxypropane (60 mL) was added to the suspension, together with 2.25 g (11.8 mmol) of tosic acid. The reaction was stirred for 24 hours at 80 °C. The mixture was cooled and subsequently treated with enough potassium carbonate to obtain a neutral solution. The reaction mixture was then filtered and concentrated under high vacuum. The concentrated crude reaction mixture was subjected to flash column silica chromatography using a solvent system increasing in polarity from 1 to 2% methanol in chloroform, affording the title compound as a caramel coloured viscous syrup (7.35 g, 57%). ^{1}H-NMR (500 MHz, $CDCl_3$) δ (ppm) 5.94 (d, J = 10.0 Hz, 1H), 4.17 (dd, J = 9.8, 6.8 Hz, 1H), 4.09 (d, J = 6.6 Hz, 1H), 3.95 (d, J = 8.1 Hz, 1H), 3.80 (m, 2H), 3.66 (q, J = 4.4 Hz, 1H), 3.45 (s, 2H), 3.40 (t, J = 7.8 Hz, 1H), 3.16 (s, 3H), 3.10 (s, 3H), 1.79 (s, 3H), 1.23 (s, 2H), 1.16 (s, 2H), 1.13 (s, 3H), 1.10 (s, 3H); ^{13}C-NMR (125 MHz,

$CDCl_3$) δ (ppm) 169.50, 109.59, 109.09, 102.86, 77.63, 77.56, 76.78, 67.04, 66.75, 54.08, 52.57, 48.87, 26.79, 26.72, 26.11, 25.00, 22.91.

2-Acetamido-2-deoxy-3,4-O-isopropylidine-aldehydo-D-glucose dimethyl acetal (**11**).[145] 10.35 g (29.80 mmol) of **10** was dissolved in a solution of 80% acetic acid in water and stirred at 40 °C for 2 hours. Upon completion of the reaction aliquots of the mixture were concentrated under high vacuum until the whole reaction mixture was concentrated to afford a thick oil. This oil was dried directly under high vacuum until the acetic acid was removed. The crude reaction mixture was then purified *via* flash column silica chromatography using a solvent system of increasing polarity, beginning at 7% and increasing to 10% methanol in chloroform. The pure fractions were concentrated and dried under high vacuum to afford the title compound as yellow syrup. (8.55 g, 86%). ^{1}H-NMR (500 MHz, $CDCl_3$) δ (ppm) 6.32 (d, J = 9.7 Hz, 1H), 4.42 (d, J = 7.0 Hz, 1H), 4.34 (t, J = 9.7 Hz, 1H), 9.48 (d, J = 9.5 Hz, 1H), 3.73 (dd, J = 11.2, 3.1 Hz, 1H), 3.60 (m, 3H), 3.36 (s, 3H), 3.27 (s, 3H), 2.02 (s, 3H), 1.33 (s, 3H); ^{13}C-NMR (125 MHz, $CDCl_3$) δ (ppm) 171.23, 109.08, 102.64, 78.02, 76.21, 73.45, 64.17, 54.61, 52.48, 50.04, 26.96, 23.19.

2-Acetamido-6-O-benzoyl-2-deoxy-3,4-O-isopropylidene-aldehydo-D-glucose dimethyl acetal (**12**).[144] To a stirred solution of **11** (7.70 g, 22.2 mmol) in pyridine at -20°C, dry benzoyl chloride (3.14 g, 22.2 mmol) was added. The mixture was stirred for 6 hours while maintaining the temperature between -10 and -5 °C. Upon completion of the reaction the mixture was diluted with chloroform. The crude mixture was washed twice with each of 2 M HCl, saturated

sodium carbonate, and water. Each aqueous layer was back extracted with chloroform. The combined organic layers were dried with magnesium sulphate, filtered, and concentrated *in vacuo*. The concentrated crude residue was subjected to flash column silica chromatography using a solvent system of increasing polarity starting with 1% and increasing to 2% methanol in chloroform. The pure fractions were concentrated *in vacuo*, dried with $MgSO_4$, and then the desired material was crystallized from ethyl acetate and hexanes to afford the title compound as white needles (7.68 g, 87%). ^{1}H-NMR (500 MHz, $CDCl_3$) δ (ppm) 8.11 (dd, J = 8.5, 1.3 Hz, 2H), 7.53 (t, J = 7.5 Hz, 1H), 7.41 (t, J = 8.2 Hz, 2H), 4.45 (m, 4H), 4.24 (d, J = 10.1 Hz, 1H), 3.90 (m, 1H), 3.71 (t, J = 8.7 Hz, 1H), 3.36 (s, 3H), 3.26 (s, 3H), 2.03 (s, 3H), 1.35 (s, 3H), 1.35 (s, 3H), 1.32 (s, 3H); ^{13}C-NMR (125 MHz, $CDCl_3$) δ (ppm) 171.20, 166.62, 132.99, 129.82, 128.29, 109.07, 102.16, 79.03, 75.38, 71.62, 66.83, 54.67, 51.95, 50.36, 26.95, 26.93, 23.12.

2-Acetamido-6-O-benzoyl-2-deoxy-3,4-O-isopropylidine-5-O-mesyl-aldehydo-D-glucose dimethyl acetal (**13**).[144] 6.52 g (16.4 mmol) of **12** was cooled to 0 °C in pyridine (14 mL). To this solution mesyl chloride (2.50 g, 20.8 mmol) was added. The reaction was kept at 0 °C until judged complete by TLC analysis (2 hours). The mixture was then concentrated under high vacuum. The resulting residue was dissolved in chloroform and the solution was successively washed twice with each of 2 M HCl, saturated sodium carbonate solution, and water. Each aqueous layer was back extracted with chloroform. All organic layers were combined, dried with $MgSO_4$, concentrated *in vacuo*, and placed under high

vacuum until residual pyridine was removed. The crude reaction mixture was purified *via* flash column silica chromatography using a solvent system of increasing polarity from 1% to 2% methanol in chloroform. Pure fractions were concentrated *in vacuo* and dried under high vacuum, giving rise to the pure product as an amorphous white solid (7.64 g, 98%). ^{1}H-NMR (500 MHz, $CDCl_3$) δ (ppm) 8.12 (d, J = 7.1 Hz, 1H), 7.60 (t, J = 7.4 Hz, 1H), 7.48 (t, J = 8.1 Hz, 2H), 5.84 (d, J = 9.7 Hz, 1H), 5.14 (m, 1H), 4.80 (dd, J = 12.5, 2.6 Hz, 1H), 4.49 (dd, J = 12.5, 7.1 Hz, 1H), 4.45 (m, 2H), 4.39 (m, 1H), 4.00 (dd, J = 7.9, 6.2 Hz, 1H), 3.45 (s, 3H), 3.34 (s, 3H), 3.16 (s, 3H), 2.07 (s, 3H), 1.78 (s, 3H), 1.45 (s, 3H), 1.43 (s, 3H); ^{13}C-NMR (125 MHz, $CDCl_3$) δ (ppm) 170.07, 166.10, 133.29, 129.91, 128.48, 110.39, 103.18, 78.40, 75.65, 63.55, 55.78, 52.79, 49.69, 38.89, 26.99, 26.90, 23.36.

2-Acetamido-5,6-anhydro-2-deoxy-3,4-O-isopropylidene-aldehydo-L-idose dimethyl acetal (**14**).[144] To a solution of **13** (6.23 g, 13.1 mmol) in dry chloroform (62 mL) at -20 °C was added drop-wise a fresh solution of sodium methoxide (0.50 g Na in 20 mL of methanol). The temperature of the reaction mixture was maintained between -10 °C and 0 °C until the reaction was judged complete by TLC analysis (5 hours). Upon completion of the reaction, additional methanol (102 mL) was added to the mixture. The reaction mixture was treated with H^+ amberlite ion exchange resin (IR-120) until the reaction mixture reached a pH of 7. In a small number of cases, if the pH of the solution became acidic, enough K_2CO_3 was added to increase the pH back to 7. The resin was filtered and washed with additional methanol. The filtrate was concentrated *in vacuo* and the

resulting residue triturated with ether and hexanes to afford a white amorphous solid (3.51 g, 92%). ^{1}H-NMR (500 MHz, $CDCl_3$) δ (ppm) 5.91 (d, J = 9.8 Hz, 1H), 4.37 (d, J = 7.1 Hz, 1H), 4.18 (m, 2H), 3.36 (s, 3H), 3.35 (m, 1H), 3.25 (s, 3H), 2.98 (m, 1H), 2.80 (m, 1H), 2.75 (dd, J = 5.1, 4.2 Hz, 1H), 1.97 (s, 3H), 1.35 (s, 3H), 1.32 (s, 3H); ^{13}C-NMR (125 MHz, $CDCl_3$) δ (ppm) 170.03, 109.79, 102.72, 78.36, 76.00, 55.43, 52.20, 50.92, 48.67, 43.75, 26.88, 26.76, 23.17.

2-Acetamido-2,5,6-trideoxy-5,6-epithio-3,4-O-isopropylidine-aldehydo-D-glucose dimethyl acetal (**15**).[144] To a solution of **14** (3.65 g, 12.6 mmol) in dry methanol (78 mL) was added thiourea (2.88 g, 37.9 mmol) after which the mixture was stirred at 60 °C for 2 h Upon completion of the reaction, the mixture was cooled to room temperature and then concentrated *in vacuo.* The title compound was purified using flash column silica chromatography using a solvent system of 2% methanol in chloroform (3.77 g, 98%). ^{1}H-NMR (500 MHz, $CDCl_3$) δ (ppm) 5.85 (d, J = 9.4 Hz, 1H), 4.33 (m, 3H), 3.40 (s, 3H), 3.36 (s, 3H), 3.26 (t, J = 7.9 Hz, 1H), 2.92 (m, 1H), 2.51 (d, J = 6.0 Hz, 1H), 2.26 (d, J = 5.2 Hz, 1H), 1.99 (s, 3H), 1.44 (s, 3H), 1.39 (s, 3H); ^{13}C-NMR (125 MHz, $CDCl_3$) δ (ppm) 169.67, 109.95, 103.38, 81.91, 78.22, 55.38, 53.56, 49.39, 33.92, 27.04, 27.03, 22.96.

2-Acetamido-6-O-acetyl-5-S-acetyl-2-deoxy-3,4-O-isopropylidine-5-thio-aldehydo-D-glucose dimethyl acetal (**16**).[144] A solution of **15** (1.02 g, 3.34 mmol), acetic anhydride (31 mL), potassium acetate (1.53 g, 15.6 mmol), and acetic acid (5 mL) was brought to reflux at 160 °C with stirring for 20 hours. After completion of the reaction, the mixture was cooled to room temperature and

concentrated under high vacuum. The remaining residue was extracted with chloroform and successively washed with 2 M HCl, saturated sodium bicarbonate, and brine. Each aqueous layer was back extracted with chloroform. The pooled organic layers were dried with $MgSO_4$, and evaporated under vacuum to afford a dark syrup. Flash column silica chromatography using a solvent system of 30% hexanes in ethyl acetate furnished the title compound as a white crystalline solid (0.980 g, 72%).^{1}H-NMR (500 MHz, $CDCl_3$) δ (ppm) 5.83 (d, J = 9.7 Hz, 1H), 4.37 (m, 2H), 4.32 (d, J = 6.8 Hz, 1H), 4.26 (dd, J = 11.5, 5.1 Hz, 1H), 4.16 (d, J = 7.5 Hz, 1H), 3.96 (m, 1H), 3.82 (t, J = 7.9 Hz, 1H), 3.37 (s, 3H), 3.30 (s, 3H), 2.36 (s, 3H), 2.04 (s, 3H), 2.02 (s, 3H), 1.42 (s, 3H), 1.39 (s, 3H); ^{13}C-NMR (125 MHz, $CDCl_3$) δ (ppm) 191.92, 168.67, 167.93, 107.89, 101.17, 75.71, 74.70, 61.90, 53.50, 50.68, 48.37, 43.03, 28.58, 25.13, 24.90, 21.38, 18.77.

2-Acetamido-1,3,4,6-tetra-O-acetyl-2-deoxy-5-thio-α-D-glucopyranose (**17**).[144] In a solution of 10:1 acetic acid:2 M HCl (77 mL) **16** (2.57 g, 6.31 mmol) was dissolved and the mixture was warmed to 40 °C for 24 hours under an atmosphere of nitrogen. The reaction mixture turned a bright pink colour. Upon completion of the reaction, the mixture was concentrated without heating under high vacuum. The resulting dark brown residue was dried thoroughly under high vacuum until residual acetic acid was removed and a dark brown syrup was obtained. The syrup was dissolved in acetic anhydride (13 mL) and pyridine (51 mL) and stirred overnight at 0°C. Upon completion of the reaction, the mixture was concentrated under high vacuum without heating. The resulting syrup was

subjected to flash column silica chromatography using a solvent system increasing in polarity 2 to 3% methanol in chloroform to give the title compound as an off-white solid that crystallized from ethyl acetate and hexanes to give pure white needles of the title compound (1.74 g, 68% over two steps). ^{1}H-NMR (500 MHz, $CDCl_3$) δ (ppm) 5.92 (d, J = 3.0 Hz, 1H), 5.70 (d, J = 8.9 Hz, 1H), 5.37 (dd, J = 10.7, 9.6 Hz, 1H), 5.16 (dd, J = 10.9, 9.7 Hz, 1H), 4.63 (m, 1H), 4.34 (dd, J = 12.1, 5.0 Hz, 1H), 4.03 (dd, J = 12.1, 3.2 Hz, 1H), 3.50 (m, 1H), 2.17 (s, 3H), 2.05 (s, 3H), 2.03 (s, 3H), 1.90 (s, 3H), 1.60 (s, 3H); ^{13}C-NMR (125 MHz, $CDCl_3$) δ (ppm) 171.73, 170.60, 169.52, 169.16, 168.77, 72.79, 71.78, 71.47, 61.10, 55.20, 39.75, 23.08, 21.14, 20.65, 20.53.

2-Acetamido-2-deoxy-5-thio-α-D-glucopyranose (**18**).[144] In a solution of methanol (1.9 mL), 0.050 g (0.12 mmol) of **17** was dissolved and a catalytic amount of sodium methoxide (enough to raise the pH of the reaction solution to between 9 and 10) was added. The reaction was followed closely by TLC and was found to be complete after 1 hour at room temperature. The solution was then neutralized by the drop-wise addition of a dilute solution of acetic acid in methanol (pH 4) until the pH was adjusted to 7. The reaction mixture was concentrated without heating under high vacuum. The final product was isolated as a white solid by flash silica column chromatography using a solvent system of 12:2:1 ethyl acetate:methanol:water (0.017 g, 58%).^{1}H-NMR (600 MHz, MeOH, d_4) δ (ppm) 4.89 (d, J = 3.2 Hz, 1H), 4.12 (dd, J = 10.5, 2.8 Hz, 1H), 3.88 (m, 2H), 3.70 (dd, J = 10.5, 8.82 Hz, 1H), 3.60 (dd, J = 10.5, 8.8 Hz, 1H), 3.60 (dd, J =

10.4, 9.0 Hz, 1H), 3.28 (m, 1H), 2.00 (s, 3H); ^{13}C-NMR (150 MHz, MeOH, d_4) δ (ppm) 171.91, 75.43, 72.07, 72.05, 61.20, 58.56, 43.44, 21.27.

3.6.2 Detailed synthetic methods for the synthesis of *p*MP- 5SGlcNAc (26).

***2-acetamido-3,4,6-tri-O-acetyl-2-deoxy-5-thio-α-D-glucopyranosyl chloride* (20).** A procedure analogous to that for generating 2-acetamido-3,4,6-tri-*O*-acetyl-2-deoxy-α-D-glucopyranosyl chloride was used here.[146] **17** (0.025 g, 0.062 mmol) was dissolved in acetyl chloride (0.5 mL) and cooled to 0 °C. HCl gas was bubbled into the cooled solution. Once the mixture was saturated with HCl gas, the mixture was capped and allowed to stir at room temperature for 72 hours. Upon completion of the reaction, the mixture was diluted with dichloromethane and cooled by directly adding ice to the solution. The cooled mixture was washed two times with saturated sodium bicarbonate, water, and brine. Each aqueous layer was back extracted with dichloromethane. The organic layers were pooled, dried with $MgSO_4$, and concentrated *in vacuo*. The reaction gave rise to a bright yellow oil (0.016 g, 73%). ^{1}H-NMR (600 MHz, $CDCl_3$) δ (ppm) 5.98 (d, *J* = 8.4 Hz, 1H), 5.31 (m, 2H), 5.21 (m, 1H), 4.58 (m, 1H), 4.36 (dd, *J* = 12.2, 5.0 Hz, 1H), 4.05 (dd, *J* = 12.2, 3.0 Hz, 1H), 3.61 (m, 1H), 2.01 (s, 3H), 1.99 (s, 3H), 1.98 (s, 3H), 1.91 (s, 3H); ^{13}C-NMR (150 MHz, $CDCl_3$) δ (ppm) 171.52, 170.53, 169.84, 169.22, 71.40, 71.25, 64.95, 60.76, 57.42, 40.52, 23.13, 20.61, 20.52; HRMS (*m*/*z*): $[M+H]^+$ calcd for $C_{14}H_{20}ClNO_7S$: 382.0727; found 382.0726.

2-Acetamido-3,4,6-tri-O-acetyl-2-deoxy-5-thio-α-D-glucopyranose (**21**). Anomeric deacetylation was effected in a manner similar to that reported previously for different saccharides.[151,153,157] To a solution of **17** (0.200 g, 0.490

mmol) in DMF (1 mL) at room temperature, was added hydrazine acetate (0.050 g, 0.54 mmol). The mixture was left to stir until all starting material was consumed (6 hours) as judged by TLC. The mixture was then concentrated under high vacuum, and co-evaporated twice with toluene, without heating. The resulting residue was taken up in ethyl acetate and washed two times with saturated sodium bicarbonate, water (until a neutral pH was obtained), and brine. Each aqueous layer was back extracted with ethyl acetate. The pooled organic layers were dried using $MgSO_4$, filtered, and concentrated *in vacuo*. The residue was subjected to flash column silica chromatography using a solvent system of 30% hexanes in ethyl acetate, and subsequently concentrated under high vacuum to afford the title compound as a white solid. Crystallization from ethyl acetate and hexanes afforded a white powder (0.144 g, 80%). ^{1}H-NMR (600 MHz, $CDCl_3$) δ (ppm) 4.89 (dd, J = 10.5, 2.8 Hz, 1H), 3.88 (m, 2H), 3.70 (dd, J = 10.5, 8.8 Hz, 1H), 3.60 (dd, J = 10.4, 8.9 Hz, 1H), 3.28 (m, 1H), 2.00 (s, 3H); ^{13}C-NMR (150 MHz, $CDCl_3$) δ (ppm) 171.91, 75.43, 72.07, 72.05, 61.20, 58.56, 43.44, 21.27. HRMS (*m*/*z*): $[M+H]^+$ calcd for $C_{14}H_{21}NO_8S$: 364.1066; found 364.1070.

2-Acetamido-3,4,6-tri-O-acetyl-2-deoxy-5-thio-α-D-glucopyranosyl trichloroacetimidate (**22**). Preparation of the trichloroacetimidate donor was carried out by modification of a previously described procedure used for different saccharides.[157] **21** was dissolved in dichloromethane at 0 °C, and to this solution was added trichloroacetonitrile (0.181 g, 1.27 mmol) and a catalytic amount of DBU (~1 drop). The reaction was allowed to stir at 0 °C until completion (0.5

hours). The mixture was then diluted with benzene and concentrated under high vacuum. The crude residue was subjected to flash column silica chromatography using a solvent system of 40% hexanes in ethyl acetate. The desired material was isolated as a clear oil, which upon standing, solidified to give a white solid (0.086 g, 76%).^{1}H-NMR (600 MHz, $CDCl_3$) δ (ppm) 8.77 (s, 1H), 6.08 (d, J = 3.0 Hz, 1H), 5.79 (d, J = 8.8 Hz, 1H), 5.37 (dd, J = 10.7, 9.8 Hz, 1H), 5.20 (dd, J = 10.7, 9.8 Hz, 1H), 4.65 (m, 1H), 4.29 (dd, J =12.1, 5.0 Hz, 1H), 4.00 (dd, J = 12.1, 3.1 Hz, 1H), 3.49 (m, 1H), 2.00 (s, 3H), 1.99 (s, 3H), 1.98 (s, 3H);^{13}C-NMR (150 MHz, $CDCl_3$) δ (ppm) 171.51, 170.49, 169.59, 169.21, 159.20, 90.79, 77.82, 71.69, 71.31, 60.99, 55.80, 40.14, 23.06, 20.63, 20.60, 20.52. HRMS (*m*/*z*): $[M+H]^+$ calcd for $C_{16}H_{121}N_2O_8SCl_3$: 507.0162; found 507.0173.

para-Methoxyphenyl 2-acetamido-3,4,6-tri-O-acetyl-2-deoxy-5-thio-β-D-glucopyranoside (**24**). Glycosylation was effected by adaptation of a reported method used for glycosylation of trichloroacetimidate donors of other saccharides.[149,153,157] A solution of **22** (0.050 g, 0.100 mmol) and *p*-methoxyphenol (0.025 g, 0.20 mmol) in dichloromethane (0.77 mL) was stirred at -20 °C. To this solution a catalytic amount of $BF_3{\cdot}OEt_2$ (~ 1 drop) was added, and the reaction was immediately allowed to warm to room temperature. The reaction was stirred for 1 hour, after which time the reaction was judged complete by TLC. Two equivalents of triethylamine (0.026 mL) were then added to the reaction mixture. The mixture was concentrated under high vacuum without heating. Flash column silica chromatography was carried out to isolate the products and the ^{1}H NMR spectrum revealed a mixture of two products; the α- and β-anomers in a ratio of

70% α and 30% β. The two anomers were separated *via* flash column silica chromatography using a solvent system 40% hexanes in ethyl acetate to afford the pure β-glycoside (0.056 g, 12%) and α-glycoside (0.096 g, 21%). Data provided for the β-glycoside: ^{1}H-NMR (600 MHz, $CDCl_3$) *δ* (ppm) 6.89 (d, *J* = 9.1 Hz, 2H), 6.77 (d, *J* = 9.1 Hz, 2H), 5.88 (d, *J* = 8.8 Hz, 1H), 5.31 (m, 1H), 5.13 (d, *J* = 6.3 Hz, 1H), 5.04 (m, 1H), 4.52 (m, 1H), 4.28 (m, 2H), 3.70 (s, 3H), 3.14 (m, 1H), 2.02 (s, 3H), 2.01 (s, 3H), 1.99 (s, 3H), 1.92 (s, 3H); ^{13}C-NMR (150 MHz, $CDCl_3$) *δ* (ppm) 170.55, 170.15, 169.70, 168.95, 155.44, 150.46, 118.20, 114.71, 80.57, 71.04, 69.16, 63.44, 55.67, 40.60, 29.72, 23.41, 20.81, 20.72, 20.70. HRMS (*m*/*z*): $[M+H]^+$ calcd for $C_{21}H_{27}N_2O_9S$: 470.1485; found 470.1478.

para-Methoxyphenyl 2-acetamido-2-deoxy-5-thio-β-D-glucopyranoside (**26**). To a solution of **24** (0.0062 g, 0.013 mmol) in methanol (0.25 mL) was added a catalytic amount of sodium methoxide (enough to bring the reaction solution to pH 10). The reaction was allowed to stir at room temperature. After twenty minutes a white solid began to precipitate out of solution. The reaction was complete after 30 minutes as judged by TLC. The reaction was then diluted with additional methanol (5 mL) and subsequently brought to a neutral pH value by the drop-wise addition of a dilute mixture of acetic acid in methanol (pH 4). The mixture was concentrated under high vacuum without heating. The title compound was isolated by precipitation from ethanol and ether as a fine white powder (0.0033 g, 66%). ^{1}H-NMR (600 MHz, MeOH, D_4) *δ* (ppm) 6.99 (d, *J* = 9.2 Hz, 2H), 6.83 (d, *J* = 9.2 Hz, 2H), 5.10 (d, *J* = 9.3 Hz, 1H), 4.19 (dd, *J* = 9.6 Hz, 1H), 3.96 (dd, *J* = 11.4, 3.7 Hz,1H), 3.79 (dd, *J* = 11.4, 6.5 Hz, 1H), 3.74 (s, 3H),

3.60 (dd, *J* = 10.1 Hz, 1H), 3.38 (dd, *J* = 9.9 Hz, 1H), 2.89 (m, 1H), 1.96 (s, 3H); ^{13}C-NMR (150 MHz, D_2O) δ (ppm) 172.44, 155.27, 151.78, 117.50, 114.14, 80.79, 75.08, 74.32, 61.23, 59.86, 54.64, 46.08, 21.58. HRMS (*m*/*z*): $[M+H]^+$ calcd for $C_{15}H_{21}NO_6S$: 344.1168; found 344.1157.

CHAPTER 4: CONCLUSIONS AND FUTURE WORK

4.1 Conclusions

The goal for synthesizing the compounds described in this thesis was to gain a greater understanding of the role of *O*-GlcNAc and its significance in the cell. One way of addressing questions relating to the significance of *O*-GlcNAc is through the design of cell permeable, potent, and selective inhibitors. By introducing such inhibitors into cells we have the opportunity to manipulate the levels of *O*-GlcNAc and evaluate the effects. In order to accomplish this goal however, it was first necessary to reflect on the active site of the enzymes and on previous inhibitors already synthesized for *O*-GlcNAcase and OGT, both in terms of their successes and shortcomings. A crucial requirement in furthering the understanding of this enzyme was the development of inhibitors that had a more acute potency and selectivity than inhibitors already developed.[40]

Studies presented in the first part of this thesis introduce a second generation of *O*-GlcNAcase inhibitors, many of which improved upon both the binding affinity and selectivity of previous inhibitors developed by colleagues Whitworth and Macauley and coworkers.[40] Several potent, nanomolar affinity inhibitors were created. A key discovery that accounts for much of the improvements made in some of these second generation inhibitors was the introduction of an electron rich amino moiety at the 2'-position the thiazoline ring. By introducing this group we were able to increase the probability of the

endocyclic nitrogen of the thiazoline ring being protonated at physiological pH. The positive charge generated through protonation of the endocyclic nitrogen of such inhibitors was able to provide the predicted ionic interaction with a key catalytic aspartate residue within the active site of *O*-GlcNAcase.[107]

It was also found that maintaining some steric bulk attached to the 2'-position of the thiazoline ring on the inhibitors was important for selectivity for human *O*-GlcNAcase over the functionally related human lysosomal β-hexosaminidases. This was first noted during the development of the first generation of inhibitors.[40] *O*-GlcNAcase is well known to possess a considerably deeper binding pocket that can accommodate greater steric bulk[129] compared to the relatively shallow binding pocket of the hexosaminidase enzymes.[158] Therefore, despite there being several inhibitors that were created with low nanomolar binding to *O*-GlcNAcase, it was the inhibitor Thiamet-G, which possesses a 2'-aminoethyl group, that gained most attention in our laboratory. It has a K_i value of 22 nM while maintaining an impressive 37,000 fold selectivity for *O*-GlcNAcase over functionally related lysosomal β-hexosaminidase enzymes.[107]

Due to Thiamet-G's potency and selectivity, it was evaluated in several cellular studies relating to the reciprocal relationship observed between the *O*-GlcNAc modification and phosphorylation of the cellular protein tau.[107] This reciprocal relationship has been of special interest to our laboratory as there have been several studies documenting the correlation between the hyper-phosphorylated state of the cellular protein tau and the development and

incidence of Alzheimer's disease. One hypothesis developed in the Vocadlo laboratory is that by increasing levels of the *O*-GlcNAc modification of tau, the levels of phosphorylation may be decreased.[107] Promising results observed by the group have prompted evaluating the long-term effects of treating animals with Thiamet-G, with the hope that it may serve to validate a potential therapeutic strategy to tau hyperphosphorylation.

The second part of this thesis involved synthesis of 5SGlcNAc. This compound was originally sought out for its potential to serve as a probe of *O*-GlcNAcase. Upon treating cells with 5SGlcNAc, however, it was found that the *O*-GlcNAc modification on proteins decreased. This observation led to the hypothesis that UDP-5SGlcNAc may act as an inhibitor of OGT. This was an exciting prospect, as there were no previous reports of a cell permeable inhibitor of OGT. UDP-5SGlcNAc was chemoenzymatically synthesized by Wesley Zandberg and was found through kinetic studies performed by David Shen that it does act as an inhibitor of OGT, with a K_i value of 8 μM. Although this inhibitor has a moderate binding affinity, it is the first cell permeable inhibitor of OGT, and will most likely be modified in the future to create new inhibitors, hopefully with improved binding affinity. This inhibitor, as well as future variants, may act as useful research tools.

Derivatives of 5SGlcNAc were also prepared including one bearing a para-methoxyphenyl leaving group. This allowed us to conduct kinetic tests with this putative substrate and it was found that *O*-GlcNAcase was capable of

efficiently processing this substrate. Undoubtedly, these findings are only the beginning of further investigations for these two related enzymes.

4.2 Future Work

Regardless of what is accomplished in science, there is always more work to be done! Often one discovery simply opens up a new set of questions, and the requirement for more experiments to address them all! The accomplishments presented in this thesis are no exception to this observation. Many studies could be done to further our understanding and knowledge in the areas discussed throughout this body of work.

In chapter 2 the focus was on the development of a potent and selective inhibitor for *O*-GlcNAcase. Despite our success in developing Thiamet-G, there is still potential for creating new, equally effective or even better inhibitors for this enzyme. This possibility is worth exploring, particularly in light of the potential *O*-GlcNAcase inhibition has as a therapeutic strategy. If Thiamet-G does prove to be effective in treating Alzheimer disease, then relying completely on this one compound would be unwise. One never knows at what stage in drug development something can go awry, and having alternative compounds one can turn to is important.

It would be interesting if a series of inhibitors for *O*-GlcNAcase could be designed that do not contain a carbohydrate moiety. It may also be possible to design a set of compounds that have comparable steric bulk to previous inhibitors, while introducing new electronic properties that would produce favorable binding interactions with key residues in the active site of *O*-

GlcNAcase. Another possibility for future *O*-GlcNAcase inhibitors would be maintaining the thiazoline ring moiety, as well as the attached 2'-aminoethyl group seen in Thiamet-G, while changing some of the portions of the carbohydrate ring. Introducing heteroatoms within the pyranose ring or as alternatives to the hydroxyl groups attached to the sugar may produce interesting new binding interactions.

In light of the discovery that UDP-5SGlcNAc acts as an inhibitor of OGT, it would be worth investigating the binding capabilities of variants of this scaffold. Introducing other heteroatoms within the carbohydrate portion of UDP-5SGlcNAc may also provide an effective scaffold for an OGT inhibitor. Investigating the inhibitory capabilities of other variants of 5-thiosugars may also be interesting. For example, it would be worth investigating the effects of 5-thio mannose, 5-thiofucose, 5-thioxylose, among others, on inhibition of other targets *in vitro*. Looking at whether these other compounds have inhibitory capabilities in cells would also be worth investigating.

Discovering that *p*MP-5SGlcNAc can act as a substrate for *O*-GlcNAcase makes it worth looking at analogues of this compound. This could be accomplished by making a small library of putative *O*-GlcNAcase substrates containing the 5SGlcNAc core bearing various leaving groups. It would be interesting to see how different leaving groups affect the rate of turnover by this enzyme. Are larger leaving groups advantageous for *O*-GlcNAcase processing? Are leaving groups with electron withdrawing or electron donating moieties advantageous for *O*-GlcNAcase processing? If so, to what extent? These are a

sampling of some of the questions that could be investigated in further studies. These experiments would be valuable, as they would provide information as to which aspects of the substrate are important for successful turnover by *O*-GlcNAcase and could broaden our understanding of this interesting enzyme.

APPENDIX

Dixon plots were used to determine K_i values of the inhibitors presented in chapter 2. Dixon plots were generated by plotting $1/V$ as a function of inhibitor concentration. Rates of substrate processing (V) were plotted as the absorbance values of *p*NP released from *p*NP-GlcNAc (400 nm) or fluorescence of 4-methylumbelliferone (excitation: 368 nm, emmision 450 nm) released from 4-methylumbelliferyl 2-acetamido-2-deoxy-β-D-glucopyranoside by *O*-GlcNAcase as a function of time. The resulting data was fitted by linear regression. Using this regression, the line can be extrapolated as described below. By plotting the horizontal line that defines $1/V_{max}$ perpendicular to the y-axis we can determine the intersection with the linear regression, which is the $-K_i$ value for the particular inhibitor of interest.

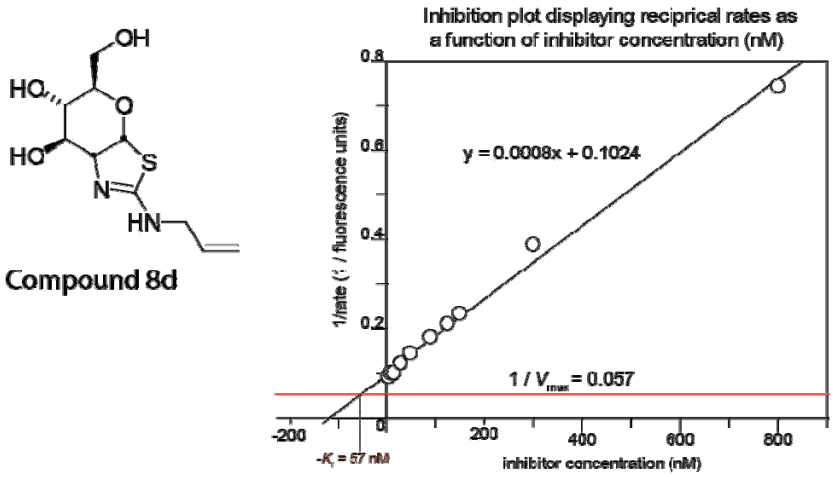

Appendix Figure 1 Reciprocal inhibition plot for compound **8d**. Rates of substrate processing at several inhibition concentrations were recorded. The reciprocal value of each of these rates were calculated and plotted as a function of inhibition concentration.To calculate our K_i value, 'x' was solved for according to its representation of $-K_i$, when y= $1/V_{max}$.

REFERENCES

1. Ghosh S., Blumenthal H., Davidson E. & Roseman, A.S. Glucosamine Metabolism: V. ENZYMATIC SYNTHESIS OF GLUCOSAMINE 6-PHOSPHATE *J Biol Chem* **235**, 1265-73 (1960).

2. Chavan, M. & Lennarz, W. The molecular basis of coupling of translocation and *N*-glycosylation. *Trends Biochem Sci* **31**, 17-20 (2006).

3. Dennis, J.W., Lau, K.S., Demetriou, M. & Nabi, I.R. Adaptive regulation at the cell surface by N-glycosylation. *Traffic* **10**, 1569-78 (2009).

4. Gu, J. *et al.* A mutual regulation between cell-cell adhesion and *N*-glycosylation: implication of the bisecting GlcNAc for biological functions. *J Proteome Res* **8**, 431-5 (2009).

5. Neville, D.C., Field, R.A. & Ferguson, M.A. Hydrophobic glycosides of *N*-acetylglucosamine can act as primers for polylactosamine synthesis and can affect glycolipid synthesis *in vivo*. *Biochem J* **307 (Pt 3)**, 791-7 (1995).

6. Yuzwa, S.A. & Vocadlo, D.J. *O*-GlcNAc modification and the tauopathies: insights from chemical biology. *Curr Alzheimer Res* **6**, 451-4 (2009).

7. Hart, G.W., Housley, M.P. & Slawson, C. Cycling of *O*-linked β-*N*-acetylglucosamine on nucleocytoplasmic proteins. *Nature* **446**, 1017-22 (2007).

8. Hanover, J.A., Krause, M.W. & Love, D.C. The hexosamine signaling pathway: *O*-GlcNAc cycling in feast or famine. *Biochim Biophys Acta* **1800**, 80-95 (2009).

9. Torres, C.R. & Hart, G.W. Topography and polypeptide distribution of terminal *N*-acetylglucosamine residues on the surfaces of intact lymphocytes. Evidence for *O*-linked GlcNAc. *J Biol Chem* **259**, 3308-17 (1984).

10. Wells, L., Vosseller, K. & Hart, G.W. Glycosylation of nucleocytoplasmic proteins: signal transduction and *O*-GlcNAc. *Science* **291**, 2376-8 (2001).

11. Chou, C.F., Smith, A.J. & Omary, M.B. Characterization and dynamics of *O*-linked glycosylation of human cytokeratin 8 and 18. *J Biol Chem* **267**, 3901-6 (1992).

12. Roquemore, E.P., Chevrier, M.R., Cotter, R.J. & Hart, G.W. Dynamic *O*-GlcNAcylation of the small heat shock protein α B-crystallin. *Biochemistry* **35**, 3578-86 (1996).

13. Zeidan, Q. & Hart, G.W. The intersections between *O*-GlcNAcylation and phosphorylation: implications for multiple signaling pathways. *J Cell Sci* **123**, 13-22 (2010).

14. Kreppel, L.K., Blomberg, M.A. & Hart, G.W. Dynamic glycosylation of nuclear and cytosolic proteins. Cloning and characterization of a unique *O*-GlcNAc transferase with multiple tetratricopeptide repeats. *J Biol Chem* **272**, 9308-15 (1997).

15. Lubas, W.A., Frank, D.W., Krause, M. & Hanover, J.A. *O*-Linked GlcNAc transferase is a conserved nucleocytoplasmic protein containing tetratricopeptide repeats. *J Biol Chem* **272**, 9316-24 (1997).

16. Dong, D.L. & Hart, G.W. Purification and characterization of an *O*-GlcNAc selective *N*-acetyl-β-D-glucosaminidase from rat spleen cytosol. *J Biol Chem* **269**, 19321-30 (1994).

17. Gao, Y., Wells, L., Comer, F.I., Parker, G.J. & Hart, G.W. Dynamic *O*-glycosylation of nuclear and cytosolic proteins: cloning and characterization of a neutral, cytosolic β-*N*-acetylglucosaminidase from human brain. *J Biol Chem* **276**, 9838-45 (2001).

18. Haltiwanger, R.S., Holt, G.D. & Hart, G.W. Enzymatic addition of *O*-GlcNAc to nuclear and cytoplasmic proteins. Identification of a uridine diphospho-*N*-acetylglucosamine:peptide β-acetylglucosaminyltransferase.

    J Biol Chem **265**, 2563-8 (1990).

19. Hanks, S.K. & Hunter, T. Protein kinases 6. The eukaryotic protein kinase superfamily: kinase (catalytic) domain structure and classification. *Faseb J* **9**, 576-96 (1995).

20. Barford, D. Molecular mechanisms of the protein serine/threonine phosphatases. *Trends Biochem Sci* **21**, 407-12 (1996).

21. Kamemura, K., Hayes, B.K., Comer, F.I. & Hart, G.W. Dynamic interplay between *O*-glycosylation and *O*-phosphorylation of nucleocytoplasmic proteins: alternative glycosylation/phosphorylation of THR-58, a known mutational hot spot of c-Myc in lymphomas, is regulated by mitogens. *J Biol Chem* **277**, 19229-35 (2002).

22. Shafi, R. *et al*. The *O*-GlcNAc transferase gene resides on the X chromosome and is essential for embryonic stem cell viability and mouse ontogeny. *Proc Natl Acad Sci U S A* **97**, 5735-9 (2000).

23. McClain, D.A. *et al.* Altered glycan-dependent signaling induces insulin resistance and hyperleptinemia. *Proc Natl Acad Sci U S A* **99**, 10695-9 (2002).

24. Vosseller, K., Wells, L., Lane, M.D. & Hart, G.W. Elevated nucleocytoplasmic glycosylation by *O*-GlcNAc results in insulin resistance associated with defects in Akt activation in 3T3-L1 adipocytes. *Proc Natl Acad Sci U S A* **99**, 5313-8 (2002).

25. Liu, F., Iqbal, K., Grundke-Iqbal, I., Hart, G.W. & Gong, C.X. *O*-GlcNAcylation regulates phosphorylation of tau: a mechanism involved in Alzheimer's disease. *Proc Natl Acad Sci U S A* **101**, 10804-9 (2004).

26. Liu, F. *et al.* Reduced *O*-GlcNAcylation links lower brain glucose metabolism and tau pathology in Alzheimer's disease. *Brain* **132**, 1820-32 (2009).

27. Lefebvre, T. *et al*. Evidence of a balance between phosphorylation and *O*-GlcNAc glycosylation of Tau proteins--a role in nuclear localization. *Biochim Biophys Acta* **1619**, 167-76 (2003).

28. Ngoh, G.A. & Jones, S.P. New insights into metabolic signaling and cell survival: the role of β-*O*-linkage of *N*-acetylglucosamine. *J Pharmacol Exp Ther* **327**, 602-9 (2008).

29. Chatham, J.C. & Marchase, R.B. The role of protein *O*-linked β-*N*-acetylglucosamine in mediating cardiac stress responses. *Biochim Biophys Acta* **1800**, 57-66 (2009).

30. Chatham, J.C., Not, L.G., Fulop, N. & Marchase, R.B. Hexosamine biosynthesis and protein *O*-glycosylation: the first line of defense against stress, ischemia, and trauma. *Shock* **29**, 431-40 (2008).

31. Shi, Y. *et al*. Aberrant *O*-GlcNAcylation characterizes chronic lymphocytic leukemia. *Leukemia* (2010).

32. Caldwell, S.A. *et al.* Nutrient sensor *O*-GlcNAc transferase regulates breast cancer tumorigenesis through targeting of the oncogenic transcription factor FoxM1. *Oncogene* **29**, 2831-42.

33. Golks, A., Tran, T.T., Goetschy, J.F. & Guerini, D. Requirement for *O*-linked *N*-acetylglucosaminyltransferase in lymphocytes activation. *Embo J* **26**, 4368-79 (2007).

34. Golks, A. & Guerini, D. The *O*-linked *N*-acetylglucosamine modification in cellular signalling and the immune system. 'Protein modifications: beyond the usual suspects' review series. *EMBO Rep* **9**, 748-53 (2008).

35. Vocadlo, D.J. & Davies, G.J. Mechanistic insights into glycosidase chemistry. *Curr Opin Chem Biol* **12**, 539-55 (2008).

36. Yip, V.L. & Withers, S.G. Nature's many mechanisms for the degradation of oligosaccharides. *Org Biomol Chem* **2**, 2707-13 (2004).

37. Wolfenden, R., Lu, X.D. & Young, G. Spontaneous hydrolysis of glycosides. *Journal of the American Chemical Society* **120**, 6814-6815 (1998).

38. Cantarel, B.L. *et al.* The Carbohydrate-Active EnZymes database (CAZy): an expert resource for Glycogenomics. *Nucleic Acids Res* **37**, D233-8 (2009).

39. Wade, L.G. *Organic Chemistry, 6th ed*, (Pearson/Prentice Hall, Upper Saddle River, New Jersey, USA, 2005).

40. Macauley, M.S., Whitworth, G.E., Debowski, A.W., Chin, D. & Vocadlo, D.J. *O*-GlcNAcase uses substrate-assisted catalysis: kinetic analysis and development of highly selective mechanism-inspired inhibitors. *J Biol Chem* **280**, 25313-22 (2005).

41. Cetinbas, N., Macauley, M.S., Stubbs, K.A., Drapala, R. & Vocadlo, D.J. Identification of Asp174 and Asp175 as the key catalytic residues of human *O*-GlcNAcase by functional analysis of site-directed mutants. *Biochemistry* **45**, 3835-44 (2006).

42. Rempel, B.P. & Withers, S.G. Covalent inhibitors of glycosidases and their applications in biochemistry and biology. *Glycobiology* **18**, 570-86 (2008).

43. Withers, S.G. & Aebersold, R. Approaches to labeling and identification of active site residues in glycosidases. *Protein Sci* **4**, 361-72 (1995).

44. Legler, G.C. Glycoside hydrolases: mechanistic information from studies with reversible and irreversible inhibitors. *Adv Carbohydr Chem Biochem* **48**, 319-84 (1990).

45. He, Y., Martinez-Fleites, C., Bubb, A., Gloster, T.M. & Davies, G.J. Structural insight into the mechanism of streptozotocin inhibition of *O*-GlcNAcase. *Carbohydr Res* **344**, 627-31 (2009).

46. Bryk, R. & Wolff, D.J. Pharmacological modulation of nitric oxide synthesis by mechanism-based inactivators and related inhibitors. *Pharmacol Ther* **84**, 157-78 (1999).

47. Pauling, L. Molecular architecture and biological reactions. *Chem Eng News* **24**, 1375-77 (1946).

48. Pauling, L. The forces of nature between large molecules of biological interest. *Nature* **161**, 707-709 (1948).

49. Davies, G.J., Withers S.G. *Comprehensive biological catalysis. A mechanistic reference, ed.*, (M. L. Sinnott, Academic Press, London, 1998).

50. Davies, G.J., Ducros, V.M.A., Varrot, A. & Zechel, D.L. Mapping the conformational itinerary of β-glycosidases by X-ray crystallography. *Biochem Soc Trans* **31**, 523-527 (2003).

51. Gloster, T.M. *et al.* Glycosidase inhibition: an assessment of the binding of 18 putative transition-state mimics. *J Am Chem Soc* **129**, 2345-54 (2007).

52. Inouye, S., Tsuruoka, T. & Nida, T. The structure of nojirimycin, a piperidinose sugar antibiotic. *J Antibiot (Tokyo)* **19**, 288-92 (1966).

53. Inouye, S., Tsuruoka, T., Ito, T. & Niida, T. Structure and synthesis of nojirimycin. *Tetrahedron* **24**, 2125-44 (1968).

54. Lillelund, V.H., Jensen, H.H., Liang, X. & Bols, M. Recent developments of transition-state analogue glycosidase inhibitors of non-natural product origin. *Chem Rev* **102**, 515-53 (2002).

55. Gloster, T.M. & Davies, G.J. Glycosidase inhibition: assessing mimicry of the transition state. *J Am Chem Soc* **129**, 305-20 (2009).

56. Payan, F. *et al.* The dual nature of the wheat xylanase protein inhibitor XIP-I: structural basis for the inhibition of family 10 and family 11 xylanases. *J Biol Chem* **279**, 36029-37 (2004).

57. Sansen, S. *et al.* Structural basis for inhibition of Aspergillus niger xylanase by triticum aestivum xylanase inhibitor-I. *J Biol Chem* **279**, 36022-8 (2004).

58. Houston, D.R., K. Shiomi, N. Arai, S. Omura, M.G. Peter, A. Turberg, B. Synstad, V.G.H. Eijsink and D.M.F. Aalten. High-resolution structures of chitinase complexed with natural product cyclopentapeptide inhibitors: Mimicry of carbohydrate substrate. *Proc Natl Acad Sci U S A* **99**, 9127-32 (2002).

59. Dale, M.P., Ensley, H.E., Kern, K., Sastry, K.A. & Byers, L.D. Reversible inhibitors of β-glucosidase. *Biochemistry* **24**, 3530-9 (1985).

60. Lairson, L.L., Henrissat, B., Davies, G.J. & Withers, S.G. Glycosyltransferases: structures, functions, and mechanisms. *Annu Rev Biochem* **77**, 521-55 (2008).

61. Chan, P.H. *et al.* NMR spectroscopic characterization of the sialyltransferase CstII from Campylobacter jejuni: histidine 188 is the general base. *Biochemistry* **48**, 11220-30 (2009).

62. Garinot-Schneider, C., Lellouch, A.C. & Geremia, R.A. Identification of essential amino acid residues in the Sinorhizobium meliloti glucosyltransferase ExoM. *J Biol Chem* **275**, 31407-13 (2000).

63. Lewis ES, B.C. The kinetic and stereochemistry of decomposition of secondary alkyl chloro sulphites. *J Am Chem Soc* **74**, 308–11

(1952).

64. Compain, P. & Martin, O.R. Carbohydrate mimetics-based glycosyltransferase inhibitors. *Bioorg Med Chem* **9**, 3077-92 (2001).

65. Roychoudhury, R. & Pohl, N.L. New structures, chemical functions, and inhibitors for glycosyltransferases. *Curr Opin Chem Biol* **14**, 168-73.

66. Brockhausen, I. *et al.* UDP-Gal: GlcNAc-R beta1,4-galactosyltransferase--a target enzyme for drug design. Acceptor specificity and inhibition of the enzyme. *Glycoconj J* **23**, 525-41 (2006).

67. Vidal, S., Bruyere, I., Malleron, A., Auge, C. & Praly, J.P. Non-isosteric C-glycosyl analogues of natural nucleotide diphosphate sugars as glycosyltransferase inhibitors. *Bioorg Med Chem* **14**, 7293-301 (2006).

68. Gross, B.J., Kraybill, B.C. & Walker, S. Discovery of *O*-GlcNAc transferase inhibitors. *J Am Chem Soc* **127**, 14588-9 (2005).

69. Lenzen, S. & Panten, U. Alloxan: history and mechanism of action. *Diabetologia* **31**, 337-42 (1988).

70. Lyons, S.D., Sant, M.E. & Christopherson, R.I. Cytotoxic mechanisms of glutamine antagonists in mouse L1210 leukemia. *J Biol Chem* **265**, 11377-81 (1990).

71. Platt, F.M., Neises, G.R., Dwek, R.A. & Butters, T.D. *N*-butyldeoxynojirimycin is a novel inhibitor of glycolipid biosynthesis. *J Biol Chem* **269**, 8362-5 (1994).

72. Lee, K.Y. *et al.* The Hexapeptide inhibitor of Galbeta 1,3GalNAc-specific alpha 2,3-sialyltransferase as a generic inhibitor of sialyltransferases. *J Biol Chem* **277**, 49341-51 (2002).

73. Schneider, E.G., Nguyen, H.T. & Lennarz, W.J. The effect of tunicamycin, an inhibitor of protein glycosylation, on embryonic development in the sea urchin. *J Biol Chem* **253**, 2348-55 (1978).

74. Jefferies, I. *et al.* Synthesis of Inhibitors α-1,3-fucosyl transferase. *Bioorg Med Chem Lett* **7**, 1171-1174 (1997).

75. Miura, T. *et al.* Synthesis and evaluation of morpholino- and pyrrolidinosphingolipids as inhibitors of glucosylceramide synthase. *Med Chem Lett* **6**, 1481-1489 (1998).

76. Kim, Y. *et al.* A rationally designed inhibitor of α-1,3-galactosyltransferase. *J Am Chem Soc* **121**, 5829-5830 (1999).

77. Hashimoto, H., Endo, T. & Kajihara, Y. Synthesis of the First Tricomponent Bisubstrate Analogue That Exhibits Potent Inhibition against GlcNAc:β -1,4-Galactosyltransferase. *J Org Chem* **62**, 1914-1915 (1997).

78. Muller, B.S., C.; Schmidt, R. R. Efficient Sialyltransferase Inhibitors Based on Transition-State Analogues of the Sialyl Donor. *Angew. Chem., Int. Ed. Engl.* **37**, 2893-2897 (1998).

79. Unligil, U.M. & Rini, J.M. Glycosyltransferase structure and mechanism. *Curr Opin Struct Biol* **10**, 510-7 (2000).

80. Yeoh, K.K., Butters, T.D., Wilkinson, B.L. & Fairbanks, A.J. Probing replacement of pyrophosphate *via* click chemistry; synthesis of UDP-sugar analogues as potential glycosyl transferase inhibitors. *Carbohydr Res* **344**, 586-91 (2009).

81. Martinez-Fleites, C. *et al.* Structure of an *O*-GlcNAc transferase homolog provides insight into intracellular glycosylation. *Nat Struct Mol Biol* **15**, 764-5 (2008).

82. Charnock, S.J. & Davies, G.J. Structure of the nucleotide-diphospho-sugar transferase, SpsA from Bacillus subtilis, in native and nucleotide-complexed forms. *Biochemistry* **38**, 6380-5 (1999).

83. Jackson, S.P. & Tjian, R. *O*-glycosylation of eukaryotic transcription factors: implications for mechanisms of transcriptional regulation. *Cell* **55**, 125-33 (1988).

84. Kelly, W.G., Dahmus, M.E. & Hart, G.W. RNA polymerase II is a glycoprotein. Modification of the COOH-terminal domain by *O*-GlcNAc. *J Biol Chem* **268**, 10416-24 (1993).

85. Han, I., Roos, M.D. & Kudlow, J.E. Interaction of the transcription factor Sp1 with the nuclear pore protein p62 requires the C-terminal domain of p62. *J Cell Biochem* **68**, 50-61 (1998).

86. Roos, M.D., Su, K., Baker, J.R. & Kudlow, J.E. *O*-glycosylation of an Sp1-derived peptide blocks known Sp1 protein interactions. *Mol Cell Biol* **17**, 6472-80 (1997).

87. Federici, M. *et al.* Insulin-dependant activation of endothelial nitric oxide synthase is impaired by *O*-linked glycosylation modification of signaling proteins in human coronary endothelial cells *Circulation* **106**, 466-72 (2002).

88. Yang, X. *et al. O*-linkage of *N*-acetylglucosamine to Sp1 activation domain inhibits its transcriptional capability. *Proc Natl Acad Sci U S A* **98**, 6611-6 (2001).

89. Gao, Y., Miyazaki, J. & Hart, G.W. The transcription factor PDX-1 is post-translationally modified by *O*-linked *N*-acetylglucosamine and this modification is correlated with its DNA binding activity and insulin secretion in min6 β-cells. *Arch Biochem Biophys* **415**, 155-63 (2003).

90. Du, X.L. *et al.* Hyperglycemia inhibits endothelial nitric oxide synthase activity by posttranslational modification at the Akt site. *J Clin Invest* **108**, 1341-8 (2001).

91. Parker, G.J., Lund, K.C., Taylor, R.P. & McClain, D.A. Insulin resistance of glycogen synthase mediated by *O*-linked *N*-acetylglucosamine. *J Biol Chem* **278**, 10022-7 (2003).

92. Chou, T.Y., Hart, G.W. & Dang, C.V. c-Myc is glycosylated at threonine 58, a known phosphorylation site and a mutational hot spot in lymphomas. *J Biol Chem* **270**, 18961-5 (1995).

93. Comer, F.I. & Hart, G.W. Reciprocity between *O*-GlcNAc and *O*-phosphate on the carboxyl terminal domain of RNA polymerase II. *Biochemistry* **40**, 7845-52 (2001).

94. Cheng, X., Cole, R.N., Zaia, J. & Hart, G.W. Alternative *O*-glycosylation/*O*-phosphorylation of the murine estrogen receptor beta. *Biochemistry* **39**, 11609-20 (2000).

95. Macauley, M.S., Bubb, A.K., Martinez-Fleites, C., Davies, G.J. & Vocadlo, D.J. Elevation of global O-GlcNAc levels in 3T3-L1 adipocytes by selective inhibition of *O*-GlcNAcase does not induce insulin resistance. *J Biol Chem* **283**, 34687-95 (2008).

96. Grundke-Iqbal, I. *et al.* Abnormal phosphorylation of the microtubule-associated protein tau (tau) in Alzheimer cytoskeletal pathology. *Proc Natl Acad Sci U S A* **83**, 4913-7 (1986).

97. Lindwall, G. & Cole, R.D. Phosphorylation affects the ability of tau protein to promote microtubule assembly. *J Biol Chem* **259**, 5301-5 (1984).

98. Braak, H., Braak, E., Grundke-Iqbal, I. & Iqbal, K. Occurrence of neuropil threads in the senile human brain and in Alzheimer's disease: a third location of paired helical filaments outside of neurofibrillary tangles and neuritic plaques. *Neurosci Lett* **65**, 351-5 (1986).

99. Sippel, K.H. *et al.* High-resolution structure of human carbonic anhydrase II complexed with acetazolamide reveals insights into inhibitor drug design. *Acta Crystallogr Sect F Struct Biol* **65**, 992-5 (2009).

100. Ko, S., Lee, M.K., Shin, D. & Park, H. Structure-based virtual screening approach to the discovery of novel inhibitors of factor-inhibiting HIF-1: identification of new chelating groups for the active-site ferrous ion. *Bioorg Med Chem Lett* **17**, 7769-74 (2009).

101. Alterio, V. *et al.* Crystal structure of the catalytic domain of the tumor-associated human carbonic anhydrase IX. *Proc Natl Acad Sci U S A* **106**, 16233-8 (2009).

102. Hamza, A.Z., C.G. Determination of the structure of human phosphodiesterase-2 in a bound state and its binding with inhibitors by molecular modeling, docking, and dynamics simulation. . *J Phys Chem B* **113**, 2896-908 (2009).

103. Cowan-Jacob, S.W., Mobitz, H. & Fabbro, D. Structural biology contributions to tyrosine kinase drug discovery. . *Curr Opin Cell Biol* **21**, 280-7 (2009).

104. Wang H. *et al.* Bioisoterism of urea-based GCP II inhibitors: Synthesis and structure activity relationship studies. *Bioorg Med Chem Lett* **20**, 392-7 (2009).

105. Gibson, R.P. *et al.* Molecular basis for trehalase inhibition revealed by the structure of trehalase in complex with potent inhibitors. *Angew Chem Int Ed Engl* **46**, 4115-9 (2007).

106. Aguilar, M. *et al.* Molecular basis for β-glucosidase inhibition by ring-modified calystegine analogues. . *Chembiochem* **9**, 2612-8 (2008).

107. Yuzwa, S.A. *et al.* A potent mechanism-inspired *O*-GlcNAcase inhibitor that blocks phosphorylation of tau in vivo. *Nat Chem Biol* **4**, 483-90 (2008).

108. Le Calvez, P.B., Scott, C.J. & Migaud, M.E. Multisubstrate adduct inhibitors: drug design and biological tools. *J Enzyme Inhib Med Chem* **24**, 1291-1318 (2009).

109. Plapp, B.V. Conformational changes and catalysis by alcohol dehydrogenase. *Arch Biochem Biophys* **493**, 3-12 (2009).

110. Xu, C., Maxwell, B.A., Brown, J.A., Zhang, L. & Suo, Z. Global conformational dynamics of a Y-family DNA polymerase during catalysis. . *PLoS Biol* **7**, e1000225 (2009).

111. Hammes, G.G., Chang, Y.C. & Oas, T.G. Conformational selection or induced fit: a flux description of reaction mechanism. *Proc Natl Acad Sci U S A* **106**, 13737-41 (2009).

112. Gutteridge, A. *et al.* Conformational change in substrate binding, catalysis and product release: an open and shut case? *FEBS Lett* **567**, 67-73 (2004).

113. Ho, M.C., Sturm, M.B., Almo, S.C. & Schramm, V.L. Transition state analogues in structures of ricin and saporin ribosome-inactivating proteins. *Proc Natl Acad Sci U S A* **106**, 20276-81 (2009).

114. Sturm, M.B., Tyler, P.C., Evans, G.B. & Schramm, V.L.Transition state analogues rescue ribosomes from saporin-L1 ribosome inactivating protein. *Biochemistry* **48**, 9941-8 (2009).

115. Mimoto, T. *et al.* Rational design and synthesis of a novel class of active site-targeted HIV protease inhibitors containing a hydroxymethylcarbonyl isostere. Use of phenylnorstatine or allophenylnorstatine as a transition-state mimic. *Chem Pharm Bull(Tokyo)* **39**, 2465-7 (1991).

116. Gloster, T.M. *et al.* Structural studies of the β-glycosidase from Sulfolobus solfataricus in complex with covalently and noncovalently bound inhibitors. *Biochemistry* **43**, 6101-9 (2004).

117. Whitworth, G.E. *et al.* Analysis of PUGNAc and NAG-thiazoline as transition state analogues for human *O*-GlcNAcase: mechanistic and structural insights into inhibitor selectivity and transition state poise. *J Am Chem Soc* **129**, 635-44 (2007).

118. Butler, K.V.K., A.P. Chemical origins of isoform selectivity in histone deacetylase inhibitors. *Curr Pharm Des* **14**, 505-28 (2008).

119. Branda, K.J., Tomczak, J. & Natowicz, M.R. Heterozygosity for Tay-Sachs and Sandhoff diseases in non-Jewish Americans with ancestry from Ireland, Great Britain, or Italy. *Genet Test* **8**, 174-80 (2004).

120. Parker, G., Taylor, R., Jones, D. & McClain, D. Hyperglycemia and inhibition of glycogen synthase in streptozotocin-treated mice: role of *O*-linked *N*-acetylglucosamine. *J Biol Chem* **279**, 20636-42 (2004).

121. Konrad, R.J., Mikolaenko, I., Tolar, J.F., Liu, K. & Kudlow, J.E. The potential mechanism of the diabetogenic action of streptozotocin: inhibition of pancreatic β-cell *O*-GlcNAc-selective *N*-acetyl-β-D-glucosaminidase. *Biochem J* **356**, 31-41 (2001).

122. Arias, E.B., Kim, J. & Cartee, G.D. Prolonged incubation in PUGNAc results in increased protein *O*-Linked glycosylation and insulin resistance in rat skeletal muscle. *Diabetes* **53**, 921-30 (2004).

123. Junod, A. *et al.* Studies of the diabetogenic action of streptozotocin. *Proc Soc Exp Biol Med* **126**, 201-5 (1967).

124. Bennett, R. *et al.* Alkylation of DNA in rat tissues following administration of streptozotocin. *Cancer Res* **41**, 2786-90 (1981).

125. Burkart, V. *et al.* Mice lacking the poly(ADP-ribose) polymerase gene are resistant to pancreatic β-cell destruction and diabetes development induced by streptozocin. *Nat Med* **5**, 314-9 (1999).

126. Mark, B.L. *et al.* Crystallographic evidence for substrate-assisted catalysis in a bacterial β-hexosaminidase. *J Biol Chem* **276**, 10330-7 (2001).

127. Hanover, J.A., Lai, Z., Lee, G., Lubas, W.A. & Sato, S.M. Elevated *O*-linked *N*-acetylglucosamine metabolism in pancreatic β-cells. *Arch Biochem Biophys* **362**, 38-45 (1999).

128. Macauley, M.S., Stubbs, K.A. & Vocadlo, D.J. *O*-GlcNAcase catalyzes cleavage of thioglycosides without general acid catalysis. *J Amer Chem Soc* **127**, 17202-17203 (2005).

129. Dennis, R.J. *et al.* Structure and mechanism of a bacterial β-glucosaminidase having *O*-GlcNAcase activity. *Nat Struct & Mol Biol* **13**, 365-371 (2006).

130. Sheltinga, T.C. *et al.* Stereochemistry of chitin hydrolysis by a plant chitinase/lysozyme and X-ray structure of a complex with allosamidin: evidence for substrate assisted catalysis. *Biochemistry* **34**, 15619-15623 (1995).

131. Avalos, M., Babino, R. & Cintas, P. Condensation of 2-amino-2-deoxy sugars with isothiocyanates, Synthesis of cis-1,2-fused glucopyranoheterocycles. *Tetrahedron* **50**, 3273-96 (1994).

132. Knapp, S. *et al.* Tautomeric modification of GlcNAc-thiazoline. *Org Lett* **9**, 2321-4 (2007).

133. Gonzaleza, M.A. *et al.* Synthesis of 1,3,4,6-tetra-*O*-acetyl-2-[3-alkyl-(aryl)-thioreido]-2-deoxy-α-D-glucopyranoses and their transformation into 2-alkyl(aryl)amino-(1,2-dideoxy-α-d-glucopyrano)[2,1-d]-2-thiazolines. *Carb Res* **154**, 49-62 (1986).

134. Knapp, S., Vocadlo, D.V., Gao, G., Kirk, B., Lou, J., & Withers, S. NAG-Thiazoline, An *N*-Acetyl-β-hexosaminidase Inhibitor that implicates acetamido participation. *Jour Amer Chem Soc* **118**, 6804-6805 (1996).

135. Avalos, M. *et al.* Synthesis of 1,3,4,6-tetra-*O*-acetyl-2-[3-alkyl-(aryl)-thioreido]-2-deoxy-α-D-glucopyranoses and their transformation into 2-alkyl(aryl)amino-(1,2-dideoxy-α-d-glucopyrano)[2,1-d]-2-thiazolines.*Carb Res* **154**, 49-62 (1986).

136. Fuentes J. *et al.* Stereocontrolled preparation of 2,3 and 4-isothionato aldopyranose derivatives.*Tetrahedron: Asymmetry* **11**, 2471-2482 (2000).

137. Gonzalez, M.A. *et al.* Synthesis of 1,3,4,6-tetra-*O*-acetyl-2-[3-alkyl-(aryl)-thioreido]-2-deoxy-α-D-glucopyranoses and their transformation into 2-alkyl(aryl)amino-(1,2-dideoxy-α-d-glucopyrano)[2,1-d]-2-thiazolines. *Carb Res* **154**, 49-62 (1986).

138. Toshiaki, O. *et al.* Nitrogen-containing Sugars. IX. Influence of the substituent at C-2 on the Chlorination at C-1 in *N*-Acyl-1,3,4,6-tetra-*O*-acetyl-β-D-glucosamines *Chem & pharm bull* **8**, 597-610 (1960).

139. Avalos, M., Babiano, R. & Cintas, P. Synthesis of sugar-(2-thiazolin-2-yl) thioureas. *Carb Res* **198**, 247-258 (1990).

140. Knapp, S., Kirk, B.A., Vocadlo, D. & Withers, S.G. An Allosamizoline/Glucosamine Hybrid NAGase Inhibitor. *Synlett*, 435-436 (1997).

141. Kiso, M. & Anderson, L. Ferric Chloride-Catalyzed Glycosylation of Alcohols by 2-Acylamido-2-Deoxy- β -D-Glucopyranose 1-Acetates. *Carbohydrate Research* **72**, C12-C14 (1979).

142. Rao, F. *et al.* Structural insights into the mechanism and inhibition of eukaryotic *O*-GlcNAc hydrolysis. *Embo Journal* **25**, 1569-78 (2006).

143. Schultz, J. *et al.* Prediction of structure and functional residues for *O*-GlcNAcase, a divergent homologue of acetyltransferases. *Febs Letters* **529**, 179-182 (2002).

144. Tanahashi, E. & Hasegawa A. A facile synthesis of 2-acetamido-2-deoxy-5-thio-D-glucopyranose. *Carb Res* **117**, 304-308 (1983).

145. Hasegawa, A. Tanahashi, E. A Simple Preparation of 2-(Acylamino)-2-deoxy-3,4:5,6-di-*O*-isopropyladine-aldehydo-D-glucose dimethyl and dibenzylacetal. *Carb Res* **79**, 265-270 (1980).

146. Greig, I.R., Macauley, M.S., Williams, I.H. & Vocadlo, D.J. Probing synergy between two catalytic strategies in the glycoside hydrolase *O*-GlcNAcase using multiple linear free energy relationships. *J Am Chem Soc* **131**, 13415-22 (2009).

147. Yuasa, H. *et al.* β-Selective Glycosidation of a 5-Thioglucosamine Derivative. *Chemistry Letters* **37**, 1288-1289 (2008).

148. Tsuruta, O., Yuasa, H., Hashimoto, H., Kurono, S. & Yazawa, S. Affinity of 5-thio-L-fucose-containing Lewis X (Le(X)) trisaccharide analogs to anti-Le(X) monoclonal antibody. *Bioor Med Chem Lett* **9**, 1019-1022 (1999).

149. Izumi, M., Tsuruta, O., Hashimoto, H. & Yazawa, S. Synthesis of 5-thio-L-fucose-containing blood group antigens H-type 2 and Lewis X (Le(x)). *Tet Lett* **37**, 1809-1812 (1996).

150. Mehta S. *et al.* Synthesis of sulphur analogues of methyl and allyl kojibiosides and methyl isomaltoside and conformational analysis of the kojibiosides. *Tet Asym* **5**, 2367-2396 (1994).

151. Hashimoto, H. *et al.* Efficient and stereoselective 1,2-cis-glycoside formation of 5-thioaldopyranoses - Glycosylation with peracetylated 5-thio-D-arabinopyranosyl and 5-thio-L-fucopyranosyl-trichloroacetimidates. *Tet Lett* **34**, 4949-4952 (1993).

152. Mehta, S., Andrews, J.S., Johnston, B.D. & Pinto, B.M. Novel heteroanalogues of methyl maltoside containing sulfur and selenium as potential glycosidase inhibitors. *J Amer Chem Soc* **116**, 1569-70 (1994).

153. Yuasa H., & Hashimoto H. Glycosidation reactions of 5-thioxylpyranosyl donors. *Lett Org Chem* **5**, 429-431 (2008).

154. Damager, I. Synthesis and characterization of novel chromogenic substrates for human pancreatic α-amylase. *Carb Res* **339**, 1727-37 (2004).

155. Mehta, S., Andrews, J.S., Johnston, B.D., Svensson, B. & Pinto, B.M. Synthesis and enzyme-inhibitory activity of novel glycosidase inhibitors containing sulfur and selenium. *J Amer Chem Soc* **117**, 9783-90 (1995).

156. Mehta, S.P., B.M. Unprecedented chemical glycosidation of 5-thioglucose to give disaccharides. . *Tet Lett* **33**, 7675-78 (1992).

157. Izumi, M., Tsuruta, O., Harayama, S. & Hashimoto, H. Synthesis of 5-thio-L-fucose-containing disaccharides, as sequence-specific inhibitors, and 2'-fucosyllactose, as a substrate of α-L-fucosidases. *Jour Org Chem* **62**, 992-998 (1997).

158. Mark, B.L. *et al.* Structural and functional characterization of Streptomyces plicatus β-*N*-acetylhexosaminidase by comparative molecular modeling and site-directed mutagenesis. *J Biol Chem* **273**, 19618-24 (1998).